

AD-757 795

SOME CONSIDERATIONS ON THE FEASIBILITY  
OF ADVERTENT CLIMATE MODIFICATION

Henry Hidalgo

Institute for Defense Analyses

Prepared for:

Defense Advanced Research Projects Agency

October 1972

DISTRIBUTED BY:

**NTIS**

**National Technical Information Service  
U. S. DEPARTMENT OF COMMERCE  
5285 Port Royal Road, Springfield Va. 22151**

PAPER P-856

SOME CONSIDERATIONS ON THE FEASIBILITY OF  
ADVERTENT CLIMATE MODIFICATION

Henry Hidalgo

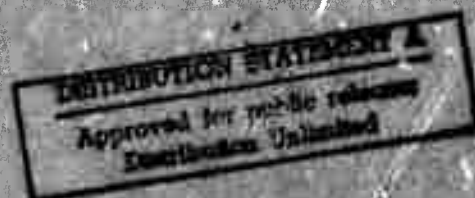
October 1972



Reproduced by  
**NATIONAL TECHNICAL  
INFORMATION SERVICE**  
U S Department of Commerce  
Springfield VA 22151



**INSTITUTE FOR DEFENSE ANALYSES  
SCIENCE AND TECHNOLOGY DIVISION**



IDA Log No. HQ 72-14325  
Copy 61 of 100 copies

138

AD 757795

## DOCUMENT CONTROL DATA - R &amp; D

(Security classification of title, body of abstract and indexing annotation must be entered when the overall report is classified)

## 1. ORIGINATING ACTIVITY (Corporate author)

INSTITUTE FOR DEFENSE ANALYSES  
400 Army-Navy Drive  
Arlington, Virginia 22202

2a. REPORT SECURITY CLASSIFICATION  
UNCLASSIFIED

2b. GROUP --

## 3. REPORT TITLE

SOME CONSIDERATIONS ON THE FEASIBILITY OF ADVERTENT CLIMATE  
MODIFICATION

## 4. DESCRIPTIVE NOTES (Type of report and inclusive dates)

PAPER P-856 October 1972

## 5. AUTHOR(S) (First name, middle initial, last name)

Henry Hidalgo

## 6. REPORT DATE

October 1972

## 7a. TOTAL NO. OF PAGES

124 138

## 7b. NO. OF REFS

54

## 8a. CONTRACT OR GRANT NO.

DAHC15 73 C 0200

## 8b. ORIGINATOR'S REPORT NUMBER(S)

P-856

## b. PROJECT NO.

ARPA Assignment 20

## 8c. OTHER REPORT NO(S) (Any other numbers that may be assigned this report)

NA

## 10. DISTRIBUTION STATEMENT

Approved for public release; distribution unlimited.

## 11. SUPPLEMENTARY NOTES

NA

## 12. SPONSORING MILITARY ACTIVITY

Defense Advanced Research  
Projects Agency  
Arlington, Virginia 22209

## 13. ABSTRACT

A general circulation model for climate, emphasizing physical phenomenology, is developed as part of an overall consideration: whether it is feasible to control or advertently modify the earth's surface climate at the middle and high northern latitudes. Ultimately, the answer to this feasibility question will be used to evaluate theoretically the current capabilities of world superpowers in their possible utilization of controlled climate modification for political or military purposes.

The use of the model, along with the most recent reduction of experimental data for the long-term statistics of the current general circulation, allows the semi-experimental determination of certain statistics which are difficult to measure directly. These are the wave and amplitude parameters of the baroclinic disturbances, and the vertical transports, which the model determines as a function of latitude. A local test of the model proved successful: for the latitude where the large-scale transport of angular momentum vanishes as the large-scale transport of sensible heat reaches a maximum, experimental and semi-experimental results show agreement.

The model indicates that the transports of angular momentum, sensible heat, and specific humidity do depend on the zonal (eastward direction) circulation. This resolves the puzzle of previous results in which wave and amplitude parameters of the baroclinic disturbances were assumed to be constant. Also, the model indicates that these transports are coupled to the vertical ones. Only one eigenvalue is required by the model. This involves the static stability of the troposphere.

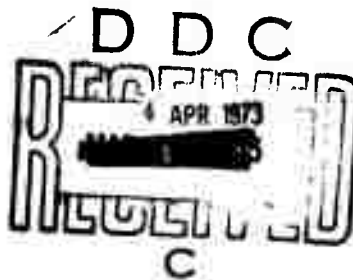
KEY WORDS	LINK A		LINK B		LINK C	
	ROLE	WT	ROLE	WT	ROLE	WT
Feasibility of Advertent Climate Modification						
Climate Modification						
Climate Control						
Model for General Circulation of Climate						

PAPER P-856

SOME CONSIDERATIONS ON THE FEASIBILITY OF  
ADVERTENT CLIMATE MODIFICATION

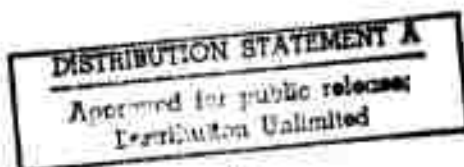
Henry Hidalgo

October 1972



INSTITUTE FOR DEFENSE ANALYSES  
SCIENCE AND TECHNOLOGY DIVISION  
400 Army-Navy Drive, Arlington, Virginia 22202

Contract DAHC15 73 C 0200  
ARPA Assignment 20



ic

## FOREWORD

This paper considers the question of whether controlled or advertent modification of the earth's climate at the middle and high northern latitudes is feasible. The work was performed by IDA for the Defense Advanced Research Projects Agency (DARPA).

The author is indebted to Dr. W.L. Gates of the Rand Corporation for his comprehensive review of the manuscript of this paper, and to Dr. W.M. Washington of the National Center for Atmospheric Research for important general comments on the main subject of this paper. One of Dr. Washington's worthwhile comments concerns the development of numerical models of the atmosphere for the prediction of climate changes, i.e., "it is the feeling among most modellers that neither simplified nor complex models are developed to the point of giving definite answers to climate change."

The author acknowledges the support of his colleagues at IDA, i.e., Dr. Ernest Bauer for reviewing the manuscript and Mr. Dennis F. Deriggi for his work on the numerical calculations for this paper. The author also thanks Dr. Robert Vaglio-Laurin for some valuable technical discussions concerning two-dimensional turbulence.

## SUMMARY

This paper considers the feasibility of controlled or advertent modification of the climate of the earth's surface at the middle and high northern latitudes.\* The ultimate aim of this feasibility question is the theoretical evaluation of the current capabilities of a world superpower to use controlled climate modification for political or military purposes. The timeliness of this feasibility question stems from two technological developments which will enhance the understanding of tropospheric phenomena: (1) the advent of meteorological satellites, which provides a capability for worldwide, near real-time measurements of the main characteristic parameters of the troposphere (e.g., the temperature field, humidity etc.); and (2) the development of large-memory, high-speed electronic computers, which will allow the reduction of large amounts of data and the performance of theoretical calculations with increasing space resolutions both over the earth's surface and along the vertical dimension of the troposphere.

Considerations of the feasibility of advertent climate modification at the middle and high northern latitudes must strive for a maximum understanding of the basic processes that control atmospheric and oceanic phenomena near the earth's surface. The study of such processes during recent years has emphasized the development of complex numerical models of the troposphere using increasing space resolutions; a trend that requires the use of large electronic computers of ever

---

\*The concept of controlled or advertent climate modification is different from that of either inadvertent climate modification caused by the impact of modern man's activities on his environment or advertent weather modification.

increasing capabilities. Such procedures yield a wealth of numerical data which do not necessarily enhance the understanding of the controlling processes. The overall considerations of the feasibility of advertent climate modification have therefore used two approaches: (1) an attempt to capitalize on the availability of the complex numerical models for the general circulation of air within the troposphere (e.g., the Mintz-Arakawa model, etc.), and (2) an investment of a limited manpower level in developing simpler complementary models of the general circulation for climate that emphasize physical phenomenology. This report is part of this second approach.

The fundamental question concerning the feasibility of advertent climate modification is broken down in this report into four basic subquestions:

1. What are the key processes that control the climate at the earth's surface?
2. Can the results of these processes be described uniquely from the use of the physical laws controlling such processes?
3. What is the sensitivity of the climate at the earth's surface to changes in these key processes?
4. Does man have the technology now to use such a sensitivity to control his climate?

A positive answer to the fundamental question of the feasibility of advertent climate modification requires conclusive positive answers to each of these subquestions. Thus, the answer to the first subquestion must take the form of an accurate model for climate, i.e., a mathematical description of the basic processes that control the long-term (e.g., annual, seasonal, monthly) statistics of the general circulation. The second subquestion is the most difficult to answer conclusively, for it requires as yet unknown ergodic criteria for the ruling out of all but one of any multiple solutions from the model that predicts changes in the earth's climate. The answer to the third subquestion must be based on the previous ones, i.e., on the use of an accurate model that yields unique predictions for changes in the earth's

climate; the earth's climate must then have an appropriate degree of sensitivity to changes in the key processes. The answer to the final subquestion must be based on the answer to the third subquestion. Because of the time lag between initiation and completion of a major project, which is usually a major fraction of a decade, a positive answer to the fourth subquestion becomes necessary if man is to control his climate as early as in the 1980s.

The results of this paper are addressed mainly to the first subquestion, i.e., the development of a model of the general circulation appropriate for climate by emphasizing physical phenomenology. For this reason, the scope of this report attempts (1) to present a rather unified picture of the main developments in meteorology during the last 30 years, which have enhanced the understanding of the basic processes that control the earth's climate, and (2) to describe the physical and mathematical arguments in the development of a model, based on physical phenomenology, with enough detail to bring out as clearly as possible all the assumptions used in such a model.

Key processes that control the earth's climate, as determined by the long-term statistics of the general circulation of air within the troposphere, are the poleward transports of angular momentum and sensible heat (or enthalpy).<sup>\*</sup> These processes involve two different but coupled types of phenomena:

1. Net heating rates of the troposphere as a function of latitude by solar and terrestrial radiation, condensation of water vapor, and eddy fluxes of sensible and latent heat to the troposphere from the surface boundary layer (about 1 km thick) next to the earth's surface (e.g., Figs. 1 and 2, Section III).
2. Large-scale turbulent or eddy motion that is triggered by the net heating rates of the troposphere; because of the condition of very small vertical winds or hydrostatic equilibrium

---

<sup>\*</sup>The troposphere is the lowest layer of the atmosphere, about 16 km thick at the equator and about 8 km at the poles.

in the direction vertical to the earth's surface, the turbulent motion is two-dimensional with its own characteristic spectra (Fig. 4, Section III). However, in contrast with the problem of long-range weather forecasting, only low hemispherical wave numbers (i.e., number of wavelengths in a latitudinal circle) are of interest for climate.

The eddy motion at low wave numbers produces the large-scale poleward transports of angular momentum and sensible heat, which in turn set up a meridional cell structure of a statistical nature for the general circulation (e.g., Fig. 5, Section III). The number of the meridional cells in each hemisphere varies between two and three, which corresponds, respectively, to the two extremes of interglacial and glacial climates in the current Pleistocene Epoch. Large-scale transports of angular momentum and sensible heat take place through a mechanism that involves the presence of streamlines with an asymmetrical sinusoidal form, which are characterized by the associated NE-SW tilt ( $\alpha$ ) from the meridian of their trough line (Fig. 12, Section VII). This mechanism produces transports of angular momentum that are countergradient at middle and higher latitudes, i.e., transport that cannot be expressed by the use of an eddy viscosity and the latitudinal gradient of the average flow. Since the transport of angular momentum is largest in the upper half of the troposphere, a model of the general circulation for climate can be set up by using a two-level model of the troposphere (Fig. 13, Section VII); i.e., the flow pattern in the upper half of the troposphere may be represented by that at the 250-mb level, while the flow pattern in the lower half of the troposphere is represented by that at the 750-mb level. The conservation equations are applied at these levels together with the analytical formulation of the flow ( $\psi^*$ ) and temperature ( $\hat{\theta}^*$ ) disturbances induced by the eddy motion (Fig. 12). Based on the meridional cell structure of the general circulation for the two extreme conditions of the interglacial and glacial climates of the current Pleistocene Epoch, a further assumption used in the model is that the

role of the angular momentum transport is always more important in the upper half as compared with that in the lower half of the troposphere.

Specific results concerning the first subquestion are then as follows:

1. A model of the general circulation for advertent climate modification has been formulated based on a variable tilt from the meridian for both the flow and temperature disturbances; a variable phase lag between the flow and temperature disturbances, and a variable amplitude of these nonlinear baroclinic disturbances.
2. The use of this model based on variable wave and amplitude parameters of the baroclinic disturbances, together with the most recent reduction of experimental data for the long-term statistics of the current general circulation, allows the semi-experimental determination as a function of latitude of statistics that are difficult to measure directly, i.e., the wave and amplitude parameters of the baroclinic disturbances as well as the vertical transports.
3. A successful local test of the fundamental formulation of the nonlinear baroclinic disturbances is obtained from the agreement between experimental and semi-experimental results for the latitude where the large-scale transport of angular momentum vanishes as the large-scale transport of sensible heat reaches a maximum value.
4. The model based on variable wave and amplitude parameters of the baroclinic disturbances indicates that the transports of angular momentum, sensible heat, and specific humidity do depend on the zonal (i.e., eastward direction) circulation, a result that resolves the puzzle of previous results assuming constant wave and amplitude parameters of the baroclinic disturbances. The model based on variable wave and amplitude parameters further indicates that the foregoing transports are also coupled to the vertical transports.

5. The model based on variable wave and amplitude parameters of the baroclinic disturbances requires only one eigenvalue parameter, which involves the static stability of the troposphere. This result implies that there is no need to use-- as in the model using constant amplitude and wave parameters-- a weak boundary condition at the north pole to establish the magnitude of the transports of angular momentum and sensible heat at latitudes lower than those near the north pole.

Integrations of this model can yield the changes in the basic statistics that control the general circulation within the troposphere, as a function of essentially the advertent modifications of the poleward heat flux at the middle and high latitudes; a modification that would result from any advertent change of the surface albedo, for example, and its related impact on the net heating rates of the troposphere at these latitudes. These integrations can use known boundary conditions at the northern edge of the unperturbed meridional cell at low latitudes, i.e., the Hadley cell, in which the ITCZ phenomena play a dominant role (Fig. 7, Section III). The changes in the long-term statistics determinable from the model involve the large-scale poleward transport of angular momentum at the 250-mb level, the mean sensible heat and specific humidity transports, the vertical transports, and the meridional as well as zonal eddy kinetic energies in the middle and in the upper half of the troposphere.

The second basic subquestion identified earlier has to do with the uniqueness (or lack of it) of a predicted change of the climate at the earth's surface as derived from the nonlinear conservation equations. This problem is again different from the predictability of weather forecasting for a few days, since the fundamental question here concerns the possible multiplicity of solutions for given nonlinear differential equations with appropriate boundary conditions. If such solution is unique, then there is only one prediction for the change of the climate; the solution then becomes deterministic or transitive. If there are multiple solutions, then there are several predictions for the change of the climate; the solutions then become

intransitive. It has been possible, for example, to devise a rather crude model of the climate of the earth's surface that is intransitive; the model is given by a nonlinear, second order, ordinary differential equation for the earth's surface temperature as a function of latitude. Integrations of this equation using the same boundary conditions yield five climates; two of these are physically unidentifiable, while the other three correspond to the current climate, a climate of the ice age, and a climate for an ice covered earth, respectively (Fig. 8, Section IV). Since the two physically unidentifiable solutions can be made to vanish by the formulation of a coefficient of the differential equation, it becomes clear that the use of an accurate model is a necessary, but not sufficient, condition for the determination of the transitive or intransitive nature of a prediction of any advertent change of the climate. In the absence of ergodic criteria to eliminate all but one of any multiple solutions from a given model, the answer to the second subquestion must be determined from numerical investigations using an accurate model.

The third subquestion, concerning the sensitivity of climate to advertent changes in its key processes, can be answered from numerical investigations using an accurate, transitive model for climate.

The fourth subquestion, concerning the capability of current technology to produce changes in the climate, can be illustrated by a potential mechanism for advertent climate modification. Although the solar inclination is low at high latitudes, the length of the solar illumination during summer at these latitudes is such that the magnitude of the incoming solar radiation can be greater than that at low latitudes for a significant fraction of each year. However, because of the high surface albedo at the high latitudes, the absorbed solar radiation becomes significantly lower than that at the low latitudes (Fig. 9, Section VI). Thus, a decrease in the surface albedo accomplished by a large-scale removal of the snow and permanent ice over the Arctic Ocean could have a significant impact on the current intensity and extent of the meridional cells at the middle and high

latitudes. The use of a transient thermodynamic model for sea ice is successful in reproducing theoretically both the thickness of the current ice layer over the Arctic Ocean and the temperature at its surface (Fig. 10, Section VI). Parametric results from this model indicate that the use of a suitable material dark enough to decrease the surface albedo from its current value of about 0.5 to only 0.4 would remove the permanent ice layer over the Arctic Ocean within a very few years.

The integrations of the foregoing model based on variable wave and amplitude parameters of the baroclinic disturbances can be applied to the conditions of an Arctic Ocean without sea ice (which is also an environment corresponding to the interglacial climate of the current Pleistocene Epoch). This procedure would provide a test of the iterative process on the temperature at the 500-mb level, which is required for the solution of the problem of advertent climate modification. This model, then, could be used to seek answers for the second and third subquestions concerning the feasibility of advertent modification of the climate of the earth's surface at middle and high northern latitudes.

The modest computer capability that is required for the use of the model for climate, based on variable wave and amplitude parameters of the baroclinic disturbances, suggests that a world superpower can solve the feasibility problem of advertent climate modification without the need of new electronic computers of larger capabilities.

## CONTENTS

Foreword	iii
Summary	v
Symbols	xv
I. Introduction	1
II. Key Questions in Advertent Climate Modification	5
III. Processes that Control the Earth's Climate	9
A. Net Heating Rate of the Atmosphere	13
B. Large-Scale Poleward Transports	19
IV. Predictability of the Climate at the Earth's Surface	27
V. Characteristics of the Climates of the Pleistocene Epoch	31
VI. Sample of a Potential Mechanism for Advertent Climate Modification	35
VII. Description of the General Circulation for Climate	43
A. Transports as a Function of Poleward Heat Flux	49
B. Transports as a Function of Wave Parameters	52
VIII. Evaluation of the Theory of the General Circulation for Climate Based on a Constant S Wave Parameter	57
IX. Formulation of the Theory of the General Circulation for Climate Based on a Variable Tilt, Phase Lag, and Amplitudes of the Baroclinic Disturbances	83
X. Results and Concluding Remarks	99
XI. References	103
Appendix A--Derivation of Zonal Momentum and Energy Equations and S-Wave Parameter	109
Appendix B--Derivation of Eddy Kinetic Energy Equation	121

## SYMBOLS

a	Mean radius of earth, 6371 km
$A_a$	Atmosphere albedo
$A_*$	Earth's albedo
$A_p$	Planetary albedo
A	Amplitude of flow disturbances, $m^2/sec$
B	Amplitude of temperature disturbances, $m^2/sec^2$
c	Specific heat
$c_v$	Specific heat of air at constant volume, $7.09 \times 10^6 \text{ cm}^2 \text{ sec}^{-2} \text{ deg}^{-1}$
$c_p$	Specific heat of air at constant pressure, $9.96 \times 10^6 \text{ cm}^2 \text{ sec}^{-2} \text{ deg}^{-1}$
C	Heat released by condensation, ly/day or $\text{cal/cm}^2 \text{ day}$
D	Horizontal divergence, $\text{sec}^{-1}$
$E_S$	Flux divergence of heat due to eddy transport of sensible heat from earth's surface
$E_L$	Flux divergence of heat due to eddy transport of latent heat from earth's surface
$E_W$	Rate of change of water vapor content per unit mass
$\vec{F}$	Horizontal frictional force vector
f	Coriolis parameter, $2\Omega \sin \theta$ , $\text{sec}^{-1}$
g	Mean magnitude of the acceleration of gravity, $981 \text{ cm sec}^{-2}$
$H_m$	Quantity proportional to transport of sensible heat or enthalpy, $m^3/\text{sec}^3$
$\vec{i}$	Unit vector directed eastward
$I_o$	Solar radiation passing through the top surface of the sea ice layer

$\vec{j}$	Unit vector directed northward
$\vec{k}$	Unit vector directed upward
$k$	Hemispherical wave number, conductivity
$K_e$	Kinetic energy per unit mass for the horizontal motion, $(\frac{1}{2}) \vec{u} \cdot \vec{u}$
$K_Z$	Zonal kinetic energy, $(\frac{1}{2}) [\vec{u}] \cdot [\vec{u}]$
$K_E$	Eddy kinetic energy, $(\frac{1}{2}) \vec{u}^* \cdot \vec{u}^* + [\vec{u}] \cdot \vec{u}^*$
$L_d$	Downward long-wave radiation, ly/day or cal/cm <sup>2</sup> day
$L_t$	Upward long-wave radiation, ly/day or cal/cm <sup>2</sup> day
$L$	Latent heat of condensation, 600 cal/gm
$m$	Sec $\theta$ , Mercator map factor
$M_m$	Quantity proportional to angular momentum transport in the Mercator plane, m <sup>2</sup> /sec <sup>2</sup>
$M_o$	Flux divergence of heat in the oceans due to lateral ocean transport, ly/day
$M_w$	Rate of condensation of water per unit volume, gm/cm <sup>3</sup> day
$p$	Pressure, mb or gm/m sec <sup>2</sup>
$Q$	Rate of heating per unit mass, cal/gm day
$q$	Specific humidity
$q_f$	Poleward heat flux, m <sup>3</sup> /sec <sup>3</sup>
$R$	Gas constant for air, $2.87 \times 10^6$ cm <sup>2</sup> sec <sup>-2</sup> deg <sup>-1</sup>
$S_o$	Solar radiation at top of atmosphere, ly/day or cal/cm <sup>2</sup> day
$S_a$	Solar radiation absorbed by the atmosphere, ly/day or cal/cm <sup>2</sup> day
$S_*$	Solar radiation absorbed by the earth's surface, ly/day
$S_i$	Sea ice salinity profile
$t$	Time
$T$	Temperature, °K or °C
$T_*$	Temperature of earth's surface, °K or °C
$T_2$	500 mb or vertical mean temperature
$u$	Eastward component of $\vec{V}$ , m/sec
$u_m$	Eastward Mercator map wind component of $\vec{V}_m$
$\vec{U}$	Horizontal wind velocity, horizontal projection of $\vec{V}$ , m/sec

$v$	Northward component of $\vec{V}$ , m/sec
$v_m$	Northward Mercator map wind component of $\vec{V}_m$
$\vec{V}$	Wind velocity, m/sec
$\vec{V}_m$	Mercator map wind velocity
$w$	Upward component of $\vec{V}$ , m/sec
$x$	Eastward Mercator map coordinate
$y$	Northward Mercator map coordinate
$z$	Elevation, measured upward
$\alpha$	Tilt from meridian of trough line of the flow and temperature disturbances
$\Gamma$	Long-wave absorptivity of the atmosphere
$\Gamma_2$	Static stability of atmosphere
$\gamma^2$	Eigenvalue parameter proportional to the static stability
$\delta$	Phase lag of temperature and flow disturbances
$\vec{\nabla}$	Two- or three-dimensional del operator
$\zeta$	Vertical component of relative vorticity, sec <sup>-1</sup>
$\theta$	Latitude, deg
$\theta_p$	Potential temperature
$\kappa_i$	Extinction coefficient for solar radiation penetrating top surface of sea ice
$\lambda$	Longitude (deg), wavelength (km)
$\nu_t$	Normalization parameter for upward long-wave atmospheric radiation
$\nu_d$	Normalization parameter for downward long-wave atmospheric radiation
$\rho$	Density, gm/cm <sup>3</sup>
$\sigma$	Stephan-Boltzmann constant, $1.177 \times 10^{-7}$ ly day <sup>-1</sup> deg <sup>-4</sup>
$\tau$	Frictional stress per unit horizontal area
$\phi$	Geopotential, gz
$\chi$	Dependent variable, opacity of atmosphere to solar radiation
$\psi$	Stream function of flow disturbances, m <sup>2</sup> /sec
$\Omega$	Angular velocity of earth, $7.292 \times 10^{-5}$ sec <sup>-1</sup>
$\omega$	Individual or total pressure change, dp/dt

- [ ( ) ] Longitudinal average of ( )  
 ( )\* Departure from longitudinal average  
 $\overline{(\ )}$  Time average (Bar is usually omitted in the annual averages.)  
 ( )' Departure from time average  
 $\int$  Vertically integrated spectral mode,  $\overline{\xi} = \xi_1 + \xi_3$   
 $\int$  Vertical shear spectral mode,  $\hat{\xi} = \xi_1 - \xi_3$

### Subscripts

- 1 250-mb level  
 2 500-mb level  
 3 750-mb level  
 4 1000-mb level or ear h's surface  
 \* Earth's surface  
 i Ice  
 i, o Pure ice  
 s Snow  
 m Mercator plane  
 w Water vapor

### Abbreviation

- ly Langley (or g cal/cm<sup>2</sup>)

## I. INTRODUCTION

The main objective of this paper is to consider the feasibility of controlled modifications of the climate of the earth's surface at middle and high northern latitudes. The concept of controlled or advertent climate modification is different from both the concept of inadvertent modifications of the earth's climate by modern man's activities and the concept of advertent weather modification. The concept of advertent climate modification stems from the trend of world superpowers to make timely exploitations of breakthroughs in technology towards the achievement of their economical, political, and military goals. The considerations of the feasibility of advertent climate modification must strive to gain a maximum understanding of the key processes that control atmospheric and oceanic phenomena near the earth's surface.

The general study of atmospheric and oceanic processes during recent years emphasizes the use of theoretical models of increasing complexity that require ever larger electronic computers. This approach yields a wealth of numerical details, which do not necessarily enhance the understanding of the relevant controlling processes. The overall considerations of advertent climate modification have therefore attempted to capitalize on the availability of such complex models (e.g., Rapp, 1970); however, as a complementary activity, a limited manpower effort has also been dedicated to the task of attempting to gain insight into the key processes that control the climate at the earth's surface through the development of simpler models that stress physical phenomenology. Such simpler models provide two additional advantages at a sacrifice in the wealth of numerical details: (1) they increase the range and number of parameters that must be considered

in preliminary numerical investigations, a task that would involve prohibitive investments of resources through the use of the more complex models; and (2) they aid in the evaluation of the capability of world superpowers that may lag in the development of ever larger electronic computers for their consideration of the feasibility of advertent climate modification. This paper, which is based on limited manpower, uses therefore this complementary approach for the considerations of the feasibility of advertent modifications of the climate of the earth's surface at middle and high latitudes.

The basic aim of emphasizing the physical phenomenology relevant to the advertent modification of the climate at the earth's surface has shaped the scope of this paper, which attempts to present the relevant physical and mathematical developments in sufficient detail to bring out as clearly as possible the physical arguments and assumptions. For this reason, the scope of this paper includes the following topics:

1. A brief description of the basic processes that control the climate of the earth's surface.
2. The predictability of changes of the climate at the earth's surface or of the long-term (i.e., monthly, seasonal, annual) statistics that result from large-scale wave phenomena in the troposphere, which control the long-term general circulation or structure of the air flow within the troposphere.
3. The characteristics of the climate at the earth's surface corresponding to the two extremes of glacial and interglacial conditions of the current Pleistocene Epoch as described by their difference in both the structure of the general circulation and the earth's surface temperature as a function of latitude.
4. A sample of a potential mechanism for advertent climate modification.
5. Description of the general circulation for climate, including a brief review of the key meteorological developments relevant to the understanding of climate over the last 30 years.

6. Evaluation of available theoretical models of the general circulation in the troposphere applicable to climate, by using the most recent reduction of experimental data.
7. Generalization of the formulation of the models so as to close the gap between the theoretical results and the measurement of the statistics that control the current general circulation and climate near the earth's surface.

The relevance of the foregoing topics becomes clear from the nature of the key questions in advertent climate modification, which are described in the next section.

## II. KEY QUESTIONS IN ADVERTENT CLIMATE MODIFICATION

The fundamental question of advertent climate modification has to do with the theoretical evaluation of the feasibility of controlled modification of the earth's climate, in the early 1980s, by a world superpower for either political or military purposes. The 1980s time scale is fixed by the time lag between initiation and operation of a major new project, which is usually measurable in a large fraction of a decade; and the fact that it must use proven and, therefore, current advanced technology. The timeliness of this feasibility question has been brought about by two breakthroughs in modern meteorology:

1. Advent of meteorological satellites, which provides a capability for near real-time, worldwide measurements of the temperature distribution throughout the troposphere (e.g., Hidalgo, 1969). This capability includes measurements of the wind field from selective cloud motion, and of course, the derived geostrophic wind at middle and high latitudes from the temperature field.
2. Development of modern electronic computers, which yields a capability for both the reduction of a large amount of satellite data and the execution of more refined theoretical calculations.

These breakthroughs can therefore accelerate the progress towards a more refined understanding of the processes that sustain the general circulation of the air in the troposphere, and the subsequent identification of the key processes for advertent climate modification, if they exist.

The meteorological merits of the subject of advertent climate modification are perhaps best addressed by quoting the late eminent meteorologist, C.G. Rossby (The Atmosphere and Sea in Motion, 1959):

Our understanding of the general circulation of the atmosphere is increasing rapidly, and the expenses that would go with a large scale experiment of changing the albedo of the earth do not seem unsurmountable. It is perhaps not surprising then that some very outstanding scientists consider the question of climate control to be a real and practical task for meteorological research. As an example, the highly judicious mathematician J. von Neumann made this statement in 1955: probably intervention in atmospheric and climatic matters will come in a few decades and will unfold on a scale difficult to imagine at present.

Rossby added:

Most meteorologists would be reluctant perhaps to accept von Neumann's forecast today, but one should remember that during the last decades the technological development has time after time shown the dreams of a visionary mind to be closer to reality than the commonsense judgment of the realists.

It may only be appropriate, more than a decade later, to emphasize Rossby's remarks concerning the understanding of the processes that control the general circulation of the atmosphere, for the execution of any large-scale experiment for the purpose of climate control would require an evaluation of the probable consequences to man's environment from the nonlinear response of the troposphere to such proposed experiment.

The fundamental question concerning the feasibility of advertent climate modification can be broken down into the following four basic subquestions:

1. What are the key processes that control the climate at the earth's surface?
2. Can the results of these key processes be predicted uniquely from the use of the physical laws controlling such processes?

3. What is the theoretical sensitivity of the climate at the earth's surface to changes in these key processes?
4. Does man have the technology now to use such sensitivities for the control of his climate?

A positive answer to the fundamental question concerning the feasibility of advertent climate modification requires positive answers to every one of these subquestions; i.e., key processes must be identified and described through a model based on physical laws, physical laws must give unique predictions of climate changes, the climate must have an appropriate degree of sensitivity to changes in the key processes, and man must possess the technology necessary for the use of such sensitivities. While these subquestions are straightforward to pose, the answer to the second one is difficult because it must invoke as yet underdeveloped ergodic theory that has to do with the long-term statistical properties of solutions of differential equations. Nevertheless, this subquestion might be answerable with the use of an accurate mathematical model of the phenomena that control the current long-term general circulation, if such model is found to be successful in describing uniquely the coupling between the main characteristics of each climate during the time the earth acquired its current geographical distribution of oceans and continents.

### III. PROCESSES THAT CONTROL THE EARTH'S CLIMATE

The climate at the earth's surface is characterized by the monthly, seasonal, and annual average magnitude of two thermodynamic variables: the surface temperature ( $T_*$ ) and the humidity ( $q$ ) of the air. These variables are, however, coupled through the conservation equations to the dynamic variables or two components of the wind, i.e., the zonal wind ( $u$ ) in the longitudinal direction ( $\lambda$ ) and the meridional wind ( $v$ ) in the latitudinal direction ( $\theta$ ); the vertical wind ( $w$ ) in the altitude direction ( $z$ ) is small, a condition that yields hydrostatic equilibrium or an exponential decrease in pressure ( $p$ ) with increasing altitude. The phenomena controlling the climate at the earth's surface take place mainly in the troposphere or lowest layer of the atmosphere, which extends to only about 16 km from the earth's surface at the equator and to about 8 km at the poles. The troposphere is characterized by a decrease in air temperature with increasing altitude (i.e.,  $dT/dz < 0$  or  $dT/dp > 0$ ); this lowest layer contains most of the air in the atmosphere, since the air density at the tropical tropopause (or upper limit of the troposphere) drops to about 15 percent of the value at the earth's surface.\* Thus, there are two immediate implications for climate:

1. Only time averages of the thermodynamic and dynamic variables become of interest; this is in contrast with weather forecasting, where emphasis must be placed on the instantaneous values of such variables.

---

\*The middle level of the next layer, the stratosphere (where  $dT/dz \geq 0$ ), is of some interest because the ozone concentration reaches a maximum there.

2. The upper rarified layers of the atmosphere (i.e., upper stratosphere, mesosphere, and thermosphere) with their complicated chemical kinetics and physics, are relatively unimportant for the climate at the earth's surface.

These two conditions allow the use of significant mathematical simplifications in the formulation of the theory of the general circulation for climate.

Another condition that allows a further mathematical simplification of the theory of the general circulation for climate is the rather remarkable fact that species present in the troposphere in small amounts play a dominant role in climate at the earth's surface. The most important of these species is water; near sea level it is present in the air by less than 4 percent by volume in the vapor phase, and less than 1 percent in the liquid and solid phases (e.g., Miller and Thompson, 1970). Water in its vapor and liquid phases in the lower levels of the troposphere influences the climate at the earth's surface mainly through its spectral properties for the absorption of long-wave terrestrial radiation. Its spectral properties allow it to absorb a fraction of the long-wave radiation emitted by the earth's surface, and emit a downward flux of long-wave radiation back to the earth's surface. This greenhouse effect maintains the temperature of the earth's surface at a higher value (i.e., by nearly 50°F, Willett and Sanders, 1959) than it would be otherwise. Water also has a significant impact on the net heating of the troposphere through its vaporization-condensation cycle, i.e., by absorbing its latent heat during vaporization at the earth's surface, and releasing it to heat the troposphere during its condensation while ascending to the middle and upper levels of the troposphere. The cloud formation that results from this condensation process has a further effect on the net heating of the troposphere, since the statistics of the cloud distribution within the troposphere have an important effect on the reflection of incoming short-wave solar radiation or albedo of the troposphere. Since the vaporization-condensation cycle introduces a variable content of water within the troposphere, the magnitude of the

air's specific humidity as a function of latitude, longitude, and altitude (or pressure, since these two variables are interchangeable from the condition of hydrostatic equilibrium in the vertical direction) must be determined from the conservation equation for water vapor. However, the small concentration of water vapor relative to the air allows a mathematical decoupling of the equations of motion from the continuity equation for the specific humidity.\*

Finally, the rotation of the earth and the orientation of its axis of rotation relative to the sun allow the use of zonal (or longitudinal) averages for the thermodynamic and dynamic variables of interest for climate; i.e., the rotation of the earth tends to average the magnitude of such variables at a given latitude whenever the time interval of interest becomes appreciably longer than one day. The zonal averaging allows the value of a dependent variable at any longitude to be expressed as the sum of its zonal average and the deviation from its zonal average. The former is usually referred to as pertaining to the "circulation," and the latter to the "eddy," or large-scale, two-dimensional turbulent motion. Since longitude and time are independent variables of the atmospheric motion, a time-average of a dependent variable at a given longitude also yields two components, i.e., the long-term time average (monthly, seasonal, or annual) or "standing" motion and its deviation from the long-term time average or "transient" motion. A dependent variable at any longitude and time is then expressible by the sum of four components: the standing and transient circulations and the standing and transient eddy motions. Thus, the meridional wind  $v$ , for example, is given by

$$v = [\bar{v}] + [v]' + \bar{v}^* + v^{*'}$$

---

\* Another specie of interest is carbon dioxide. However, since carbon dioxide is well mixed with air, its mixing ratio ( $3 \times 10^{-4}$ ) is constant.

where the bracket, star, bar, and prime denote, respectively, the zonal average, eddy, time average, and transient components. Typical examples of these types of motion are as follows (Lorenz, 1967):

1. Trade winds at low latitudes for the standing circulation.
2. Asiatic summer and winter monsoons, or features in addition to those of the standing circulation which appear when the variables are averaged with respect to time alone.
3. Fluctuations of the zonal index, or features, in addition to those of the standing circulation which appear when the variables are averaged with respect to longitude alone.
4. Migratory cyclones, or features, in addition to those of the standing circulation which appear when the variables are not averaged.

The long-term zonal average of the poleward transport of any quantity  $X$  (where  $X$  denotes any quantity such as a velocity component, temperature, specific humidity, etc.) may then be resolved into the amounts accomplished by the separate components of  $v$ , i.e.,

$$[\overline{Xv}] = [\bar{X}][\bar{v}] + \overline{[X]'[v]'} + [\bar{X}^*\bar{v}^*] + \overline{[X^*]'[v^*]'}$$

The terms at the right-hand side then represent, respectively, the standing circulation or cell transport, transient cell transport, standing eddy transport, and the transient eddy transport.

The foregoing considerations emphasize general characteristics of atmospheric and planetary phenomena that are relevant to the formulation of a theory of the general circulation for climate applications. The specific description of the key processes that control the climate at the earth's surface involves two distinct but coupled types of phenomena:

1. The net heating rate of the atmosphere, which is a result of the following four processes:

- a. Absorption of long-wave terrestrial radiation mainly by water and carbon dioxide in the troposphere.
  - b. Absorption of short-wave solar radiation mainly by oxygen and ozone in the stratosphere; the absorption of solar radiation by these species is relatively small, and the atmosphere as a whole may be assumed to be transparent to the short-wave solar radiation (Charney, 1959).
  - c. Condensation of water vapor mainly in the troposphere.
  - d. Flux of sensible heat from the earth's surface transported by small-scale, three-dimensional turbulence in the surface boundary layer or layer extending from the earth's surface to an altitude of about 1 km.
2. Large-scale poleward transports of angular momentum, sensible heat, and water vapor by the transient and standing eddy motion at the middle and upper levels of the troposphere; this motion is triggered by the net heating rate of the troposphere. The large-scale transports of angular momentum and sensible heat by the eddy motion then set up the dynamics of the general circulation in distinct cells of meridional circulation of a statistical nature.

Each of these two types of phenomena is described below in more detail.

#### A. NET HEATING RATE OF THE ATMOSPHERE

The absorption of long-wave terrestrial radiation and short-wave solar radiation by water, carbon dioxide, oxygen, and ozone is controlled by the absorptivity of these species as a function of wavelength (their spectra are shown, for example, in Miller-Thompson, 1970). The condensation of water vapor is coupled with the dynamics of the circulation and eddy motions in the troposphere (Smagorinsky, 1963), while the transport of sensible heat in the surface boundary layer is governed by the appropriate energy equation. The instability of the system is controlled by the Richardson number, i.e., a criterion

that expresses the relative role of the buoyancy and wind shear in three-dimensional turbulence (e.g., Hidalgo, 1970; Monin, 1970). A parameterization of these complex phenomena has been given by Smagorinsky (1963), using previous theoretical and experimental results by Phillips (1956), Charney (1959), Houghton (1954), Budyko (1956), and London (1957).

This parameterization is based on long-term (annual) zonal averages of the relevant parameters and is described schematically in Fig. 1, which shows three altitude or pressure levels at any given latitude: (1) top of the atmosphere; (2) the atmosphere, as represented by a column with a mean temperature corresponding to the 500-mb pressure level or altitude of about 5.6 km for a standard atmosphere; and (3) the earth's surface.

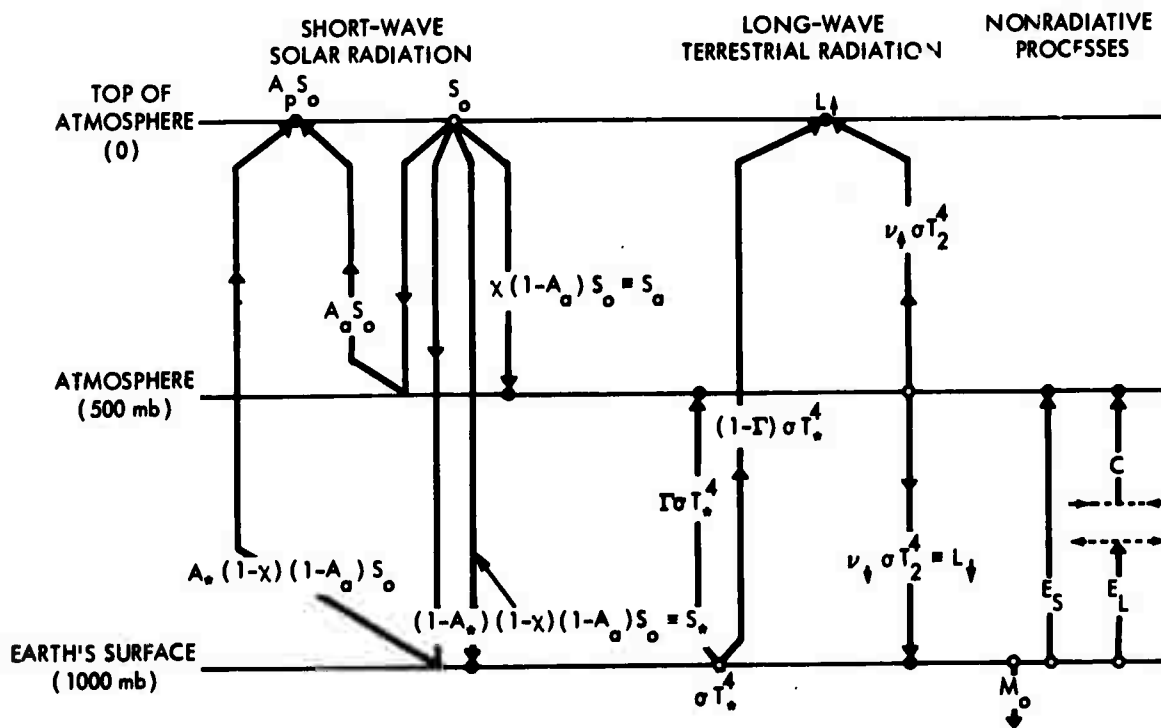


FIGURE 1. Schematic Diagram of the Processes Contributing to the Heat Balance in the Troposphere (Smagorinsky, 1963)

Figure 1 is self-explanatory; at each level, open circles denote either emission or flux divergence and closed circles signify either absorption or flux convergence. The left side of the figure describes the absorption of short-wave radiation by the atmosphere\* ( $S_a$ ) and earth's surface ( $S_*$ ), where  $S_0$  denotes the solar radiation at the top of the atmosphere,  $A_a$  the albedo (or reflection to space of short-wave radiation) of the atmosphere,  $\chi$  the short-wave absorptivity by oxygen and ozone in the atmospheric column,  $A_*$  the albedo of the earth's surface, and  $A_p$  the planetary albedo. The middle of the figure describes the emission and absorption of long-wave terrestrial radiation, where  $T_*$  denotes the temperature at the earth's surface,  $\sigma$  the Stephan-Boltzmann constant,  $\Gamma$  the long-wave absorptivity by the water and carbon dioxide in the atmospheric column, and the empirical parameters  $v^{\uparrow}$  and  $v^{\downarrow}$  pertain to the upward and downward fluxes of radiation, respectively. The figure indicates that the earth's surface absorbs and emits as a blackbody, while the atmosphere absorbs and emits as a gray body. Finally, the right-hand side of the figure shows the nonradiative processes.

As shown in Fig. 1, for the earth's surface level, flux divergence of heat in the oceans due to lateral ocean transports is indicated by  $M_o$ , and the flux divergence of both sensible and latent heat due to the eddy transports of temperature and humidity from the earth's surface to the troposphere is indicated by  $E_S$  and  $E_L$ , respectively. At the 500-mb level, the heating of the atmospheric column is indicated by both the condensation of water vapor ( $C$ ) and the heat flux  $E_S$  from the surface boundary layer.

The net average heating rate of the atmospheric column may be defined as  $Q_2$ , i.e.,

$$Q_2 = \frac{1}{p_4} \int_0^{p_4} Q dp = \int_0^1 Q d\left(\frac{p}{p_4}\right)$$

\*The notation  $[\ ]$  has been dropped to simplify this figure.

where  $Q$  is the net heating rate at any pressure level, and the limits of integration correspond to the top of the atmosphere ( $p = 0$ ) and to the earth's surface ( $p = p_4 = 1000$  mb). With this definition and the use of the principle of conservation of energy, the closed and open circles at 500 mb of Fig. 1 yield the net heating rate of the atmospheric column as follows:

$$\frac{p_4 Q_2}{g} = S_a + \Gamma \sigma T_*^4 - \nu \uparrow \sigma T_2^4 - \nu \downarrow \sigma T_2^4 + C + E_S \quad (1)$$

where the terms in the right-hand side are obtained from annual experimental data.

Figure 2 shows the magnitude of each of the terms in Eq. 1 for the current climate, and the rather dominant role of the long-wave radiation terms. If it is assumed that there is no heat accumulation at the earth's surface, the circles corresponding to the earth's surface yield

$$\sigma T_*^4 = S_* + \nu \downarrow \sigma T_2^4 - (E_S + E_L + M_O) \quad (2)$$

i.e., the surface temperature is a function of the short-wave radiation reaching the surface, its albedo, the downward flux of long-wave radiation, and the divergence of the sensible, latent, and oceanic heat fluxes. For the conditions indicated in Fig. 2 for the current climate, the surface and mean atmospheric temperatures vary as a function of latitude in the range  $260 \leq T_* \leq 300^\circ\text{K}$  and  $240 \leq T_2 \leq 270^\circ\text{K}$ . Figure 3 shows the magnitude of each of the terms in Eq. 2 for the current climate, and it is consistent with the annual mean data of the previous figure, i.e., Budyko's experimental values for the lateral oceanic transport  $M_O$  have been reduced by 9.4 to make them consistent with London's data (Smagorinsky, 1963). Figure 3 shows the dominant effect of the long-wave radiation term in the right-hand side of Eq. 2 at all latitudes, and the relatively small magnitude of the oceanic transport  $M_O$ .

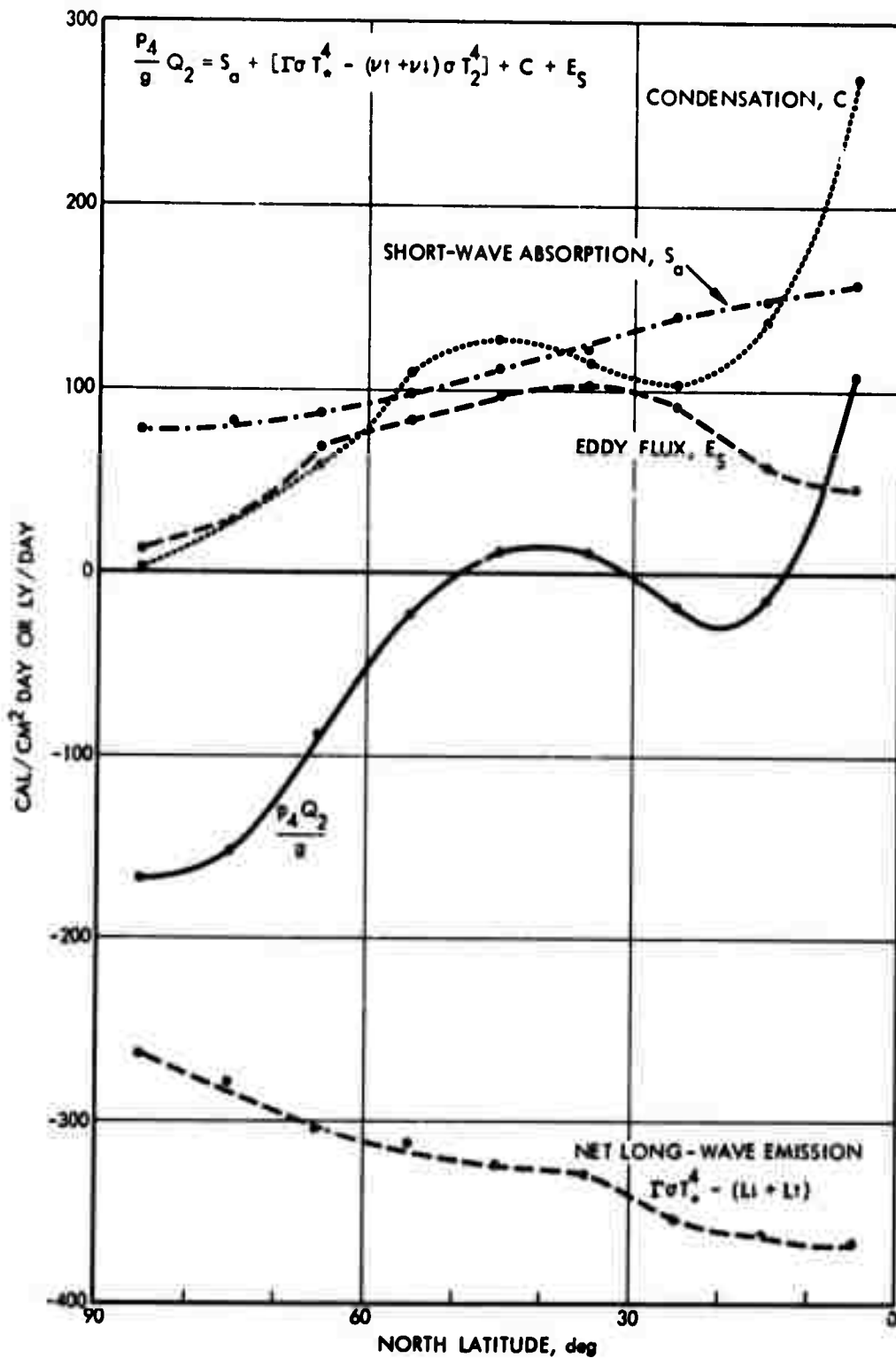


FIGURE 2. Net Heating Rate Per Unit Area of a Column,  $p_4 Q_2/g$ , Based on Annual Mean Data (Smagorinsky, 1963)

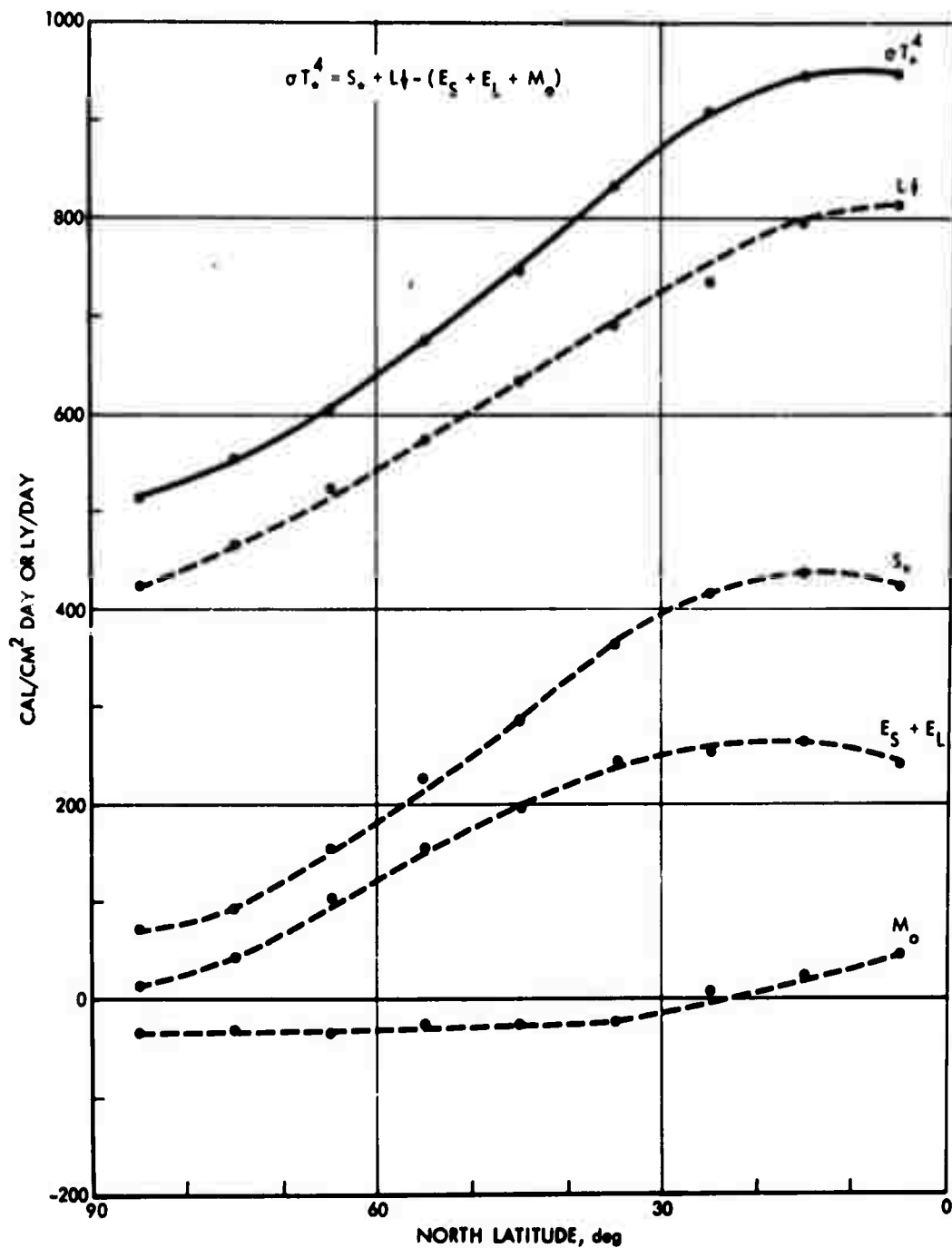


FIGURE 3. Contribution to Earth's Surface Temperature ( $T_e$ ) of Long-Wave Downward Radiation ( $L\downarrow$ ), Short-Wave Radiation ( $S_e$ ), Flux Divergence of Heat Due to Eddy Transports of Sensible and Latent Heat ( $E_s + E_l$ ) and Lateral Oceanic Transport ( $M_o$ )

## B. LARGE-SCALE POLEWARD TRANSPORTS

The turbulent nature of the eddy motion triggered by the net heating rates of the troposphere is demonstrated by the longitudinal spectrum of kinetic energy at synoptic wavelengths. Figure 4 shows the spectral distribution of large-scale atmospheric kinetic energy as a function of pressure level and latitude (Julian et al., 1970). The kinetic energy spectrum is defined as the portion of the spectrum arising from stochastic transient motion on all scales, and it is derived from both reduced wind data and untreated observed winds. The hemispheric wave number ( $k$ ) denotes the number of wavelengths ( $\lambda$ ) in a latitudinal circle with radius  $a \cdot \cos \theta$ , where  $a$  is the radius of the earth and  $\theta$  the latitude of the circle, i.e.,

$$k = \frac{2\pi a \cos \theta}{\lambda}$$

Thus, large wavelengths or large-scale phenomena correspond to small wave numbers. The kinetic energy in Fig. 4 has been normalized with respect to its value at  $k = 6$ . The two-dimensional character of the turbulent motion in the troposphere is indicated in Fig. 4 by the spectral slope at the higher wave numbers; i.e., all estimates of the spectrum suggest that the spectral slope in the 3500- to 1500-km wavelength region can be represented by a power law with an exponent in the range -2.7 to -3.0, which is different than the  $-5/3$  value for three-dimensional or isotropic turbulence at very small wavelengths. The two-dimensional nature of the turbulence at the high wave numbers becomes important for considerations of the theoretical limit on long-range weather forecasting, which is estimated to be at most no more than a few weeks. For climate, however, the interest is on large-scale phenomena or low wave numbers, since a theoretical solution of barotropic atmospheric motion (involving the use of the momentum and continuity equations) and a homogeneous earth indicate that the wave number for a large-scale stationary disturbance is given by (Haurwitz, 1940)

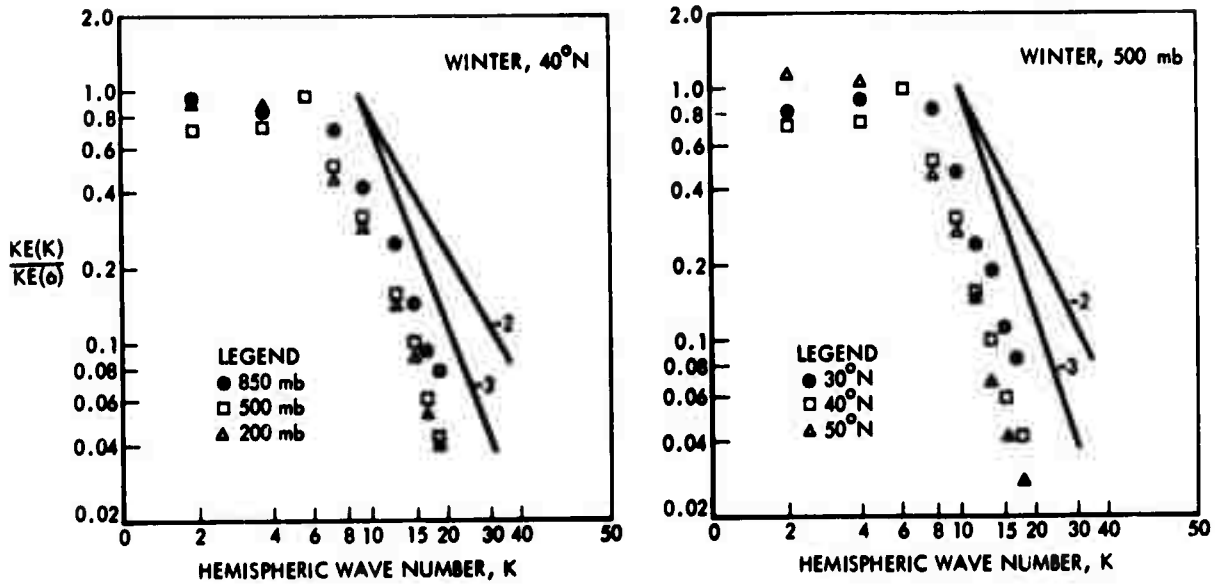


FIGURE 4. Spectral Distribution of Large-Scale Atmospheric Kinetic Energy as a Function of Altitude and Latitude (Julian et al., 1970)

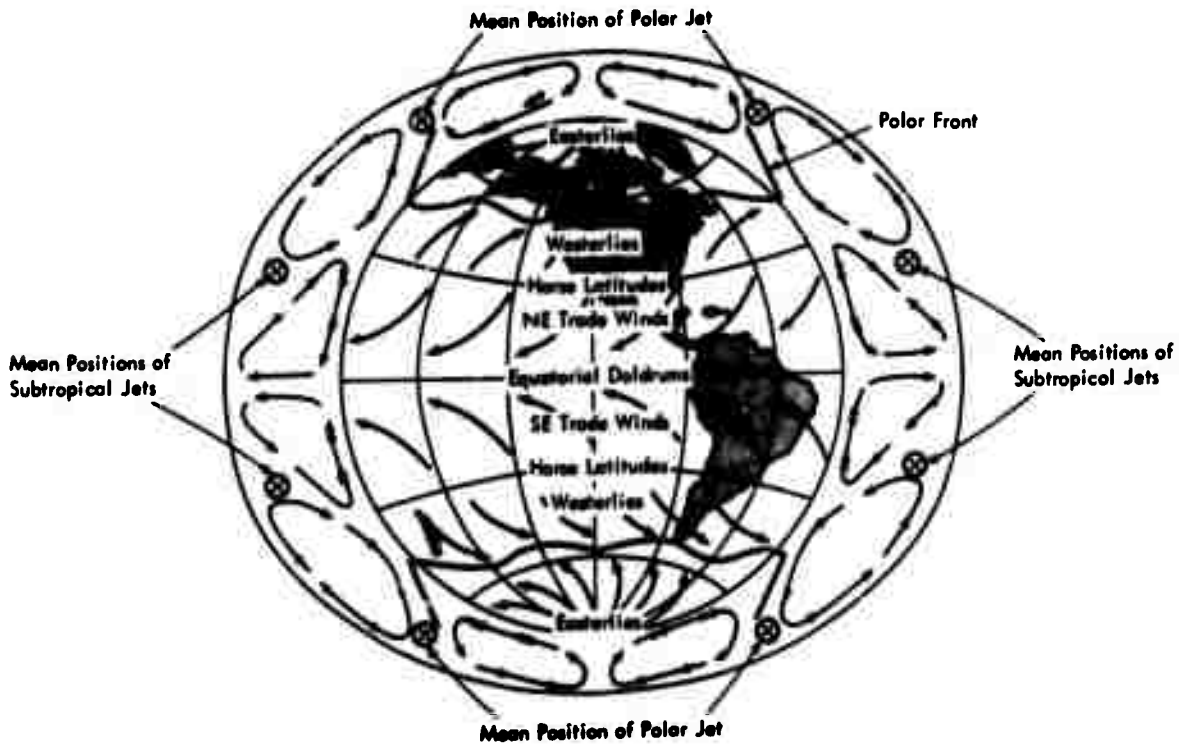


FIGURE 5. Schematic Representation of the General Circulation within the Troposphere for Current Climate (Miller & Thompson, 1970)

$$k = \sqrt{\frac{2\Omega a \cos \theta}{[\bar{u}]}}$$

where  $[\bar{u}]$  denotes the standing zonal circulation. For example, this barotropic solution yields  $k \approx 6$  when  $[\bar{u}] = 20$  m/sec at 45-deg latitude. As shown later, the effect of baroclinic disturbances (where the energy equation is used together with the momentum and continuity equations) and a nonhomogeneous earth's surface (as given by the distribution of oceans and continents) may yield a wave number appropriate for climate that is even lower than the above barotropic value. A fundamental difference of interest for climate between large-scale two-dimensional turbulence at very low wave numbers, and small-scale three-dimensional turbulence at very high wave numbers, is the fact that the transports by the former can be countergradient, i.e., the usual concepts of eddy viscosity for very small or microscale turbulence cannot be extended to the large-scale transports. The eddy viscosity or mixing-length concepts in microturbulence assume that the transports are given by the product of an eddy viscosity and the gradient of the average flow. This assumption breaks down for the large-scale transport of angular momentum at middle and high latitudes, for example, since at these latitudes the transport is positive while the latitudinal gradient of the average flow (i.e.,  $d[\bar{u}]/d\theta$ ) is negative. Since this transport and the gradient  $d[\bar{u}]/d\theta$  remain both positive at lower latitudes, even a concept of a "negative" eddy viscosity becomes unapplicable at any arbitrary latitude.

The organization of general circulation dynamics into distinct cells by the large-scale transports of angular momentum and sensible heat is illustrated in Fig. 5 for the current climate. The figure shows three meridional cells: (1) the direct Hadley cell, where humid air ascends near the equator and dry air descends near the Horse latitude; (2) the indirect Ferrel cell, where dry air descends near the Horse latitude and moist air ascends at the higher latitude; and (3) the polar cell at the high latitudes. The Hadley cell is controlled by the poleward large-scale transport of angular momentum, which reaches

a maximum at a latitude of about 30 deg and near the 250-mb pressure level (e.g., see Lorenz, 1967) or at an altitude of about 10 km for a standard atmosphere, an altitude that corresponds to that of the jet streams. The convergence of the eddy transports of angular momentum acts as a mechanical force, which induces the downward motion of the meridional cells at the 30-deg latitude. Similarly, the transport of sensible heat reaches its maximum value near the 50-deg latitude; the convergence of the eddy transport of sensible heat acts as a heat source, which induces the upward motion of the indirect Ferrel and polar cells near that latitude. The opposite directions of the meridional winds in the lower branches of the Hadley and Ferrel cells, together with the effect of the Coriolis acceleration ( $-2\vec{\Omega} \times [\vec{v}]$ ) from the earth's rotation ( $\vec{\Omega}$ ), control the direction of the zonally averaged standing winds at the earth's surface, which are as shown in Fig. 5.

Figure 6 shows the annual average precipitation and evaporation as a function of latitude for the current climate. Precipitation reaches a maximum near the equator or the ascending branch of the direct Hadley cell in the northern hemisphere. This maximum precipitation yields a corresponding maximum at the same latitude in the net heating of the troposphere by the condensation process (i.e., as implied in Fig. 2). Figure 6 also shows that the precipitation reaches a second peak near 50 deg or near the latitude of the ascending branch of the Ferrel cell. Figure 2 again indicates a corresponding second peak at the same latitude in the net heating by condensation. The maximum in precipitation near the equator, where the NE and SE surface winds converge (Fig. 5), is referred to as the intertropical convergence zone (ITCZ) or equatorial doldrums. Note that Fig. 6 does not show a double ITCZ across the equator, as would be expected from the Hadley cells in each hemisphere (Fig. 5). A numerical model based on a troposphere interacting with the oceans has been successful in reproducing the single ITCZ north of the equator (Pike, 1970).

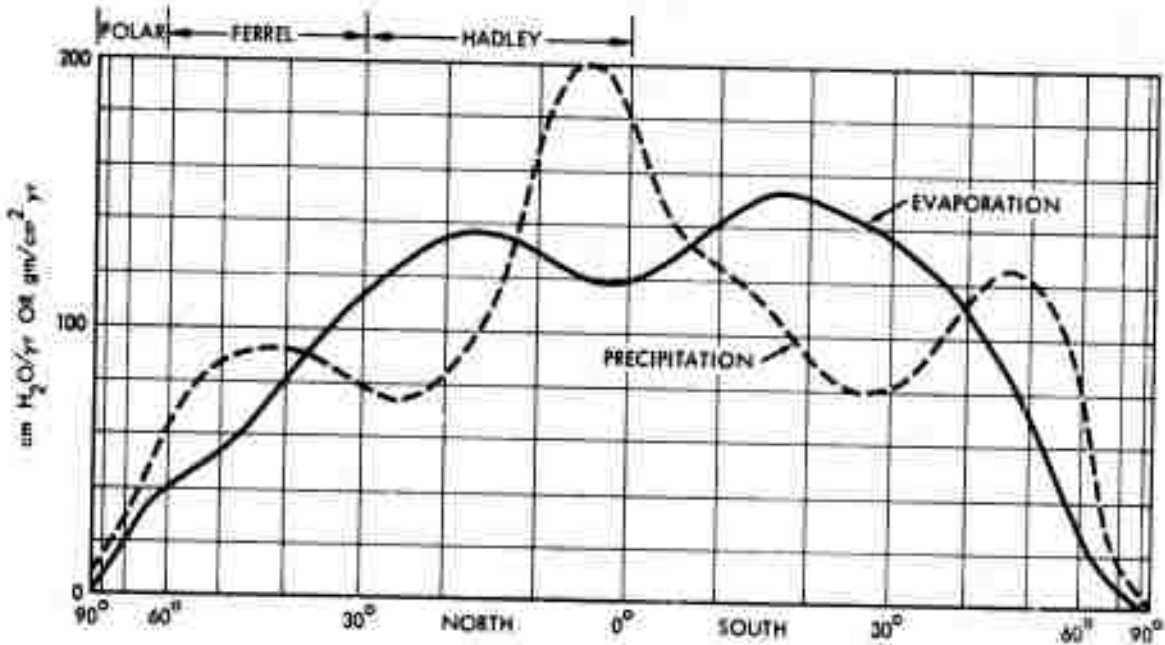
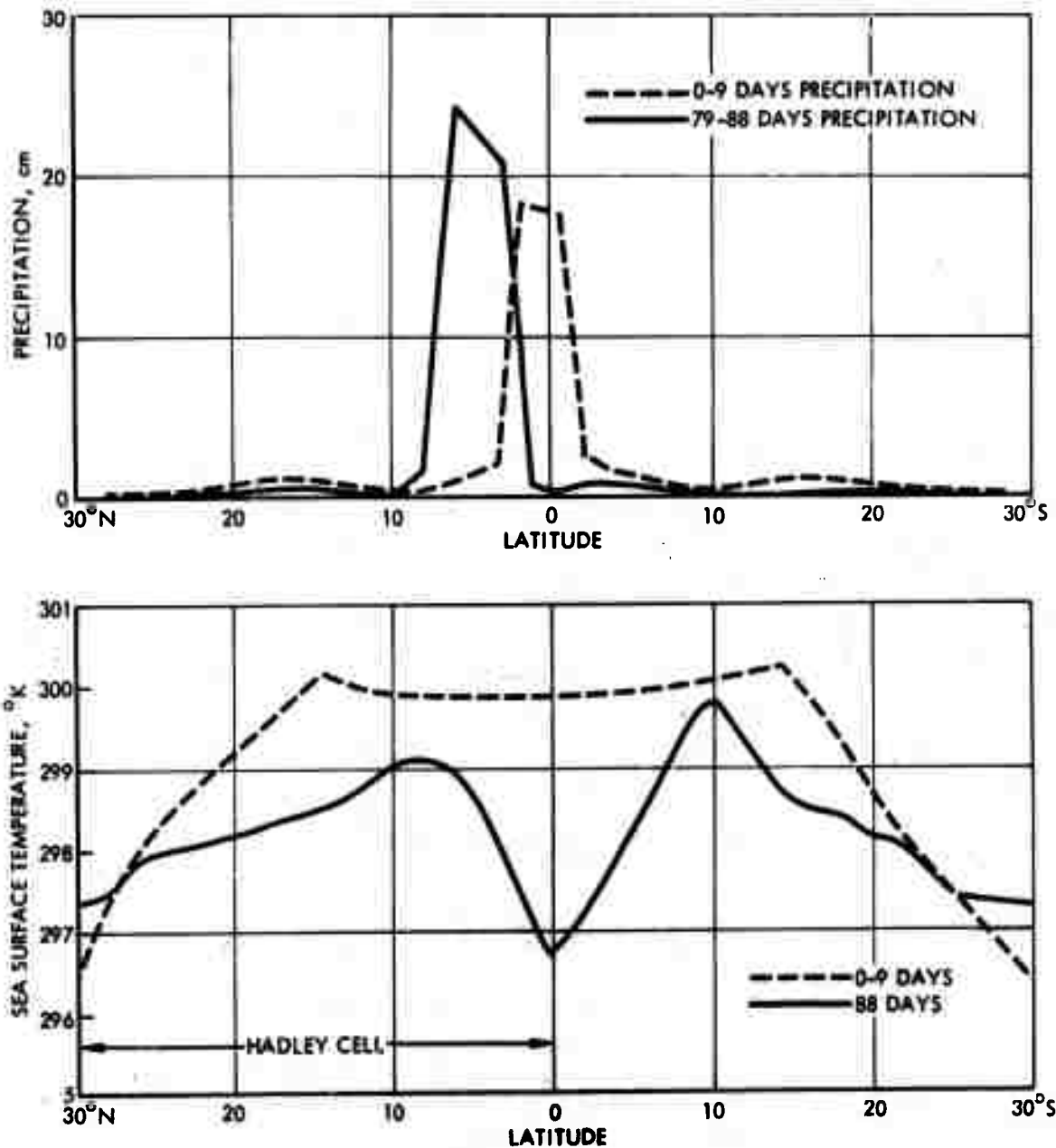


FIGURE 6. Average Annual Evaporation and Precipitation (Lorenz, 1967)

Figure 7 shows results from this model for the precipitation and ocean surface temperature as a function of time during the 88 days used in these calculations. The dashed lines show the ITCZ and the temperature during the first nine days, when the ocean's surface temperature remains constant; these lines show a single ITCZ, which remains fixed almost at the equator. The westward surface winds induce a westward sea current at the equator, while the Coriolis acceleration produces poleward (i.e., opposite) meridional sea currents in each hemisphere at the equator. The result is an entrainment of deeper, colder water at the equator; in these calculations, this effect starts to cool the sea surface temperature after the ninth day, and it becomes about 3 deg colder after 88 days (Fig. 7). As the temperature starts to cool after the ninth day, the ITCZ moves northward slowly; after 88 days it reaches 6 deg N over a predicted surface temperature maximum. Again, the model does not yield a split, in the ITCZ, into two parts, each centered over a temperature maximum. Satellite data for 1965 through 1967 indicate that the zonal average of the latitude

of maximum cloudiness (which may be associated with the maximum of precipitation) in the tropics is 5 deg N (Sadler, 1969; Kornfield and Hasler, 1969). Thus, the idea that a single ITCZ is more stable than a double ITCZ is encouraged by both theory and experiment.



**FIGURE 7. Characteristics of the Intertropical Convergence Zone (ITCZ) as Determined Numerically from an Interacting Atmosphere and Ocean Model (Pike, 1970)**

The foregoing considerations indicate that, for the current climate, the Hadley cell controls tropical meteorological phenomena, while the Ferrel and polar cells control these phenomena at the middle and high latitudes. This implies that it may be feasible to decouple tropical phenomena from considerations of the effect of advertent climate modification at the middle and high latitudes on the structure of the current Ferrel and polar cells.

The description of the key processes controlling the current climate at the earth's surface identifies the phenomena of large-scale, two-dimensional turbulence at the middle and upper levels of the troposphere as being of fundamental importance. Such phenomena control the latitudinal variation of the mean tropospheric temperature ( $T_2$ ) through the large-scale transport of sensible heat, the current configuration of the three cells in the troposphere, and therefore, the distribution of specific humidity. The mean tropospheric temperature and humidity control the downward flux of long-wave radiation (i.e.,  $\nu \downarrow \sigma T_2^4$ , Eq. 2), which has a dominant effect on the other basic variable of advertent climate modification, i.e.,  $T_*(\theta)$ , as shown in Fig. 3.

#### IV. PREDICTABILITY OF THE CLIMATE AT THE EARTH'S SURFACE

As shown later, the parameterization of the net heating rates of the troposphere (i.e., Eq. 1) can be used, together with the conservation equations and the characteristics of large-scale wave phenomena, to determine the statistics that control the cell structures of the current long-term general circulation. These statistics are, for example, the annual, large-scale transports of angular momentum (at 250 mb), sensible heat and humidity (at 500 mb), as well as the annual meridional and zonal kinetic energies and circulations. This mathematical description of the key processes becomes a model that may be used for predicting changes in the long-term, zonal averages of the surface temperature,  $T_*(\theta)$ , and humidity from advertent (or inadvertent for that matter) climate modifications. The second basic subquestion identified earlier arises then from considerations of the uniqueness (or lack of it) of the predicted  $T_*(\theta)$  that is derived, for example, from such a nonlinear mathematical model.

There are two different aspects concerning the general question of the predictability of tropospheric phenomena. One is short-term, relevant to the transient phenomena of interest for weather forecasting (e.g., Thompson, 1957; Smagorinsky, 1963; Lorenz, 1968; etc.). The other is long-term, relevant to the statistical properties of the state of the troposphere of interest for climate (e.g., Lorenz, 1967, 1968, 1970). The former is concerned with the effect of error magnitude in the initial conditions on the results of short-term numerical integrations of the conservation equations. The latter inquires into the uniqueness of the long-term statistics of the solutions. For climate, then, the nonlinear models describing the key processes can be either (1) transitive, which yield for a given set of

conditions only one set of long-term statistics or one climate; and (2) intransitive, which yield again for a given set of conditions two or more sets of statistics; consequently, each set of statistics becomes an alternative, physically possible climate. Since there is no criterion based on physical law for the selection of only one of these alternative climates, it is not currently known whether the atmosphere-ocean-earth system is transitive or intransitive. In this regard, it is of theoretical interest to consider the following example of an intransitive nonlinear equation, which is a crude approximation of the climates description, i.e.,  $T_*(\theta)$ , at the earth's surface.

The first law of thermodynamics may be applied to a control volume (e.g., Shapiro, 1953) for the earth-atmosphere-ocean system, i.e., a volume defined at a latitudinal circle by an area element  $2\pi a^2 \cos \theta d\theta$  on the earth's surface and a unit height of the planetary boundary layer. For quasi-steady conditions, the net flux of energy normal to the earth's surface must equal the net poleward flow of energy ( $\sum \rho_i v_i e_i$ ) across the area  $2\pi a \cos \theta \cdot 1$ ; hence, using the notation of Fig. 1, one obtains (Faegre, 1972):

$$\frac{1}{a \cos \theta} \frac{d}{d\theta} \left( \sum_{i=1}^3 \rho_i v_i e_i \right) \cos \theta = S_0 (1 - A_p) - L_t \quad (3)$$

The poleward flow of energy consists of three components: the transports of sensible and latent heat in the atmosphere and the transport of sensible heat in the top layer of the ocean. Recalling that there is no net flux of energy in a normal direction at the earth's surface (i.e., Eq. 2), the right-hand side of Eq. 3 denotes the net energy flux per unit area at the top of the atmosphere.\* By using the crude assumptions that  $L_t = K\sigma T_*^4$ , and that each of the three energy terms in the left-hand side of Eq. 3 is proportional to  $dT_*/d\theta$ , Eq. 3 becomes

---

\* An alternative method to derive Eq. 3 is the use of a procedure similar to that of Eq. 6.

a second-order, ordinary, nonlinear differential equation for describing the climate at the earth's surface through  $T_*(\theta)$ . The two required boundary conditions must specify that there is no energy flow off either pole, i.e.,  $dT_*/d\theta \rightarrow 0$  as  $\theta$  approaches 90 deg N and 90 deg S.

Figure 8 shows the results of numerical integrations of Eq. 3 using present values of the parameters in this model; the figure shows that there are five solutions to Eq. 3, or five climates. The solid line corresponds to the present climate, the higher dashed line to a climate that might correspond to that of an ice age, the lower dashed line to a climate for an ice-covered earth, and the two dotted lines to physically unidentifiable climates. The two assumptions used in Eq. 3 have a major impact on these solutions, i.e., (1) if  $L\uparrow$  is formulated with a constant value of  $K$  corresponding to the appropriate average value with latitude, the two dotted solutions in Fig. 8 disappear; and (2) if the formulation of the transports are modified to include effects of the meridional circulations, then the model using a variable  $K$  becomes transitive and similar to other crude models for the climate at the earth's surface (i.e., Budyko, 1969, 1970; Sellers, 1969, 1970). Thus, the transitive or intransitive nature of a model becomes sensitive to the built-in structure of such a nonlinear model. Stated in another way, the use of a most accurate structure in a nonlinear model becomes a necessary, but not sufficient, condition for defining either its transitive or intransitive nature. In the absence of ergodic criteria to eliminate all but one of the multiple solutions for a given set of conditions, the transitive or intransitive nature of a nonlinear model with a most accurate structure must depend on the results from investigations aimed at showing an absence of more than one solution.

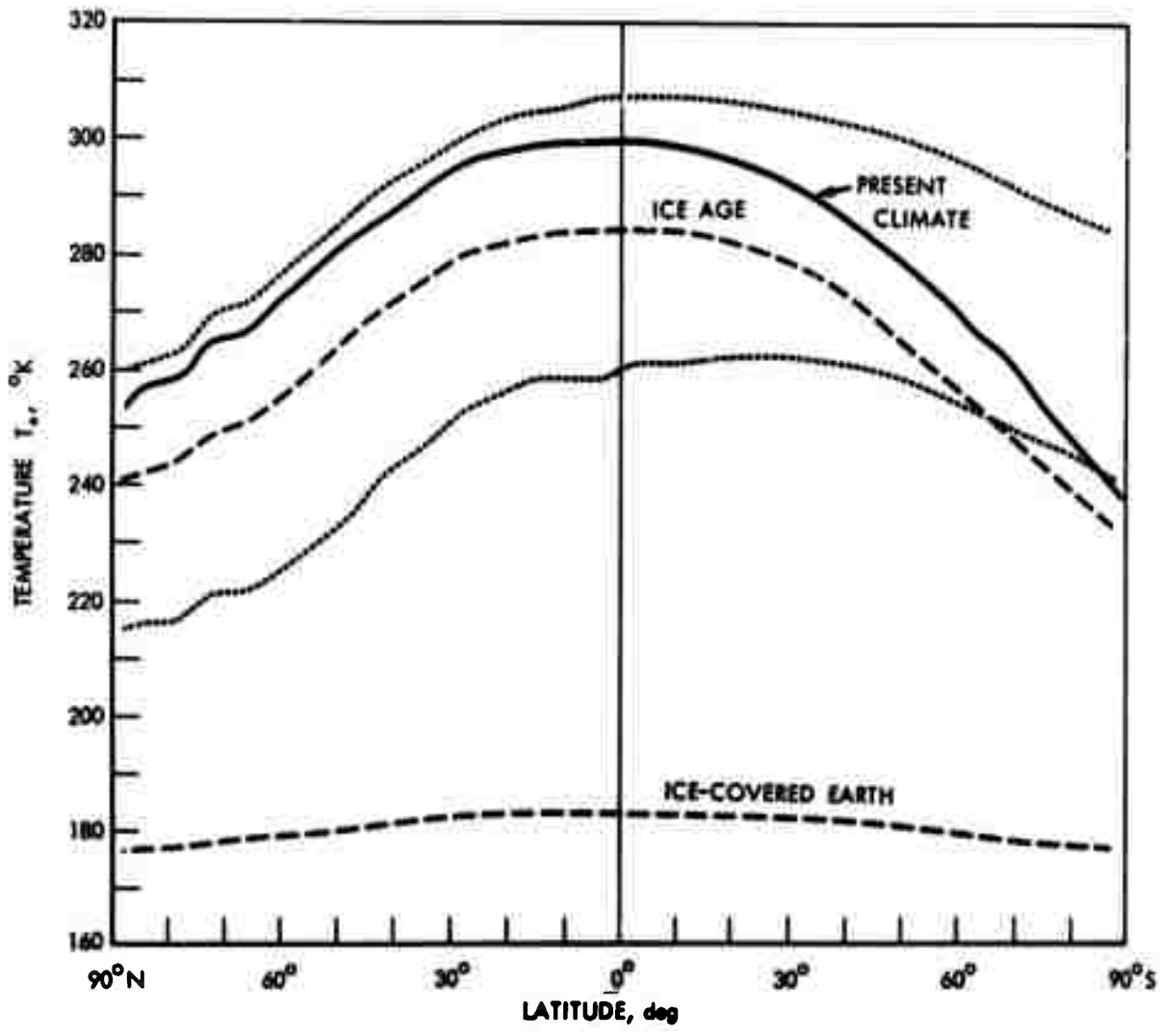


FIGURE 8. Surface Temperature as a Function of Latitude Predicted from the Same Mathematical Formulation, Eq. 3 (Faegre, 1972)

## V. CHARACTERISTICS OF THE CLIMATES OF THE PLEISTOCENE EPOCH

The transitive or intransitive nature of nonlinear models for describing changes of climate at the earth's surface leads to an interest in the main characteristics of the two extreme types of climate which have existed from the time the earth acquired its current geographical distribution of oceans and continents, i.e., the major glacial-interglacial cycles of climate and atmospheric circulation of the current Pleistocene Epoch. The problem of the changes from interglacial to glacial climates is different from that of advertent or inadvertent climate modifications. This is because the former has an additional degree of freedom through the variable magnitude of the incoming solar radiation,  $S_0(\theta)$ , as caused by changes in both solar and earth's orbital characteristics over extremely long times. Nevertheless, the characteristics of the deduced general circulations corresponding to the glacial and interglacial extremes may be used to test the transitive or intransitive nature of a model that describes the current climate accurately and uniquely. This test would involve an evaluation of the capability of the model to reproduce transitively the coupling between the deduced cell structure of the general circulation and the net heating of the troposphere under glacial or interglacial conditions. Note that such a test would avoid the difficult problem concerning a prediction of the net heating of the troposphere under glacial conditions, i.e., the rather controversial predictions of the onset and recess of ice-age phenomena (e.g., Mitchell, 1968; MacCracken, 1969; Schell, 1971).

The end of the most recent (Würm) major glacial period of the Pleistocene Epoch is usually placed at approximately 6500 B.C. It was the time at which the ice boundaries and climate conditions in

Europe had returned essentially to those of today. The probable main characteristics of the general circulation and climate during the Pleistocene glacial-interglacial cycles have been deduced from geological evidence (e.g., Willett, 1953). These characteristics indicate that the statistical cell structure of the meridional circulation (i.e., Fig. 5) persists even under the extremes of the minimum and maximum glaciations of the Pleistocene Epoch. The available evidence indicates that these major glacial-interglacial cycles are in phase rather than in opposition in the earth's northern and southern hemispheres. The general circulation for the conditions of minimum and maximum glaciation is characterized, respectively, by two and three meridional cells, i.e., by the configuration of the polar cell, which disappears for minimum glaciation but for maximum glaciation extends equatorward by about 15 deg from the latitude of its current ascending branch (e.g., Figs. 5, 6). Thus, for minimum glaciation, the surface easterlies at high latitudes disappear with the polar cell, while the westerlies of the Ferrel cell expand poleward to the poles. The poleward expansion of the westerlies induces a poleward expansion of the Hadley cell, i.e., the latitude of the descending branches of the Ferrel and Hadley cells increases from its current value. Conversely, for maximum glaciation, the easterlies of the polar cell are displaced towards the equator; this effect induces a displacement of the descending branch of the Hadley cell to latitudes lower than the current value. For conditions of maximum glaciation, the Hadley cell is characterized by an ITCZ that is stronger than the current maximum precipitation near the equator.

The climate corresponding to the two- and three-cell structures of the minimum and maximum glaciations is as follows:

1. For interglacial conditions, the ascending branch of the Ferrel cell at the poles yields an increase of warmth and precipitation relative to current values at the polar latitudes; the result is an absence of permanent glaciation on the earth's surface at these high latitudes and a displacement of the cyclonic storminess of middle latitudes into the

higher latitudes. The poleward displacement of the descending branches of the Ferrel and Hadley cells shifts the current subtropical high-pressure belts to the middle latitudes; this condition yields a generally settled, mild, storm-free climate at these latitudes. The disappearance of the easterlies at high latitudes and the poleward displacement of the westerlies produce a relaxation of the overall circulation and a decrease in the intensity of the condensation cycle.

2. For glacial conditions, the equatorward displacement of the ascending branches of the polar and Ferrel cells, coupled with a marked acceleration of the condensation cycle, sustains the precipitation of higher middle latitudes that builds the ice sheets; the current storm tracks of middle latitude are displaced to lower latitudes, and they exhibit increased storminess from the increased intensity of the circulation in the Ferrel cell. The acceleration of the condensation cycle becomes evident from the precipitation of higher middle latitudes, the extremely pluvial conditions that prevail in the lower middle latitudes, and the greatly increased rainfalls at the ITCZ.

Finally, the climate, as characterized by the mean annual surface temperature  $T_*(\theta)$ , for the current climate and corresponding temperatures for the interglacial and glacial conditions, is as given in Table 1 (Schell, 1961; Fairbridge, 1961).

TABLE 1.  $T_*(\theta)$  FOR DIFFERENT CLIMATES

Latitude	Present	Interglacial	Glacial
80°-90°N	-19°C	0°C	-70°C
40°-60°N	10	13	2
0°-20°N	26	27	23
80°-90°S	-49	-30	-110

Table 1 indicates that the current climate is closer to the interglacial climate of the Pleistocene Epoch. The table also shows a rather small difference between the interglacial and glacial values of  $T_*$  at low latitudes; this difference increases rapidly at the higher latitudes (Bell, 1953) of the expanded polar cell.

The considerations of the glacial-interglacial conditions indicate that the cell structure of the current general circulation, as induced by the large-scale transports of angular momentum and sensible heat, will also prevail under the less drastic conditions of either advertent or inadvertent climate modification. Also, the deduced general circulation for the extreme glacial and interglacial climates of the Pleistocene Epoch can be used to test the transitive or intransitive character of a nonlinear model that relates the cell structure of the general circulation to the net heating of the troposphere.

## VI. SAMPLE OF A POTENTIAL MECHANISM FOR ADVERTENT CLIMATE MODIFICATION

The  $T_*(\theta)$  values at the middle and high latitudes for the interglacial and glacial climates of the Pleistocene Epoch indicate that the climate of the earth's surface at these latitudes is very sensitive to the magnitude of the surface albedo,  $A_*$ . Thus, recalling the third and fourth basic subquestions identified earlier, it is of interest to examine briefly if man has achieved the technological capability to decrease the current high values of  $A_*$  at the high northern latitudes.

Figure 9 compares the magnitude of both the incoming solar radiation and its absorption by the earth's surface and troposphere at low and high latitudes (Budyko, 1966). Even though the solar inclination is low at high latitudes, the length of solar illumination during summers at these latitudes is such that the magnitude of the incoming solar radiation can be greater than that at low latitudes for a significant fraction of each year. However, because of the relatively high value of the surface albedo at the high latitudes, the absorbed short-wave radiation at the earth's surface at these latitudes becomes significantly lower than that at the low latitudes. Thus, a decrease in the surface albedo accomplished by a large-scale removal of the snow and ice at the high latitudes could have a significant effect on the structure of the polar and Ferrel cells at the middle and high latitudes.

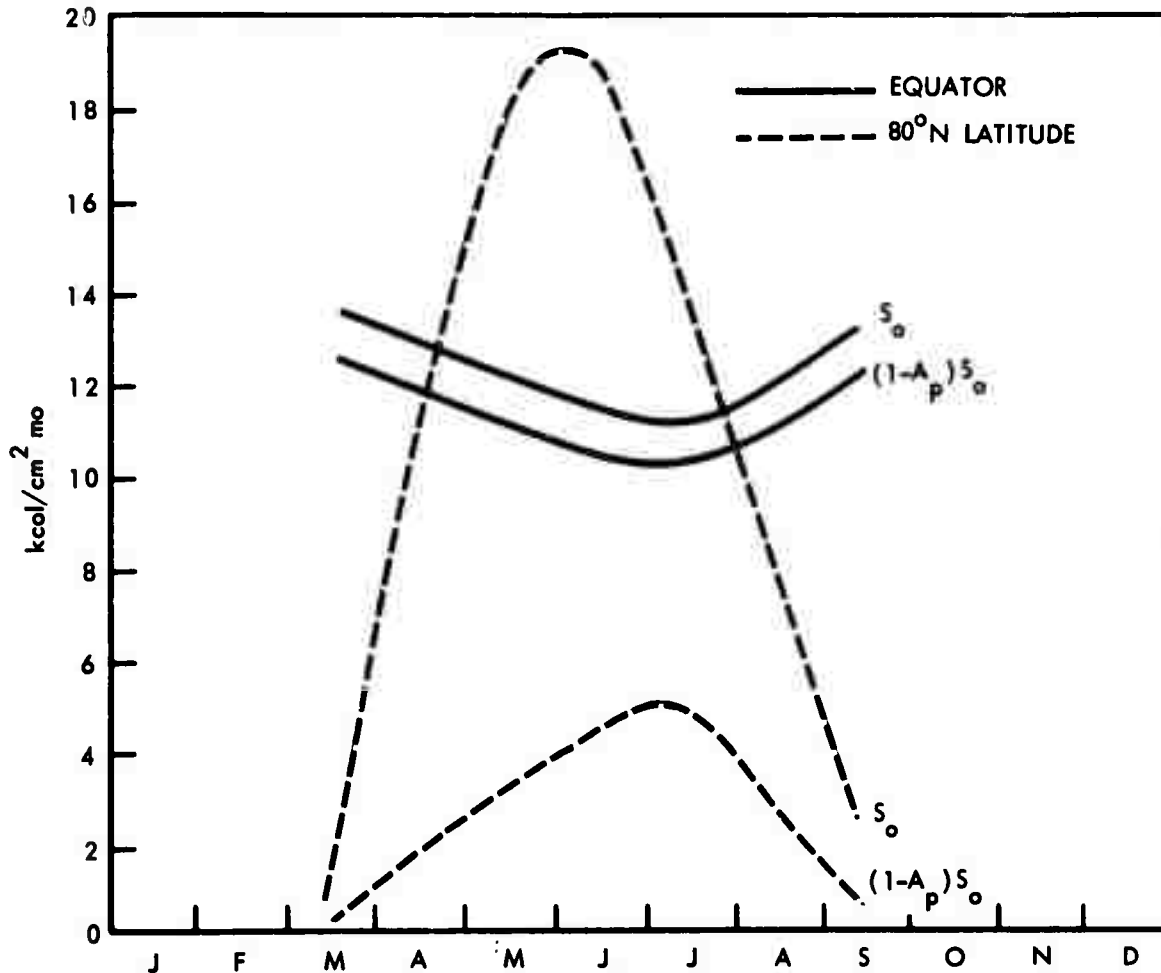


FIGURE 9. Annual Distribution of Incident and Absorbed Solar Radiation at Equator and 80°N Latitude (Budyko, 1966)

The feasibility of large-scale removal of snow and ice at high latitudes has been examined theoretically by using a thermodynamic model of sea ice (Maykut, 1969), since sea ice is a dominant feature of the Arctic Ocean, which covers an area of about  $10^7$  km<sup>2</sup>. This area is about 80 percent ice during the winter and 60 percent in the late summer. Because of the large horizontal dimensions of the surface of the Arctic Ocean relative to the thickness of the ice and snow layers over this surface, the model may consider an infinite, thin slab of ice as existing over the water and an infinite, thin slab of snow as existing over the ice. Thus, the model is reduced to the use of the

one-dimensional heat conduction equation for both the snow and ice layers, with appropriate boundary conditions for each layer. The differential equation for the snow layer is then given by

$$(\rho c)_s \frac{\partial T}{\partial t} = k_s \frac{\partial^2 T}{\partial z^2} \quad (4-a)$$

where  $(k/\rho c)_s$  is the thermal diffusivity for the snow,  $T$  the temperature in the snow layer,  $z$  the vertical coordinate, and  $t$  the time. The differential equation for the sea ice must account for the variability of the thermal diffusivity  $k_i/(\rho c)_i$  from the inclusion of small pockets of salt water entrapped when sea water freezes. Thus, the product of the density and specific heat  $(\rho c)_i$ , and conductivity  $k_i$ , for sea ice may be expressed as

$$(\rho c)_i = (\rho c)_{i,o} + \frac{4100 S_i(z)}{(T - 273)^2}$$

and

$$k_i = k_{i,o} + \frac{0.28 S_i(z)}{T - 273}$$

where the subscript  $i,o$  denotes pure ice and  $S_i$  a known ice salinity profile. Another factor that must be considered in the heat conduction equation for the snow and sea ice layers is the absorption of solar radiation per unit time, per unit volume, at depth  $z$  in the layers. This factor may be expressed by using the extinction coefficient  $\kappa$  as  $\kappa I_0 \exp(-\kappa z)$ , where  $I_0$  denotes the amount of short-wave radiation passing through the surface of the layers. However, for snow, the value of  $\kappa_s$  is large and all the incoming radiation is essentially absorbed in the first few centimeters of the snow layer. For snow-free conditions, the heat conduction equation for the ice layer is then given by

$$(\rho c)_i \frac{\partial T}{\partial t} = k_i \frac{\partial^2 T}{\partial z^2} + \kappa_i I_0 \exp(-\kappa_i z) \quad (4-b)$$

The boundary conditions for Eqs. 4-a and 4-b must allow for the melting of snow and ice at their interface with the atmospheric air, and either melting or accretion of ice at the ice-water interface. Thus, the boundary conditions are as follows:

1. At the snow-air or ice-air interface, the net energy flux is either zero when  $T < 273^\circ\text{K}$ , or equal to the heat required for melting when  $T = 273^\circ\text{K}$ .
2. At the snow-ice interface of the two layers, the heat flux by conduction in the snow side of the interface must be equal to that in the ice side of the interface.
3. At the ice-water interface, the net heat flux from conduction in the ice side of the interface and turbulence from the ocean in the water side of the interface must equal that for either melting or accretion of the ice at this interface.

Since the parameters at the interface with the atmospheric air are prescribed as a function of time (i.e., by their monthly average values), an equilibrium condition is eventually reached where the ice accretion at the ice-water interface balances the ice lost through melting at the ice-air interface. For such an equilibrium condition, the net mass balance for the year is zero, and both the mass changes and temperature profiles will repeat themselves in an annual cycle. The numerical integrations of Eqs. 4-a and 4-b yield two characteristics of the ice layer that are of interest for advertent climate modification: (1) its equilibrium thickness for a specified monthly atmospheric environment during the year; and (2) the time required for a change from one equilibrium condition to another as induced, for example, by a change in the surface albedo.

Figure 10 shows the snow and ice layers over the water for the equilibrium condition deduced from Eqs. 4-a and 4-b for the current atmospheric and oceanic environments. The specified snow layer is

based on experimental data; after the freeze-up in late August, it is assumed to grow in thickness to 30 cm by the end of October and to 40 cm during May. The figure shows no snow during the melt season. The equilibrium thickness of the ice is determined by using arbitrary initial conditions for the temperature and ice thickness in the integration of the equations. This figure shows that the model predicts an average equilibrium ice thickness for the current environments of about 3 m, a value that agrees rather well with measurements from drifting stations on pack ice. There is also good agreement between the monthly calculated and observed surface temperatures, which yield annual values of  $-18.2^{\circ}\text{C}$  and  $-18.6^{\circ}\text{C}$ , respectively.\*

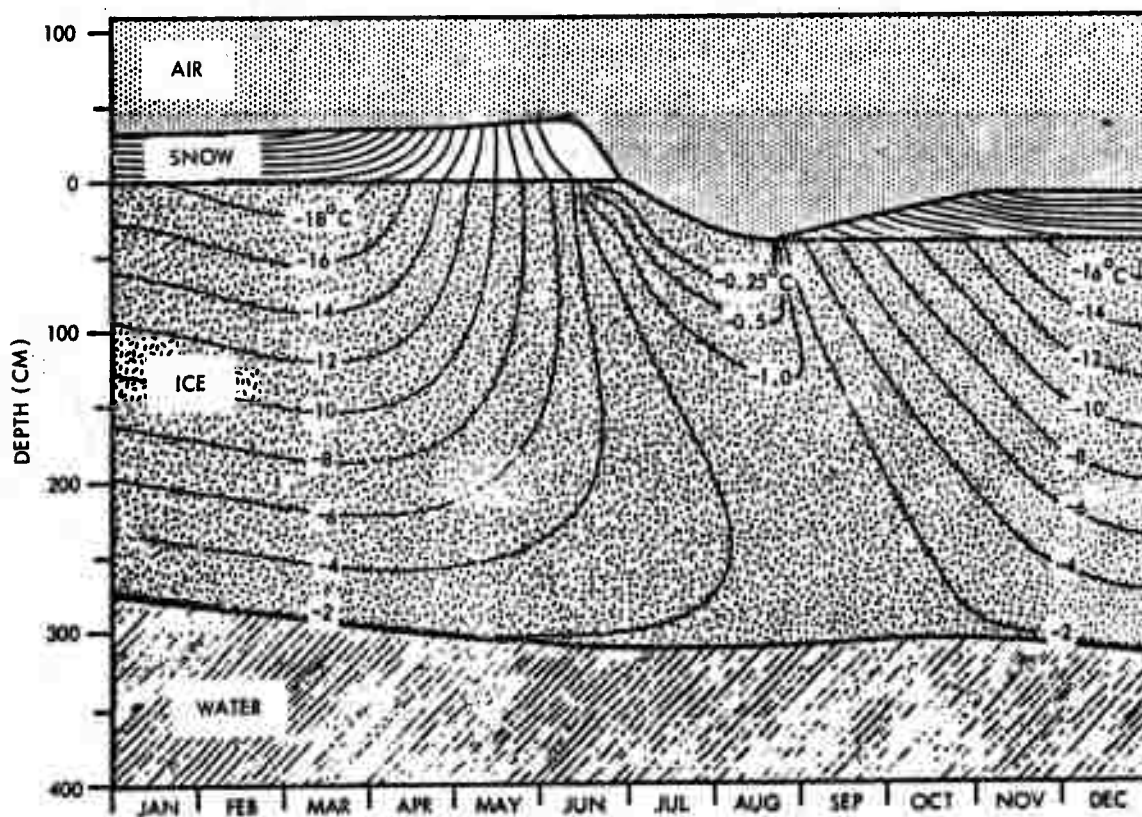


FIGURE 10. Annual Ice Equilibrium Thickness and Temperature Field as Determined from One-Dimensional Transient Thermodynamic Model of Sea Ice (Maykut, 1969)

\* Because of the relatively small thickness of the ice and snow layers, the argument that the melting of the ice and snow at the poles would flood cities does not apply to the Arctic Ocean.

The model can be used to investigate systematically the relative effect of changes in each variable defining the atmospheric and oceanic environments on the equilibrium ice thickness. Figure 11 shows, for example, the effect on the equilibrium ice thickness of changes in only the oceanic environment, which is defined by a constant heat flux from the ocean throughout the year at the ice-water interface and equals its annual average. It also shows the maximum, average, and minimum equilibrium ice thickness (as exhibited, for example, in Fig. 10) as the magnitude of the oceanic heat flux is varied parametrically between 0 and  $4.5 \text{ kcal/cm}^2 \text{ year}$ . As indicated by the figure, the equilibrium ice thickness would almost double its current value if the oceanic heat flux would vanish; the numerical results also indicate that the ice would vanish when the oceanic heat flux is increased to about 5 to  $6 \text{ kcal/cm}^2 \text{ year}$ . The relative results in Fig. 11 are useful when attempting to evaluate the merit of inducing warmer water into the Arctic for the purpose of large-scale ice removal. However, systematic investigations with this model indicate that the equilibrium ice thickness is most sensitive to the magnitude of the surface albedo. These investigations indicate the following results: (1) if the current atmospheric and oceanic environments are kept unchanged except for a 10 percent reduction in the surface albedo during June 1 to the onset of the snow only (Fig. 10), the equilibrium ice thickness is reduced to about 1 m or 1/3 of its current value; and (2) if the surface albedo is reduced by 20 percent instead of the 10 percent in the previous case, the ice vanishes during the summer of the third year. Since measurements from high towers, and calculations using satellite data, indicate a large-scale average of about 0.5 for the summer surface albedo, these relative results suggest that the use, over the Arctic surface, of a suitable material (i.e., lighter than water, slowly soluble in water, nontoxic, etc.), dark enough to yield a

large-scale summer albedo of about 0.4, would eliminate the ice layer over the Arctic within very few years.\*

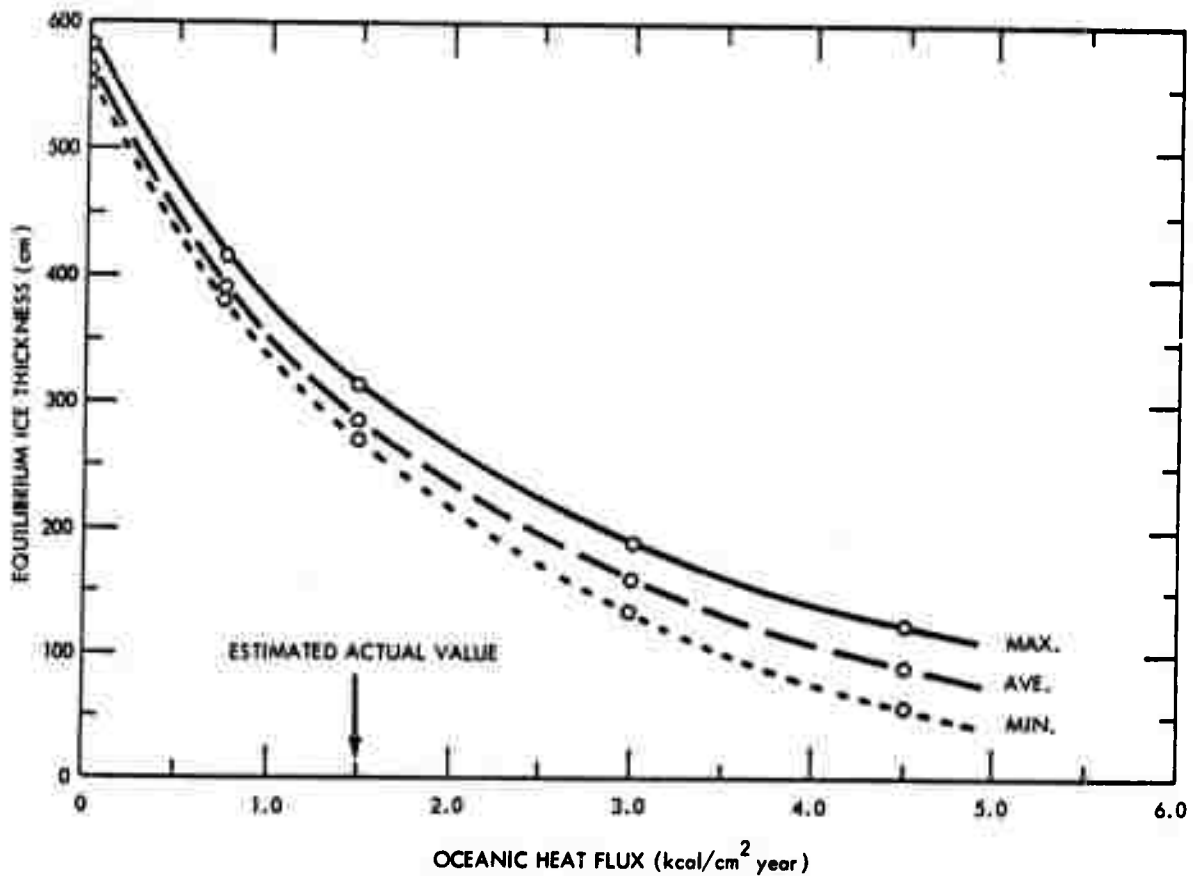


FIGURE 11. Equilibrium Ice Thickness as a Function of the Oceanic Heat Flux to the Sea Ice Layer as Determined Parametrically from Thermodynamic Model of Sea Ice (Maykut, 1969)

\* Since the model ignores the effect of melt ponds and leads (which have a lower surface albedo than that of ice), the experimental large-scale averages of the surface albedo are somewhat lower than those for melting ice used in the model.

## VII. DESCRIPTION OF THE GENERAL CIRCULATION FOR CLIMATE

The large-scale removal of the sea ice over the Arctic Ocean would have an impact on the net heating of the troposphere at high latitudes, through changes in each of the terms in Eq. 1. The change in the net heating of the troposphere at high latitudes would modify the current polar cell, which in turn would affect the atmospheric environment at these latitudes. The description of the coupling between the long-term general circulation and net heating of the troposphere becomes, then, essential in establishing both the magnitude and the transitive or intransitive nature of the changes of the climate at the earth's surface, from advertent modifications of parameters such as the surface albedo.

The statistics of the general circulation for climate can be determined from the statistics of the net heating of the troposphere by two approaches:

1. Emphasize the rather straightforward numerical integrations of the equations of motion (e.g., Holloway and Manabe, 1971; Kasahara and Washington, 1971; Arakawa, 1966; Mintz, 1964). This approach is an adaptation of the numerical methods developed for long-range weather forecasting to climate, and it requires the use of very large electronic computers to perform very long numerical experiments. It therefore yields a very detailed description of atmospheric phenomena, which are derived from difference equations approximating the differential equations of motion. The limit on the capability of a given computer introduces an upper limit to the wave number that may be considered by the difference equations.

2. Emphasize the parameterization of physical phenomena in the numerical integration of the equations of motion (e.g., Smagorinsky, 1964; Kurihara, 1970; Saltzman and Vernekar, 1971). This approach requires maximum physical insight into the key processes controlling tropospheric phenomena, e.g., the formulation of the countergradient transport of angular momentum as well as the transports of sensible heat and humidity by the large-scale two-dimensional turbulence.

As compared with the former approach, the latter approach can carry out the numerical integrations of the equations of motion through the use of smaller electronic computers, and the essential long-term statistics of the general circulation can be derived without the need of the very long time integrations that are required in the former approach. For these reasons the effort in this paper is concerned exclusively with this latter approach.

The understanding of the three-cell structure of the general circulation for the current climate was achieved only rather recently, and it was derived from the experimental evaluation of the large-scale transport of angular momentum at the upper levels of the troposphere (Lorenz, 1967). These investigations indicated that the streamlines ( $\psi^*$ ) of the flow in the troposphere at middle latitudes are as sketched in Fig. 12, i.e., the motion is defined by a westerly motion on which troughs in the general vicinity of cyclonic disturbances are superposed (Starr, 1948). The important feature of these streamlines is their departure from a symmetrical sinusoidal form and the associated NE-SW tilt from the meridian ( $\alpha$ ) of the trough line. This departure from sinusoidal form or tilt of the trough line is a function of latitude, i.e., the tilt is small at higher latitudes near the northern border of the surface westerly belt (Fig. 5) where the transport of angular momentum is small, and it becomes more pronounced at lower latitudes where the transport of angular momentum is large. Figure 12 shows also the temperature disturbances ( $\hat{\phi}^*$ ), which can be defined by introducing a longitudinal phase lag ( $\delta$ ) between the temperature and flow disturbances (Smagorinsky, 1964). The analytical representations

of these disturbances are included in Fig. 12, and they are defined by the tilt, the thermal phase lag, a zonal wave number appropriate for climate, and the disturbance's respective amplitudes A and B; thus, these formulations possess the minimum degrees of freedom necessary to effect the poleward transfer of both angular momentum and sensible heat. A brief but coherent description of the basic steps in the calculation of these statistics (e.g., the annual, zonal averages of the angular momentum and sensible heat transports) for climate from the statistics of the net heating rates of the troposphere (Eq. 1) is given below.

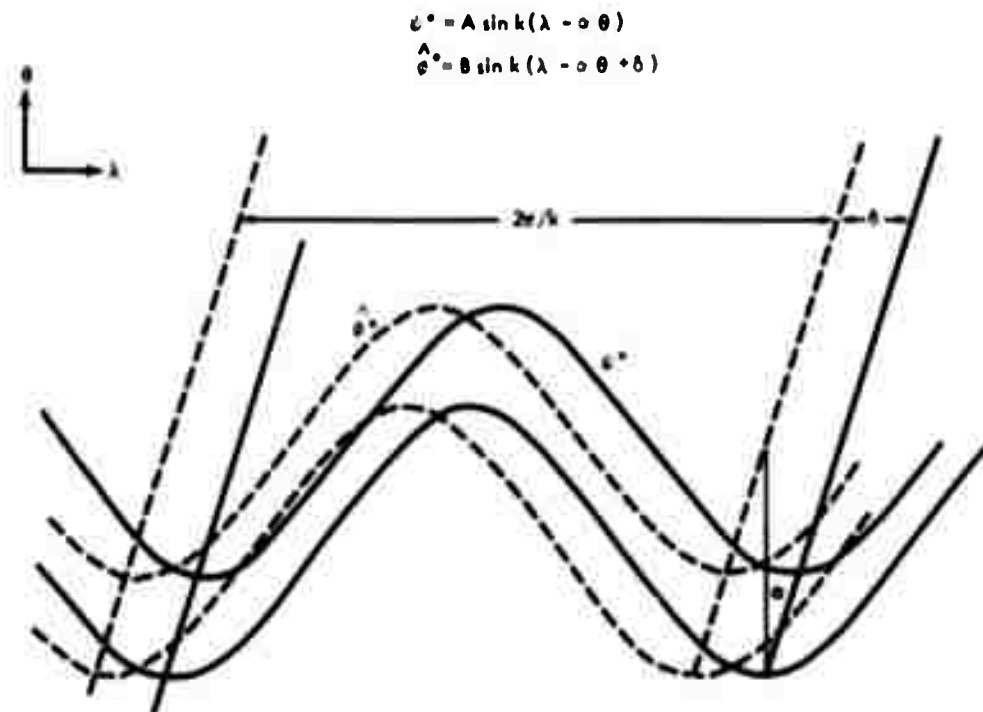


FIGURE 12. Schematic Diagram of a Baroclinic Disturbance (Starr, 1948; Smagorinsky, 1964)

The basic conservation equations for the baroclinic flow in the troposphere are as follows (e.g., Lorenz, 1967):

$$d\vec{V}/dt = -2\vec{\Omega} \times \vec{V} - \frac{1}{\rho} \vec{\nabla}p + \vec{g} + \vec{F} \quad (5-a)$$

$$dT/dt = -\left(\frac{c_p}{c_v} - 1\right) T \vec{\nabla} \cdot \vec{V} + Q/c_v \quad (5-b)$$

$$d\rho^{-1}/dt = \frac{1}{\rho} \vec{\nabla} \cdot \vec{V} \quad (5-c)$$

$$p = \rho RT \quad (5-d)$$

These equations represent, respectively, Newton's second law of motion or momentum equation, the first law of thermodynamics or energy equation, the conservation of mass or continuity equation, and the equation of state for air. The left-hand side of Eq. 5-a denotes acceleration of the three-dimensional wind  $\vec{V}$ ; the terms in the right-hand side are, respectively, the Coriolis acceleration, the pressure gradient, the earth's gravity, and the friction force per unit mass. In Eq. 5-b, the symbol  $c_p/c_v$  denotes the ratio of the specific heat of air at constant pressure to the specific heat at constant volume, and  $Q$  denotes net heating per unit mass. Using the conditions of hydrostatic equilibrium or no vertical wind, Eqs. 5-a through 5-d can be put in the so-called primitive form, where the wind field is denoted by a two-dimensional vector ( $\vec{U}$ ), and the independent variable  $z$  in the radial direction from the earth's center is replaced by the pressure  $p$ . The primitive equations are as follows (e.g., Lorenz, 1967):

$$d\vec{U}/dt = -f \vec{k} \times \vec{U} - g \vec{\nabla}z + \vec{F} \quad (5-e)$$

$$dT/dt = RT\omega/c_p p + Q/c_p \quad (5-f)$$

$$\vec{\nabla} \cdot \vec{U} + \partial\omega/\partial p = 0 \quad (5-g)$$

$$\partial z/\partial p = -RT/gp \quad (5-h)$$

where  $\vec{U} = \vec{i}u + \vec{j}v$ , with  $\vec{i}$  and  $\vec{j}$  denoting unit vectors in the eastward and northward directions,  $f$  is the Coriolis parameter  $2\Omega \sin \theta$ ,  $\vec{k}$  the unit vector in the radial direction,  $\vec{v}$  is now a horizontal differential operator holding the pressure constant, and  $w = dp/dt$ . Also, to make the kinetic energy of the horizontal motion consistent with the hydrostatic approximation,  $dr/dt = 0$  or  $r$  must be replaced by the earth's radius  $a$  (Smagorinsky, 1958). Equation 5-e describes the horizontal motion and it yields two scalar components, one for the zonal flow and the other for the meridional flow; Eq. 5-f is the energy equation, Eq. 5-g the continuity equation, and Eq. 5-h is the hydrostatic condition using Eq. 5-d. The continuity equation is put in the form 5-g from the use of both the hydrostatic equation to eliminate the density  $\rho$ , and the transformation from vertical ( $z$ ) to the pressure ( $p$ ) coordinate (e.g., Thompson, 1961). In the spherical coordinates of the earth ( $\lambda$ ,  $\theta$ ), the two scalar equations for the zonal and meridional motion are, respectively, as follows (e.g., Lorenz, 1967):

$$\frac{du}{dt} = \frac{uv}{a} \tan \theta + fv - \frac{1}{a \cos \theta} \frac{\partial \phi}{\partial \lambda} + F_{\lambda} \quad (5-i)$$

$$\frac{dv}{dt} = -\frac{u^2}{a} \tan \theta - fu - \frac{1}{a} \frac{\partial \phi}{\partial \theta} + F_{\theta} \quad (5-j)$$

where  $u = a \cos \theta d\lambda/dt$ ,  $v = a d\theta/dt$ , and  $\phi$  denotes the geopotential  $gz$ . The total or individual time derivatives in Eqs. 5-i, 5-j, and 5-f, say  $dX/dt$ , are related to their local time derivatives ( $\partial X/\partial t$ ) by the equation

$$\frac{dX}{dt} = \frac{\partial X}{\partial t} + \vec{U} \cdot \vec{\nabla} X + w \frac{\partial X}{\partial p}$$

The primitive Eqs. 5-e through 5-h can be applied to a two-level model of the atmosphere. This model represents the flow pattern in the upper half of the atmosphere by the flow pattern at the 250-mb

level, and the flow pattern in the lower half of the atmosphere is represented by the flow pattern at the 750-mb level (Charney and Phillips, 1953; Phillips 1956). Figure 13 shows these two levels, together with the dependent variables that are applicable at these levels. The momentum and continuity equations are applied at the 250-mb and 750-mb levels, while the energy equation is applied at the 500-mb level (as implied previously in Fig. 1) together with the hydrostatic equation 5-h. Figure 13 also shows the boundary conditions at the top and bottom of the atmosphere, i.e.,  $\omega_0 = \omega_4 = 0$ , which are used to filter gravity waves.

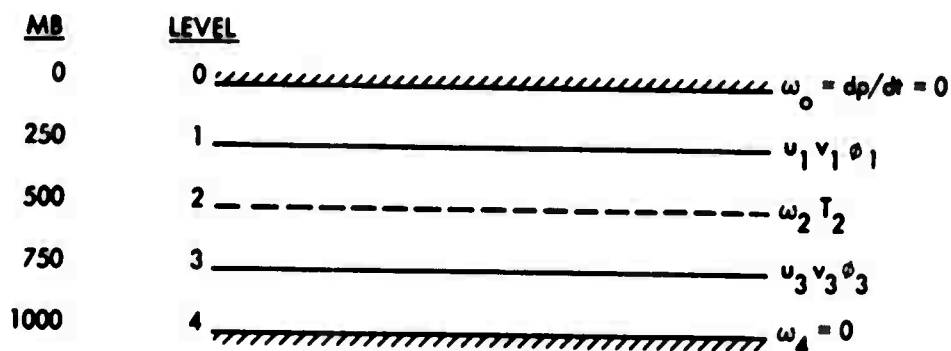


FIGURE 13. Two-Level Model of Baroclinic Flows (Phillips, 1956)

The large-scale transports of angular momentum and sensible heat were calculated by using: (1) the primitive equations, 5-i, 5-f, 5-g, and 5-h but not 5-j; (2) the two-level model of the atmosphere (Fig. 13); and (3) the mechanisms of the tilt and phase lag described in Fig. 12. The calculation of these transports was reduced to the solution of a two-parameter eigenvalue problem, which involved the numerical integration of a nonlinear, ordinary, second-order differential equation (Smagorinsky, 1958, 1963, 1964). Although a unified and somewhat detailed description of this procedure is included in Appendix A to clarify all the approximations used in this model, a broad outline of steps (1) through (3) is given by the following two results:

A. TRANSPORTS AS A FUNCTION OF POLEWARD HEAT FLUX

The use of the zonal momentum Equation 5-i, together with the continuity Equation 5-g at the 250-mb and 750-mb levels, yields two zonal equations, which after taking a zonal average of each defined by

$$[X] = \frac{1}{2\pi a} \int_0^{2\pi a} X \, dx$$

can be written as (Appendix A):

$$\frac{\partial[\bar{u}_m]}{\partial t} = -m^4 \frac{\partial}{\partial y} \frac{[\hat{u}_m][\hat{v}_m]}{2m^4} - m^4 \frac{\partial \hat{M}_m}{\partial y} + m[F_x] \quad (5-k)$$

$$\frac{\partial[\hat{u}_m]}{\partial t} = [\bar{v}_m][f + \zeta] + m^2 \left\{ -m^2 \frac{\partial \hat{M}_m}{\partial y} + \frac{[D^*u_m^*]}{m^2} \right\} + m[F_x] \quad (5-l)$$

Equations 5-k and 5-l are written in the Mercator  $(x,y)$  coordinates instead of the spherical  $(\lambda,\theta)$  coordinates by using  $dx = a \, d\lambda$  and  $dy = a \, d\theta/\cos \theta$ . The zonal and meridional winds in the Mercator plane are related to their counterparts in the spherical coordinates through the relations  $u_m = um$  and  $v_m = vm$ , where  $m = 1/\cos \theta$ . The notation  $\bar{\chi}$  and  $\hat{\chi}$  denote, respectively, the sum and the difference of the given parameters at levels one and three (Fig. 13), i.e.,  $\bar{\chi} = \chi_1 + \chi_3$  and  $\hat{\chi} = \chi_1 - \chi_3$ ;  $M_m$  denotes a quantity proportional to the eddy flux of angular momentum, i.e.,

$$M_m = [u_m^*v_m^*]/m^4$$

Finally, the symbols  $\zeta$  and  $D$  in Eq. 5-l denote, respectively, the relative vorticity and the horizontal divergence, which are given by

$$D \equiv \vec{v} \cdot \vec{u} = \frac{m}{a} \left( \frac{\partial u}{\partial \lambda} + \frac{\partial}{\partial \theta} \frac{v}{m} \right) = \frac{\partial u_m}{\partial x} + m^2 \frac{\partial}{\partial y} \left( \frac{v_m}{m^2} \right) = - \frac{\partial \omega}{\partial p}$$

$$\zeta = \partial v_m / \partial x - m^2 \partial (u_m / m^2) / \partial y$$

Similarly, the use of the energy Equation 5-f and the hydrostatic Equation 5-h at the 500-mb level (i.e., Fig. 1) yields the relation (Appendix A):

$$\frac{\partial [\hat{\phi}]}{\partial t} = -m^2 \frac{\partial}{\partial y} H_m - \gamma^2 m^2 \frac{\partial}{\partial y} \frac{[\hat{v}_m]}{m^2} + \frac{R}{c_p} [Q_2] \quad (5-m)$$

where  $H_m$  denotes a quantity proportional to the eddy flux of sensible heat, i.e.,

$$H_m = \frac{[\hat{v}_m^* \hat{\phi}^*]}{2m^2}$$

and  $\gamma^2$  is defined by

$$\gamma^2 = (1/2) p_2^2 (\partial \omega / \partial p) (\partial \ln \theta_{p_2} / \partial p)$$

where  $\theta_p$  is the potential temperature, i.e.,

$$\theta_p = (p_4/p)^{R/c_p} \cdot T$$

Introducing the condition of quasi-equilibrium in Eqs. 5-k, 5-l, and 5-m, the local time operator vanishes, i.e.,  $\partial/\partial t = 0$ . Neglecting the first term in the right-hand side of Eq. 5-k, the  $\zeta$  and  $[\widehat{D^* u_m^*}]/m^2$  in Eq. 5-l, and assuming that the frictional forces in Eqs. 5-k and 5-l are due only to the stresses at the earth's surface ( $\tau_4$ ) or

$[F] = -[\hat{F}] = g[\tau_4]/\hat{p}$ , this system of equations reduces to the following form:

$$m^4 \frac{\partial \bar{M}_m}{\partial y} = m[\bar{F}_x] = \frac{mg}{\hat{p}} [\tau_{x_4}] \quad (5-n)$$

$$f[\hat{v}_m] = m^4 \frac{\partial \hat{M}_m}{\partial y} + \frac{mg}{\hat{p}} [\tau_{x_4}] \quad (5-o)$$

$$\frac{\partial H_m}{\partial y} + \gamma^2 \frac{\partial}{\partial y} \frac{[\hat{v}_m]}{m^2} = \frac{R}{c_p} \frac{1}{m^2} [Q_2] \quad (5-p)$$

Since  $\gamma^2$  is a constant related to the static stability, integration of Eq. 5-p yields

$$H_m + \frac{\gamma^2 [\hat{v}_m]}{m^2} = q_f(y)$$

where

$$q_f(y) = \frac{R}{c_p} \int_0^y \frac{[Q_2]}{m^2} dy$$

Using the approximation  $\bar{M}_m \approx \hat{M} \approx M_{m,1}$  in Eq. 5-n, and using Eq. 5-o to eliminate  $[\hat{v}_m]$ :

$$H_m + \frac{2\gamma^2 m^2}{f} \frac{\partial \hat{M}_m}{\partial y} = q_f \quad (5-q)$$

Thus, the equations of motion yield Eq. 5-q for a relationship involving the transport of sensible heat,  $H_m$ , the latitudinal gradient of the transport of angular momentum,  $M_m$ , the annual mean energy flux,  $q_f$ , as obtained from the net heating rate of the atmospheric column (i.e.,  $[Q_2]$  as given by Eq. 1), and one eigenvalue parameter  $\gamma^2$ .

## B. TRANSPORTS AS A FUNCTION OF WAVE PARAMETERS

The use of the mechanism of the tilt and phase lag described in Fig. 12, together with the condition of geostrophic equilibrium, leads to another relation between the transports of sensible heat and angular momentum. The geostrophic equilibrium is a feature of the circulation in middle and higher latitudes that is almost as prominent as hydrostatic equilibrium; it is given by the approximate balance between the Coriolis force and the horizontal pressure gradient in Eq. 5-e, a condition that yields  $-f\vec{k} \times \vec{U} = \vec{\nabla}\phi$ , or equivalently,  $\vec{U} = (1/f)\vec{k} \times \vec{\nabla}\phi$ . The geostrophic equilibrium allows the zonal and meridional eddy winds to be expressed in terms of the temperature disturbance in Fig. 12 as follows:

$$\hat{u}_m^* = -\frac{m^2}{f} \frac{\partial \hat{\phi}^*}{\partial y} = -\frac{m}{af} \frac{\partial \hat{\phi}^*}{\partial \theta} \quad (5-r)$$

$$\hat{v}_m^* = \frac{m^2}{f} \frac{\partial \hat{\phi}^*}{\partial x} = \frac{m^2}{af} \frac{\partial \hat{\phi}^*}{\partial \lambda} \quad (5-s)$$

The continuity Equation 5-g, with the boundary conditions on  $\omega_0$  and  $\omega_4$  (Fig. 13), yields a relationship between the zonal and meridional eddy winds and the flow disturbances in Fig. 12 as follows:

$$\bar{u}_m^* = -m^2 \frac{\partial \psi^*}{\partial y} = -\frac{m}{a} \frac{\partial \psi^*}{\partial \theta} \quad (5-t)$$

$$\bar{v}_m^* = m^2 \frac{\partial \psi^*}{\partial x} = \frac{m^2}{a} \frac{\partial \psi^*}{\partial \lambda} \quad (5-u)$$

where, as indicated in Fig. 12,

$$\psi^* = A \sin \eta \quad (5-v)$$

$$\hat{\phi}^* = B \sin (\eta + k\delta) \quad (5-w)$$

with  $\eta = k(\lambda - \alpha\theta)$ . The second relationship between the transports of sensible heat and angular momentum is then obtained from differentiation of the expression for  $H_m$ , use of the definition of  $M_m$ , and the use of the relations 5-r, 5-u, and 5-w; the results can be written as follows (Appendix A):

$$\hat{M}_m = \frac{1}{f} \left( \frac{dH_m}{dy} + \frac{H_m}{mS} \right) \quad (5-x)$$

where  $S$  is a second eigenvalue parameter given by

$$S = \frac{a \tan k\delta}{2\alpha k}$$

This definition of  $S$  stems from the evaluation of the terms  $[\hat{u}_m^* \hat{v}_m^*]/m_4$  and  $H_m$  from the relations 5-r, 5-u, and 5-w, i.e.,

$$H_m = \frac{kAB}{2a} [\sin(\eta + k\delta) \cos \eta] = \frac{kAB}{4a} \sin k\delta \quad (5-y)$$

and

$$\frac{[\hat{u}_m^* \hat{v}_m^*]}{m^4} = \frac{k^2 \alpha AB}{a^2 f m} [\cos(\eta + k\delta) \cos \eta] = \frac{k^2 \alpha AB \cos k\delta}{2a^2 f m}$$

This latter expression is derived by assuming that  $B$ ,  $\alpha$ , and  $\delta$  in Eq. 5-w are nearly constant; thus, Eq. 5-y indicates then that  $H_m$  is proportional to  $A$ . The combination of these two latter expressions yields the definition of  $S$ , since  $[\hat{u}_m^* \hat{v}_m^*]/m_4$  can be written as follows:

$$\frac{[\hat{u}_m^* \hat{v}_m^*]}{m^4} = \frac{H_m}{f m S}$$

The combination of the two foregoing relations 5-q and 5-x for the transports of sensible heat and angular momentum yields:

$$\frac{2\gamma_m^2}{f} \frac{d}{dy} \left\{ \frac{1}{f} \left( \frac{dH_m}{dy} + \frac{H_m}{mS} \right) \right\} + H_m = q_f \quad (5-z)$$

If  $S$  is assumed to be constant given by a proper average, Eq. 5-z is a second-order, ordinary differential equation with two eigenvalue parameters given by the constants  $\gamma^2$  and  $S$ ; these parameters are fixed from the use of four boundary conditions, i.e.,  $H_m(0, y) = 0$  and  $dH_m/dy = 0$  at  $y = 0, y = Y$ , where  $Y$  denotes a latitude near the poles.

Either Eqs. 5-q and 5-x or 5-z and 5-x yield the large-scale transports of sensible heat and angular momentum as a function of the poleward heat flux ( $q_f$ ) induced by the net heating rates of the atmospheric column (i.e., Eq. 1). The identification of  $q_f$  as a poleward transport of energy is formally derived by integrating the product of a mass element and the individual time derivative of any dependent variable  $X$  over the volume of the region north of a latitude  $\theta_1$ , and then taking the time and zonal averages in such an integration. Thus, the use of the definition for the individual time derivative of  $X$ , the continuity Equation 5-g in spherical coordinates ( $\lambda, \theta$ ), the mass element  $g^{-1} a^2 \cos \theta d\lambda d\theta dp$ , and taking the time and zonal averages yield the following expression (e.g., Lorenz, 1967):

$$\int_0^{p_4} 2\pi a \cos \theta_1 [\overline{X\bar{v}}] g^{-1} dp = - \int_0^{p_4} \int_{\theta_1}^{\pi/2} 2\pi a^2 \cos \theta [\overline{dX/dt}] g^{-1} d\theta dp \quad (6)$$

Letting  $X$  denote the energy per unit mass  $e$  (cal/gm or  $m^2/sec^2$ ),  $Q$  the net heating rate  $de/dt$ , and  $Q_2 = \int_0^1 Q d(p/p_1)$ , Eq. 6 yields

$$\int_0^{P_4} 2\pi a \cos \theta_1 [\overline{ev}] g^{-1} dp = -2\pi a^2 \int_{\theta_1}^{\pi/2} \frac{P_4 Q_2}{g} \cos \theta d\theta$$

Using the foregoing definition of  $q_f$ , the integral in the right-hand side of this expression may be written as

$$\int_0^{P_4} 2\pi a \cos \theta_1 [\overline{ev}] g^{-1} dp = -2\pi a^2 \frac{P_4}{(R/c_p)ag} \left\{ q_f(\pi/2) - q_f(\theta) \right\}$$

or, since  $q_f(\pi/2) = 0$ ,

$$q_f(\theta_1) = \int_0^1 \frac{R}{c_p} [\overline{ev}] \cos \theta_1 d(p/P_4)$$

which relates  $q_f(\theta)$  to the average poleward transport of energy  $[\overline{ev}]$  from the atmospheric column at a latitude  $\theta_1$ . Figure 14 shows the function  $q_f$  corresponding to the processes indicated in Fig. 2 for the current climate. Figure 14 also shows schematically the modification of  $q_f$  at the higher latitudes by the advertent removal of the ice from the Arctic Ocean; this modification would, of course, result from the corresponding changes in each of the terms in Eq. 1 from the advertent change of the surface albedo  $A_*$  at these higher latitudes.

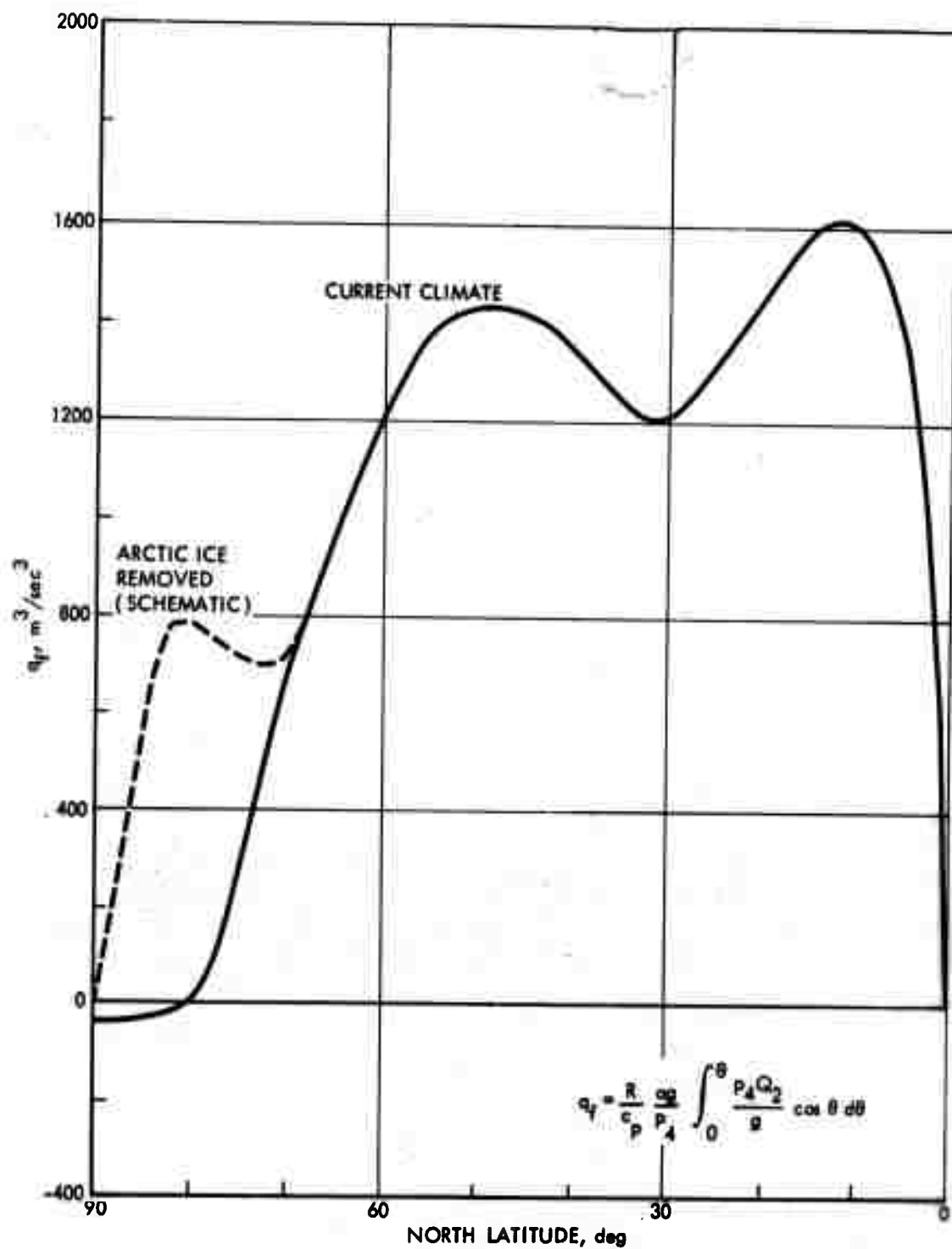


FIGURE 14. Poleward Heat Flux Required by the Net Heating Rate,  $p_4 Q_2/g$  (Smagorinsky, 1963)

VIII. EVALUATION OF THE THEORY OF THE GENERAL CIRCULATION  
FOR CLIMATE BASED ON A CONSTANT S WAVE PARAMETER.

The use of Eqs. 5-z and 5-x with a constant S wave parameter yields predictions for the two important large-scale transports of sensible heat and angular momentum as a function of latitude, i.e., the transports that control the meridional cell structure of the general circulation (Fig. 5). The results from this model can be evaluated from:

1. A comparison of the predicted transports with corresponding experimental values obtained from the reduction of data concerning the statistics of the general circulation.
2. Theoretical considerations concerning the sensitivity of the predicted values of these transports to the characteristics of the S wave parameter, which is determined from boundary conditions at the north pole.
3. A comparison of the semi-experimental behavior as a function of latitude of the amplitude and wave parameters of the baroclinic disturbances with their assumed behavior in the model.

Equations 5-q and 5-x yield power series solutions for near the equator, which are

$$M_{m \theta=0} = \frac{1}{3} \frac{a\Omega}{\gamma^2} \left( \frac{dq_f}{d\theta} \right)_{\theta=0} \theta^3$$

$$H_{m \theta=0} = \frac{2}{15} \left( \frac{a\Omega}{\gamma} \right)^2 \left( \frac{dq_f}{d\theta} \right)_{\theta=0} \theta^5$$

where

$$q_f_{\theta \rightarrow 0} = \left( \frac{dq_f}{d\theta} \right)_{\theta \rightarrow 0} \theta$$

and power series solutions for near the poles:

$$\hat{M}_{m_{\theta \rightarrow \pi/2}} = - \frac{a\Omega}{\gamma^2} \frac{C}{r+3} \left( \frac{\pi}{2} - \theta \right)^{r+3}$$

$$H_{m_{\theta \rightarrow \pi/2}} = 2 \left( \frac{a\Omega}{\gamma} \right)^2 \frac{C}{(r+3)^2} \left( \frac{\pi}{2} - \theta \right)^{r+3}$$

where

$$q_f_{\theta \rightarrow \pi/2} = C \left( \frac{\pi}{2} - \theta \right)^{r+1}$$

C and r are constants, and  $r \geq 1$  to satisfy the boundary condition  $v_m, \theta \rightarrow \pi/2 \rightarrow 0$ . The power series solutions for near the poles yield values for both  $H_m(Y)$  and  $dH_m/dy$  as  $y \rightarrow Y$ , which are required for the determination of the eigenvalue parameters  $\gamma^2$  and S from the numerical solutions of Eqs. 5-q and 5-x in the range  $0 \leq y \leq Y$ , or equivalently  $0 \leq \theta \leq \pi/2$ .

Figure 15 shows the large-scale transport of sensible heat,  $H_m$ , derived from the numerical integrations of Eqs. 5-q and 5-x and using the function  $q_f$  in Fig. 14 for the current climate. Table 2 shows experimental annual values for the northward transports of sensible heat ( $c_p T$ ) by the transient  $[\overline{v'T'}]$  and stationary  $[\overline{v^*T^*}]$  eddies as obtained from the most recent reduction of available data (Oort and Rasmusson, 1971). Using the definition of  $H_m$ , the transformation  $v_m = v_m$ , the relation  $\hat{\phi}^* = RT_2^*$  and  $\hat{v}^* = 2v_2^*$ , give  $H_m = \{[\overline{v_2'T_2'}] + [\overline{v_2^*T_2^*}]\}R \cos \theta$ . Since  $Q_2$  is defined by  $\int_0^1 Q d(p/p_4)$  in Eq. 1, the

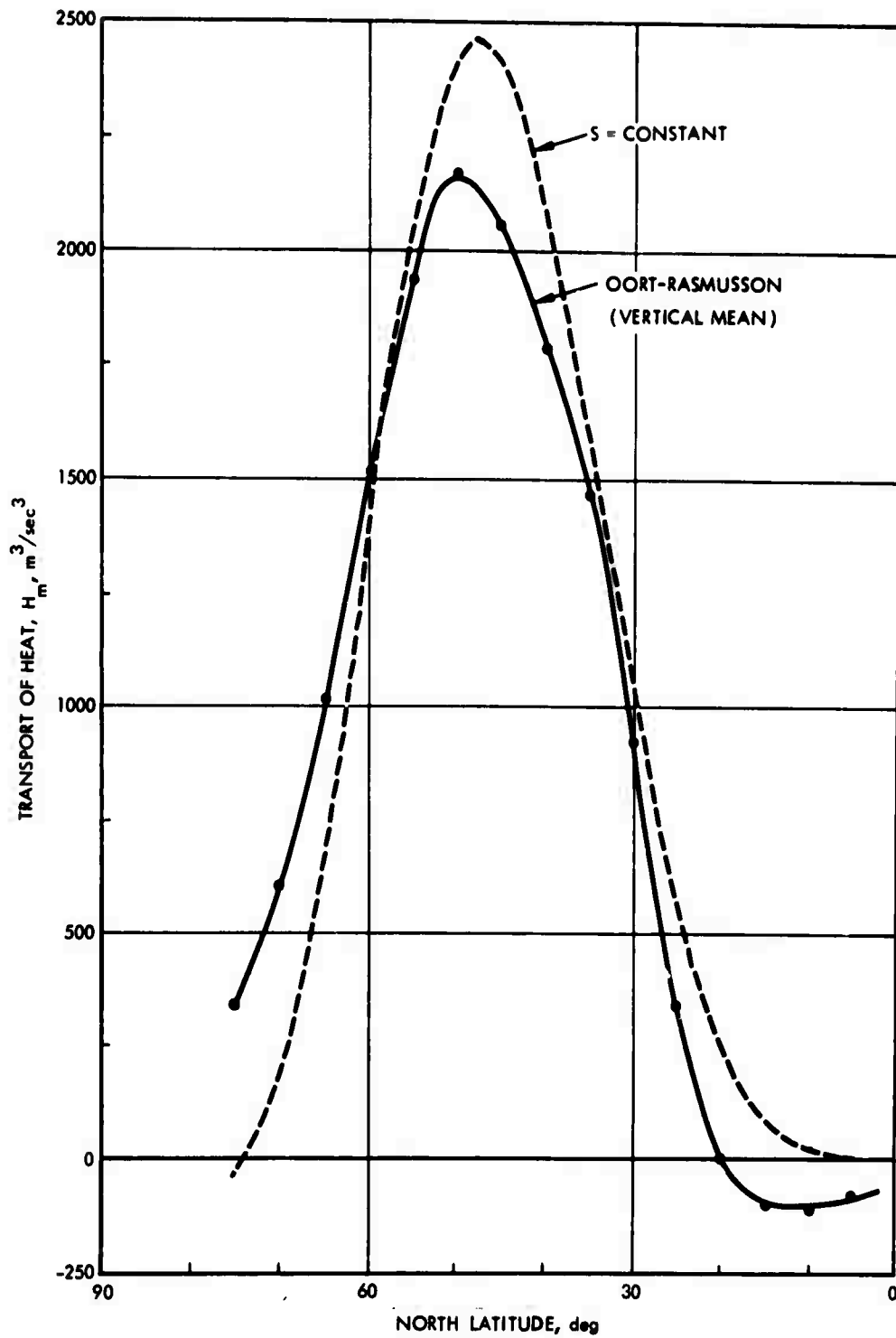


FIGURE 15. Comparison Between Theory (Smagorinsky, 1969) and Experimental Annual Data (Oort-Rasmusson, 1971) for the Transient Plus Standing Eddy Transport of Heat

TABLE 2. NORTHWARD ANNUAL TRANSPORT OF SENSIBLE HEAT  
 BY TRANSIENT EDDIES [ $\overline{v'T'}$ ] AND STATIONARY  
 EDDIES [ $\overline{v^*T^*}$ ],  $m^{\circ}C/sec$ , AT LATITUDES  
 $0 \leq \theta \leq 75^{\circ}N$

Transient Eddies

P,mb	0	5	10	15	20	25	30	35	40	45	50	55	60	65	70	75
50	-0.5	0.3	0.4	.0	-0.2	-0.1	0.4	1.1	2.4	4.4	5.9	5.9	5.1	4.6	5.0	7.1
100	-0.5	-0.2	.0	0.2	-0.1	0.1	1.3	2.4	3.7	5.4	6.6	6.7	5.8	4.5	3.7	3.2
200	0.5	0.2	-0.4	-1.5	-2.0	-0.7	2.1	5.2	7.3	8.8	9.6	8.3	6.7	4.5	3.1	1.9
300	0.5	0.2	-0.4	-0.8	-0.8	0.4	2.8	5.1	5.4	5.0	4.0	3.6	3.1	2.4	1.5	0.4
400	.0	-0.4	-0.7	-0.8	-0.9	0.1	2.4	4.6	5.3	5.7	5.7	5.1	4.9	4.3	3.5	2.5
500	0.1	-0.1	-0.4	-0.9	-1.2	-0.2	2.3	4.2	5.6	7.1	8.0	7.7	7.1	6.3	5.2	3.8
700	-0.8	-0.7	-0.6	-0.5	.0	1.4	3.5	6.4	9.1	11.4	12.5	11.5	10.1	9.0	7.9	6.6
850	-0.8	-0.7	-0.4	0.3	1.6	3.5	6.1	8.8	11.5	12.9	13.8	13.2	12.3	11.7	11.0	9.6
900	-0.7	-0.6	-0.1	0.8	2.3	4.2	7.1	9.4	11.4	12.0	12.7	12.2	11.9	11.4	10.6	9.4
950	-0.4	-0.3	0.1	1.2	2.8	4.7	7.0	8.5	9.9	9.9	10.1	9.6	9.7	9.5	8.7	8.0
1000	-0.4	-0.2	0.2	1.2	2.6	4.0	5.6	6.3	6.5	6.5	5.8	5.3	4.2	4.1	3.3	2.7
Mean	-0.2	-0.3	-0.4	-0.4	-0.1	1.2	3.4	5.8	7.5	8.6	9.2	8.6	7.7	6.8	5.8	4.6

Stationary Eddies

P,mb	0	5	10	15	20	25	30	35	40	45	50	55	60	65	70	75
50	.0	.0	0.1	0.1	0.2	0.3	0.4	0.7	1.2	2.0	2.8	3.4	4.1	4.3	3.6	2.6
100	0.1	0.3	0.6	0.8	0.7	0.4	0.3	0.4	0.9	1.7	2.6	3.4	3.8	3.5	2.5	1.4
200	0.1	.0	0.3	0.7	1.3	1.8	1.8	1.5	1.3	2.2	3.3	3.8	3.3	1.9	0.6	-0.1
300	.0	-0.1	-0.1	0.1	0.3	0.4	0.3	0.5	0.9	1.7	2.4	2.7	2.0	0.8	-0.2	-0.2
400	-.0	-.0	-.0	.0	0.1	0.2	0.2	0.2	0.6	1.4	2.1	2.4	2.0	0.8	-0.1	-.0
500	-.0	.0	0.1	0.1	0.1	0.2	0.2	0.2	0.6	1.5	2.4	2.7	2.2	0.9	-0.1	-0.1
700	-.0	-0.1	-0.1	-0.2	-0.3	-0.3	-0.1	0.3	0.9	1.8	2.8	3.4	3.0	1.4	0.1	-0.2
850	.0	0.1	-0.2	-0.7	-1.1	-1.1	-0.3	.0	0.2	1.3	2.6	3.7	3.6	1.9	-.0	-0.7
900	0.1	0.1	-.0	-0.4	-0.9	-0.9	-0.3	-0.2	-0.5	0.5	2.1	3.3	3.4	2.2	0.3	-0.9
950	-0.1	-.0	.0	.0	-0.2	-0.2	0.2	-0.1	-0.6	0.3	1.6	2.7	3.2	2.5	0.7	-0.6
1000	-0.4	-0.4	-0.2	0.2	0.4	0.7	0.9	0.5	0.2	0.9	2.0	2.6	2.9	2.4	1.0	0.1
Mean	-.0	.0	.0	.0	0.1	0.1	0.3	0.4	0.6	1.5	2.5	3.1	2.8	1.6	0.3	-0.1

transports within the bracket are also given by the mean vertical values of the atmospheric column, i.e.,  $[\overline{v_2' T_2'}] = \int_0^1 [\overline{v' T'}] d(p/p_4)$  as well as  $[\overline{v_2^* T_2^*}] = \int_0^1 [\overline{v^* T^*}] d(p/p_4)$ . The experimental values of  $H_m$  obtained in this manner from the mean values in Table 2 are also shown in Fig. 15; this figure indicates a good agreement between the theoretical and experimental values of  $H_m$ . Figure 16 shows similar data for the large-scale transport of angular momentum at the 250-mb level, i.e.,  $\hat{M}_m \approx M_{m,1}$ . The experimental values of  $M_{m,1}$  are obtained by using the definition of  $M_m$ , the transformations  $u_m = um$  and  $v_m = vm$ ; thus,  $M_{m,1} = \{[\overline{u'v'}] + [\overline{u^*v^*}]\} \cos^2 \theta$ , where the transports are shown in Table 3. Figure 16 indicates that the theory underestimates the transport of angular momentum at midlatitudes by as much as about 40 percent. Figure 16 shows a good agreement for the latitudes of the largest positive and negative absolute magnitudes of the angular momentum transports, or the latitudinal widths of the Hadley and Ferrel cells, i.e., where  $dM_{m,1}/d\theta = 0$ . This latter condition is obtained from Eqs. 5-n and 5-o, which yield

$$[\hat{v}_m] = (2m^3/af) \cdot dM_{m,1}/d\theta$$

since the continuity equation, together with the boundary conditions for the meridional wind,  $v_m = 0$  at the equator and the poles at both levels (Fig. 13), gives  $[\overline{v}_m] = 0$ , i.e.,  $[v_{m,1}] = -[v_{m,3}]$ . Then

$$[v_{m,1}] = (m^3/af) \cdot dM_{m,1}/d\theta$$

Thus, the result  $[v_{m,1}] = -[v_{m,3}]$  indicates that the meridional circulations in the upper and lower branches of each cell (Fig. 5) are equal but opposite in direction, while the two conditions  $dM_{m,1}/d\theta = 0$  in Fig. 16 yield the three-cell structure of the current long-term general circulation.

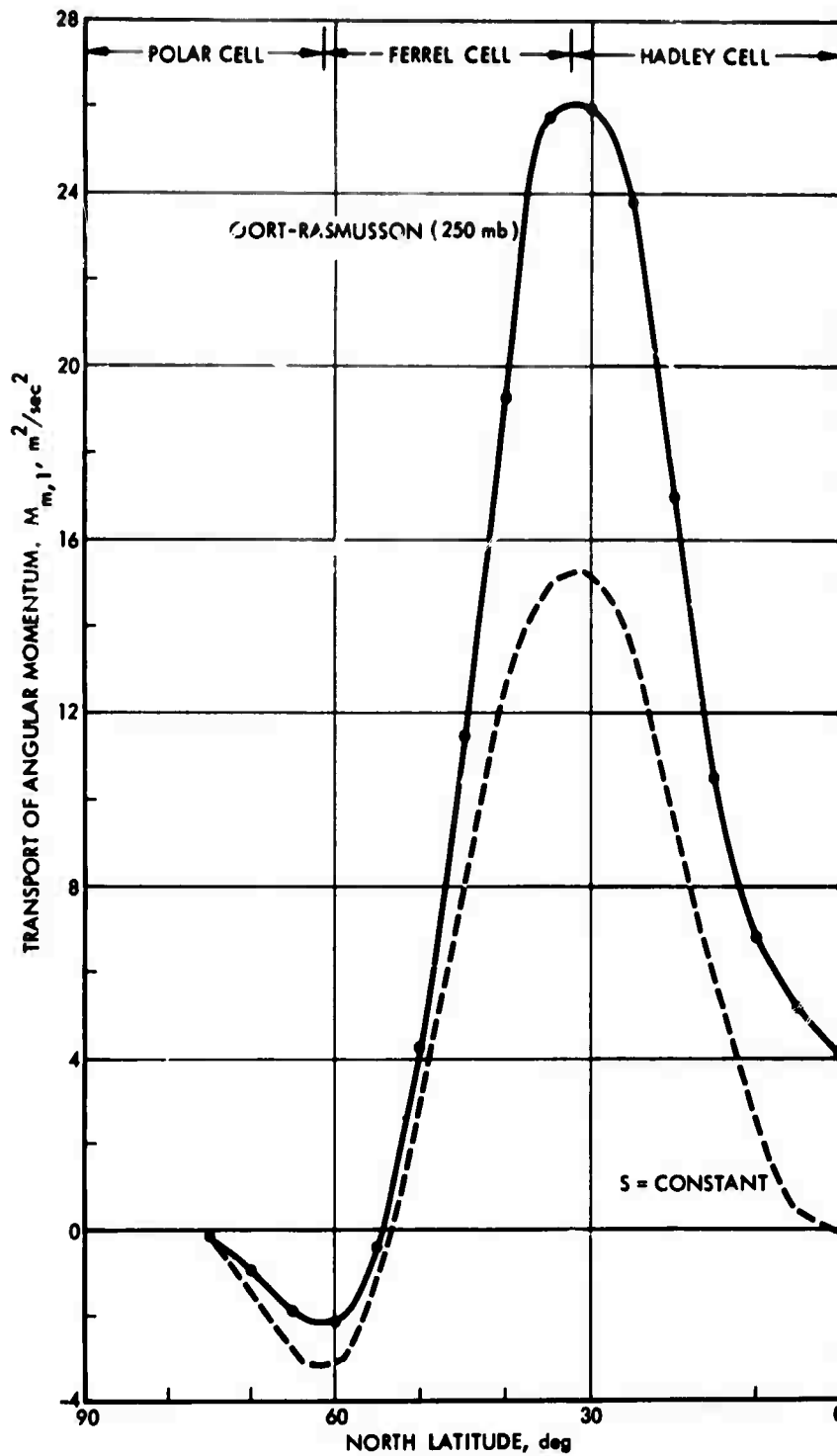


FIGURE 16. Comparison Between Theory (Smagorinsky, 1964) and Experimental Annual Data (Oort-Rasmusson, 1971) for the Transient Plus Standing Eddy Transport of Angular Momentum

TABLE 3. NORTHWARD ANNUAL TRANSPORT OF WESTERLY MOMENTUM  
 BY TRANSIENT EDDIES [ $\overline{v'u'}$ ] AND STATIONARY  
 EDDIES [ $\overline{v^*u^*}$ ],  $m^2/sec^2$ , AT LATITUDES  
 $0 \leq \theta \leq 75^\circ N$

Transient Eddies

P,mb	0	5	10	15	20	25	30	35	40	45	50	55	60	65	70	75
50	2.2	2.8	1.1	0.1	0.8	2.3	4.2	5.1	5.7	6.0	5.1	3.8	2.1	-2.6	-8.3	-13.2
100	0.3	-0.4	0.7	4.3	8.5	11.6	12.7	11.2	9.0	7.1	3.8	2.0	0.6	-1.5	-3.5	-2.6
200	4.5	6.3	8.9	16.0	24.3	30.4	36.7	38.0	29.8	18.8	7.8	-0.1	-3.9	-5.3	-5.6	-4.0
300	2.4	3.7	5.8	8.9	13.3	19.9	28.2	33.3	29.7	19.6	6.9	-3.0	-7.6	-7.7	-6.6	-5.2
400	-0.1	1.1	2.3	4.1	7.3	11.2	15.0	17.3	16.3	11.4	3.6	-3.0	-6.8	-6.6	-4.6	-3.2
500	-0.2	0.6	1.7	3.4	5.6	7.5	9.0	9.9	9.1	6.5	2.4	-0.8	-3.1	-3.8	-2.9	-2.6
700	0.4	1.4	1.8	2.3	2.3	2.7	4.1	4.7	3.8	2.5	1.0	-0.7	-1.3	-0.9	-0.3	-0.1
850	- .0	1.5	2.3	1.7	1.5	2.2	2.8	3.0	2.1	0.4	-1.6	-2.0	-1.1	-0.3	-0.7	-1.6
900	- .0	1.5	2.7	2.2	1.5	1.6	2.3	2.2	1.3	.0	-1.4	-1.8	-0.8	-0.3	-1.0	-1.3
950	.0	1.4	2.6	2.5	1.8	1.5	1.5	1.3	0.3	-0.6	-1.5	-1.3	-0.3	-0.5	-1.4	-1.2
1000	- .0	1.2	2.2	2.1	1.3	0.7	0.5	0.1	-0.4	-0.9	-1.5	-1.3	-0.6	-0.9	-1.7	-1.7
Mean	0.8	1.9	3.1	5.0	7.3	9.7	12.3	13.3	11.3	7.4	2.5	-1.2	-2.8	-3.1	-2.8	-2.2

Stationary Eddies

P,mb	0	5	10	15	20	25	30	35	40	45	50	55	60	65	70	75
50	- .0	- .0	.0	.0	0.1	0.2	0.2	-0.1	-0.4	- .0	-0.3	-1.3	-2.1	-3.0	-2.6	-1.2
100	0.2	0.1	0.1	0.1	0.4	1.4	1.6	1.0	0.4	0.5	-0.4	-1.7	-3.0	-3.4	-2.3	0.2
200	1.2	0.4	-0.6	-1.6	-1.3	1.6	3.5	3.4	3.1	3.5	2.5	0.2	-2.5	-3.7	-2.3	0.3
300	.0	-0.1	-0.3	-0.4	-0.2	0.6	1.2	2.4	3.5	4.2	3.4	0.7	-2.9	-4.7	-3.3	-0.2
400	-0.1	-0.1	-0.2	-0.3	-0.1	0.2	0.7	1.7	2.2	2.3	1.5	-0.5	-3.5	-5.1	-3.6	-0.6
500	-0.1	-0.2	-0.3	-0.3	-0.2	.0	0.2	0.7	0.9	1.2	0.9	-0.8	-3.2	-4.3	-3.1	-0.8
700	-0.1	-0.4	-0.6	-0.7	-0.6	-0.1	0.4	0.3	0.1	0.5	0.7	-0.4	-1.7	-2.2	-1.6	-0.6
850	-0.9	-0.8	-0.7	-0.7	-0.7	-0.4	0.4	0.8	0.6	0.7	0.8	0.2	-0.4	-0.6	-0.6	-0.5
900	-0.4	-0.4	-0.3	-0.3	-0.5	-0.5	0.3	0.9	0.9	0.9	0.8	0.1	-0.1	-0.1	-0.3	-0.4
950	-0.1	0.1	0.5	0.5	0.1	-0.4	-0.1	0.6	0.9	1.0	0.7	0.2	0.2	0.1	-0.1	-0.3
1000	-0.3	1.0	1.6	1.4	0.5	.0	.0	0.4	0.9	1.0	0.7	0.4	0.3	0.1	-0.1	.0
Mean	- .0	-0.1	-0.3	-0.4	-0.3	0.3	0.9	1.2	1.3	1.6	1.2	-0.3	-2.0	-2.9	-2.1	-0.4

If Eqs. 5-x and 5-z are multiplied by an arbitrary constant, both the transports of angular momentum and sensible heat are directly proportional to  $q_f$ . Thus, the magnitude of the parameters  $\gamma^2$  and  $S$  remains fixed for a given shape of the  $q_f$  curve, and the discrepancy between theory and experiment for the angular momentum transport in Fig. 16 could not be corrected by an increase in the magnitude of  $q_f$  without degrading the agreement for the transport of sensible heat in the previous figure.

The foregoing constant  $S$  theory of the general circulation for climate is successful in the accurate prediction of the large-scale transport of sensible heat, and in the determination with a lower degree of accuracy of the countergradient transport of angular momentum for the upper levels of the troposphere at middle and higher latitudes where  $d[\bar{u}]/d\theta < 0$ . However, a more decisive test of this theory can be made from both theoretical considerations and the use of experimental data for other statistics of the long-term general circulation.

To test the sensitivity of the transports' magnitude to the boundary conditions that are used to fix the constant  $S$ , an arbitrary variable  $S_p(\theta)$ , defined as  $S_{\max} \sin 2\theta$ , can be used in either Eq. 5-x or 5-z. The expression for  $S_p(\theta)$  has a maximum value  $S_{\max}$  at 45-deg latitude and it becomes zero at both the equator and the north pole. The boundary conditions for  $H_m$  and  $dH_m/d\theta$  as  $\theta \rightarrow 90$  deg are now used to determine the constants  $\gamma^2$  and  $S_{\max}$ . Numerical integrations of Eqs. 5-q and 5-x, using  $S_p(\theta)$  instead of a constant  $S$ , indicate that the transports are insensitive to  $S_p(\theta)$ ; i.e., the theoretical results shown in Figs. 15 and 16 apply essentially to both  $S_p(\theta)$  and a constant  $S$ . The use of  $S_p(\theta)$  yields maximum values for  $H_m$  and  $M_{m,1}$  that are, respectively, only about 2 percent and 4 percent higher than the corresponding values for a constant  $S$ ; the value of  $\gamma^2$  for  $S_p(\theta)$  is only 2 percent higher than that for a constant  $S$ , while the value of  $S_{\max}$  is about 5 percent lower than the constant  $S$  value. Thus, this particular change in  $S$  implies that the transports at middle latitudes can be insensitive to the boundary condition  $dH_m/d\theta$  at the pole, and that only the tilt and phase lags at middle latitudes are important.

Other theoretical limitations in the use of the constant S theory are as follows:

1. It cannot verify the assumptions used in the derivation of essentially the parameter S of the behavior of the parameters B,  $\alpha$ , and  $\delta$ , which are held constant. These latter assumptions become important for the verification of a consistency between  $dH_m/d\theta$  as derived from Eq. 5-y and the results shown in Fig. 15.
2. The use of the theory for very low latitudes, where the geostrophic equilibrium given by Eqs. 5-r and 5-s do not hold.
3. The lack of justification for the independence of the transports from the zonal circulation, a condition that is brought about by the dropping of Eqs. 5-j.

The latitudinal variation of the tilt and phase lag wave parameters can be determined from the experimental values for the transports of angular momentum and sensible heat, respectively. Likewise, the latitudinal variation of the amplitude of the stream function can be determined from the meridional eddy kinetic energy at Level 2, while the latitudinal variation of the amplitude of the temperature disturbances may be deduced from the experimental measurements of the meridional eddy kinetic energy at Level 1. Measurements of the zonal eddy kinetic energy may then be used to fix the wave number. Thus, using Eqs. 5-r, 5-s, 5-t, and 5-u, together with Eqs. 5-v and 5-w:

$$\hat{u}_m^* = -\frac{m}{af} \left\{ -kB \left( \frac{d\alpha\theta}{d\theta} - \frac{d\delta}{d\theta} \right) \cos(\eta + k\delta) + \frac{dB}{d\theta} \sin(\eta + k\delta) \right\} \quad (7-a)$$

$$\hat{v}_m^* = -\frac{m}{a} \left\{ -kA \left( \frac{d\alpha\theta}{d\theta} \right) \cos \eta + \frac{dA}{d\theta} \sin \eta \right\} \quad (7-b)$$

$$\hat{v}_m^* = \frac{m^2}{af} kB \cos(\eta + k\delta) \quad (7-c)$$

$$\hat{v}_m^* = \frac{m^2}{a} kA \cos \eta \quad (7-d)$$

Using the definition of  $\bar{M}_m$ , the identity  $\overline{u_m^* v_m^*} = (1/2)\{\hat{u}_m^* \hat{v}_m^* + \hat{u}_m^* \hat{v}_m^*\}$ , the angular momentum transport may be written as:

$$\bar{M}_m = \frac{1}{4} \frac{k^2 A^2}{ma^2} \left\{ \frac{d\alpha\theta}{d\theta} + \left( \frac{d\alpha\theta}{d\theta} - \frac{d\delta}{d\theta} \right) \left( \frac{B}{Af} \right)^2 \right\} \quad (7-e)$$

Since

$$v_1^{*2} = \frac{1}{4} (v_1^* + v_3^* + v_1^* - v_3^*)^2 = \frac{1}{4} (\hat{v}^* + \hat{v}^*)^2 = \frac{1}{4m^2} (\hat{v}_m^* + \hat{v}_m^*)^2$$

the use of Eqs. 7-c and 7-d yields:

$$[v_1^{*2}] = \frac{k^2 A^2}{8a^2 \cos^2 \theta} \left\{ 1 + \left( \frac{B}{Af} \right)^2 \right\} + \frac{1}{4} \frac{k^2}{a^2 \cos^2 \theta} \frac{AB}{f} \cos k\delta \quad (7-f)$$

The meridional eddy kinetic energy at Level 2 is obtained from the geostrophic equilibrium, Eq. 5-s, which yields:

$$fv_1^* = m \frac{\partial \phi_1^*}{\partial x}$$

$$fv_3^* = m \frac{\partial \phi_3^*}{\partial x}$$

or

$$f(v_1^* + v_3^*) = m \frac{\partial (\phi_1^* + \phi_3^*)}{\partial x}$$

Using  $\phi_1^* + \phi_3^* = 2\phi_2^*$

$$f(v_1^* + v_3^*) = 2m \frac{\partial \phi_2^*}{\partial x} = 2fv_2^*$$

whence

$$v_2^* = \frac{v_1^* + v_3^*}{2} = \frac{1}{2} v^* = \frac{1}{2} \frac{v_m^*}{m}$$

which, with Eq. 7-d, yields:

$$k^2 A^2 = 8a^2 [v_2^{*2}] \cos^2 \theta \quad (7-g)$$

The combination of Eqs. 7-f and 7-g gives the expression

$$\left(\frac{B}{Af}\right)^2 + 2 \cos k\delta \left(\frac{B}{Af}\right) - \left\{ \frac{[v_1^{*2}]}{[v_2^{*2}]} - 1 \right\} = 0$$

or

$$\frac{B}{Af} = \sqrt{\cos^2 k\delta + \frac{[v_1^{*2}]}{[v_2^{*2}]} - 1} - \cos k\delta \quad (7-h)$$

while Eqs. 5-y and 7-g yield:

$$\frac{B}{Af} = \frac{kH_m}{2af[v_2^{*2}] \cos^2 \theta} \frac{1}{\sqrt{1 - \cos^2 k\delta}} \quad (7-i)$$

and Eq. 7-e with 7-g:

$$\frac{d\alpha\theta}{d\theta} = \left\{ 1 + \left(\frac{B}{Af}\right)^2 \right\}^{-1} \left\{ \frac{M_{m1}}{2[v_2^{*2}] \cos^3 \theta} + \left(\frac{B}{Af}\right)^2 \frac{d\delta}{d\theta} \right\} \quad (7-j)$$

Thus, Eqs. 7-h and 7-i yield  $B/Af$  and  $k\delta$  as a function of the statistics of the long-term general circulation involving the meridional eddy kinetic energies at Levels 1 and 2, and the transport of sensible heat; Eq. 7-j yields  $d\alpha\theta/d\theta$  as a function of the transports of angular momentum and sensible heat as well as the meridional eddy kinetic energies at Levels 1 and 2. Differentiation of Eq. 7-g yields:

$$\frac{1}{A} \frac{dA}{d\theta} = \frac{1}{2} \frac{1}{[v_2^{*2}]} \frac{d[v_2^{*2}]}{d\theta} - \tan \theta \quad (7-k)$$

while differentiation of the quadratic equation for  $(B/Af)$  gives the expression

$$\frac{1}{B} \frac{dB}{d\theta} = \frac{1}{A} \frac{dA}{d\theta} + \cotn \theta + \left\{ \frac{1}{2} \frac{Af}{B} \frac{d}{d\theta} \frac{[v_1^{*2}]}{[v_2^{*2}]} + k \sin k\delta \cdot \frac{d\delta}{d\theta} \right\} \left\{ \frac{B}{Af} + \cos k\delta \right\}^{-1} \quad (7-l)$$

Similarly,  $d\delta/d\theta$  can be obtained either by differentiation of Eq. 7-i or numerically from  $k^{-1} d(k\delta)/d\theta$ . Since  $u_1^{*2} = \left(\frac{1}{4m^2}\right)(\bar{u}_m^* + \hat{u}_m^*)^2$ , Eqs.

7-a and 7-b yield the following expression for the zonal eddy kinetic energy at Level 1:

$$\frac{[u_1^{*2}]}{[v_2^{*2}] \cos^2 \theta} = \left(\frac{d\alpha\theta}{d\theta}\right)^2 + \frac{1}{k^2} \left(\frac{1}{A} \frac{dA}{d\theta}\right)^2 + \left(\frac{B}{Af}\right)^2 \left\{ \left(\frac{d\alpha\theta}{d\theta} - \frac{d\delta}{d\theta}\right)^2 + \frac{1}{k^2} \left(\frac{1}{B} \frac{dB}{d\theta}\right)^2 \right\} + T_{e_1} \quad (7-m)$$

Where the term  $T_{e_1}$  is given by

$$T_{e1} = \frac{H_m}{af[v_2^{*2}] \cos^2 \theta} \left\{ k \operatorname{ctn} k\delta \cdot \frac{d\alpha\theta}{d\theta} \left( \frac{d\alpha\theta}{d\theta} - \frac{d\delta}{d\theta} \right) + \frac{1}{k} \operatorname{ctn} k\delta \cdot \frac{1}{A} \frac{dA}{d\theta} \cdot \frac{1}{B} \frac{dB}{d\theta} \right. \\ \left. + \frac{1}{A} \frac{dA}{d\theta} \left( \frac{d\alpha\theta}{d\theta} - \frac{d\delta}{d\theta} \right) - \frac{1}{B} \frac{dB}{d\theta} \frac{d\alpha\theta}{d\theta} \right\}$$

Using Eqs. 7-a and 7-d, the expression  $(1/m^4)[\hat{u}_m^* \hat{v}_m^*]$  is modified to the general form:

$$\frac{[\hat{u}_m^* \hat{v}_m^*]}{m^4} = \frac{1}{2} \frac{k^2 AB}{a^2 f_m} \left\{ \left( \frac{d\alpha\theta}{d\theta} - \frac{d\delta}{d\theta} \right) \cos k\delta - \frac{1}{k} \frac{1}{B} \frac{dB}{d\theta} \sin k\delta \right\} \quad (7-n)$$

Using the expression  $[\hat{u}_m^* \hat{v}_m^*]/m^4 = H_m/f_m S$  and Eq. 7-n, the definition for S is modified to yield  $S(\theta)$  as follows:

$$S(\theta) = \frac{a}{2} \frac{1}{k} \frac{\sin k\delta}{\left( \frac{d\alpha\theta}{d\theta} - \frac{d\delta}{d\theta} \right) \cos k\delta - \frac{1}{k} \frac{1}{B} \frac{dB}{d\theta} \sin k\delta} \quad (7-o)$$

Figure 17 shows the annual variance of the meridional wind component resulting from both the transient  $[\overline{v'^2}]$  and stationary  $[\bar{v}^{*2}]$  eddies for the three levels as given by the most recent reduction of available data (Oort and Rasmusson, 1971). Figure 18 shows similar data for the zonal wind component. Figure 19 indicates the behavior of the ratio  $[\overline{v_1'^2}]/[\bar{v}_2^{*2}]$  as obtained from the data in Fig. 17, a ratio that appears in Eqs. 7-h and 7-l.

Figure 20 shows the phase lag parameter as a function of the wave number in the range  $1 \leq k \leq 8$ . The parameter  $k\delta$  in this figure is derived from the simultaneous solution of Eqs. 7-h and 7-i, a procedure that requires the use of the experimental data shown in Figs. 15, 17, and 19. Note that for low latitudes there are no solutions from Eqs. 7-i and 7-h for the specified behavior of  $[\overline{v_1'^2}]/[\bar{v}_2^{*2}]$  in Fig. 19 at those latitudes; since as  $k\delta \rightarrow 0$  in Fig. 20,  $B/Af$  becomes very large in Eq. 7-i but remains finite in Eq. 7-h. This is a result that is expected from the breakdown of the geostrophic equilibrium, i.e., Eqs.

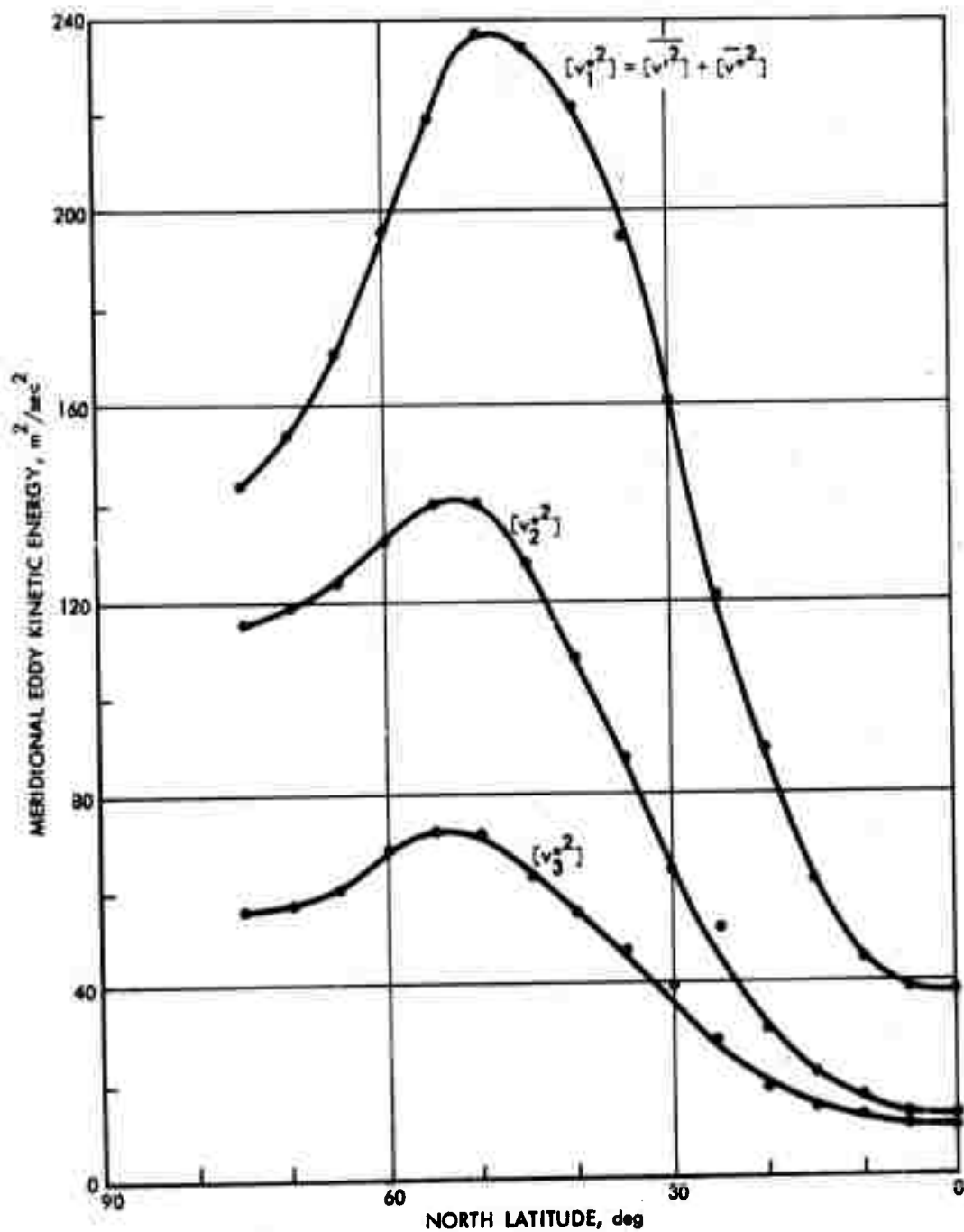


FIGURE 17. Experimental Transient Plus Standing Meridional Eddy Kinetic Energy at Levels 1, 2, and 3 (250, 500, and 750 mb, respectively) as Obtained from Oort-Rasmusson Annual Data (1971)

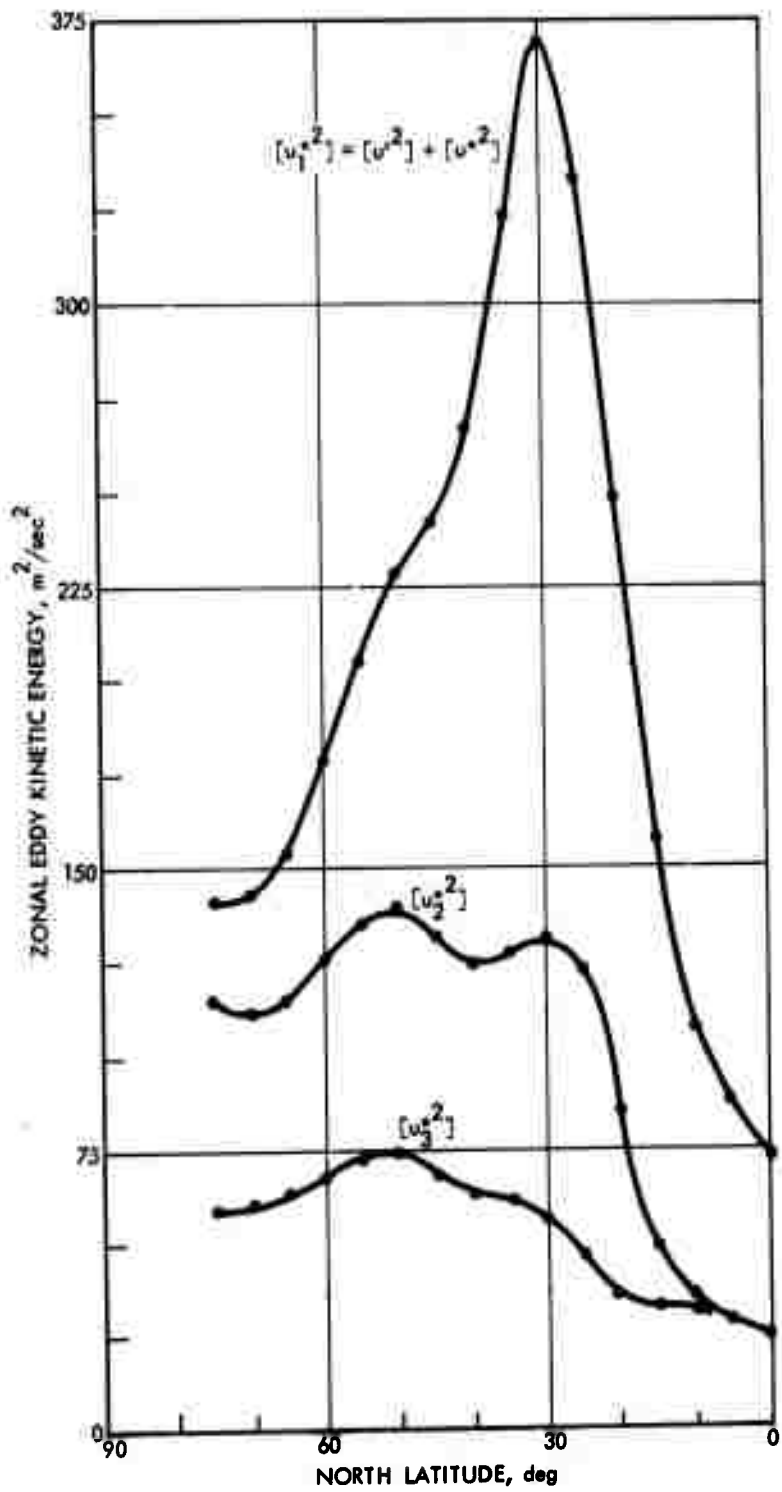


FIGURE 18. Experimental Transient Plus Standing Eddy Kinetic Energy at Levels 1, 2, and 3 (250, 500, and 750 mb, respectively) as Obtained from Oort-Rasmusson Annual Data (1971)

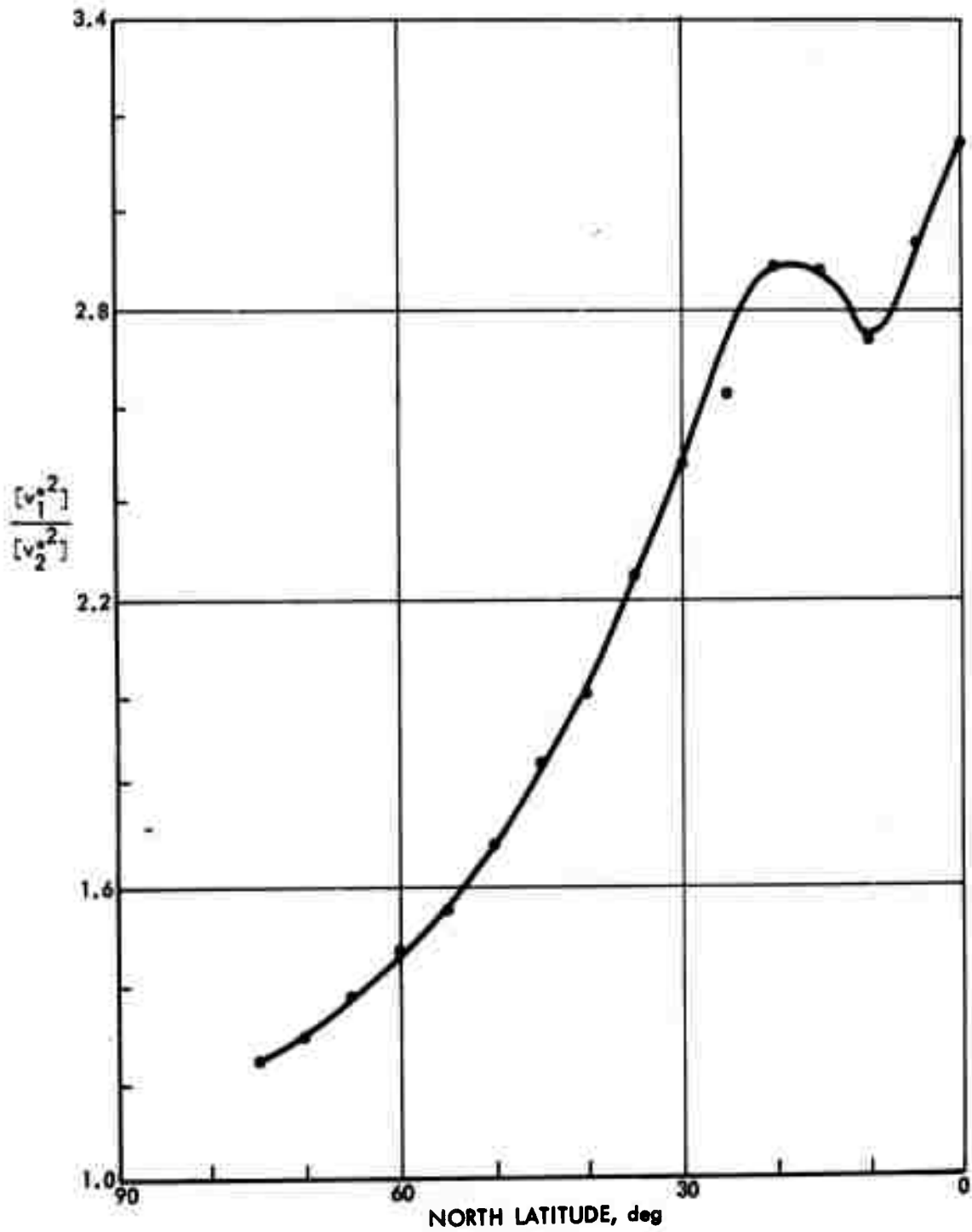


FIGURE 19. Experimental Ratio of Transient Plus Standing Meridional Eddy Kinetic Energy at Level 1 (250 mb) to that of Level 2 (500 mb) as Obtained from Oort-Rasmusson Annual Data (1971)

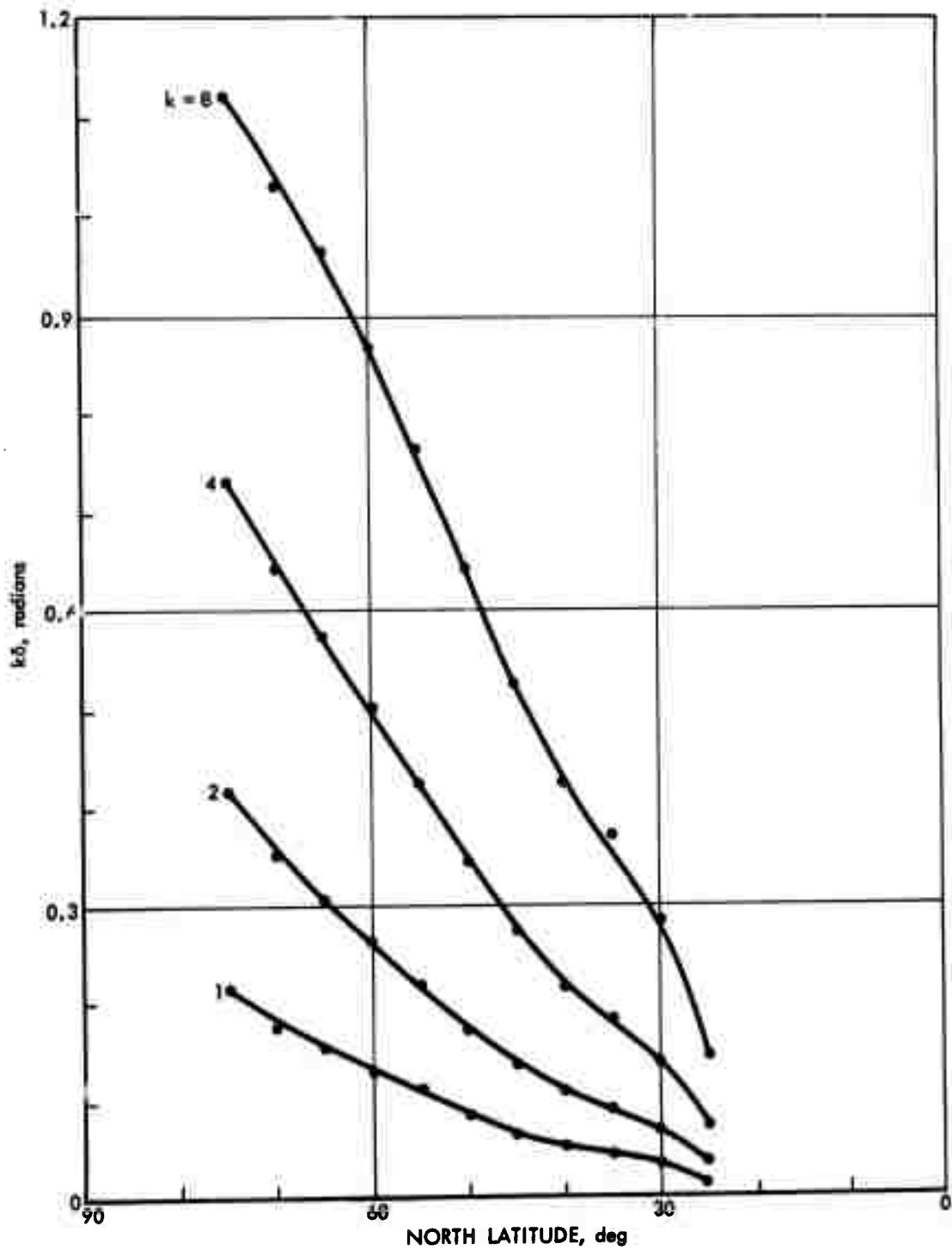


FIGURE 20. Value of  $k\delta$  as Determined from the Oort-Rasmusson Annual Data (1971) for the Meridional Eddy Kinetic Energy and the Transport of Sensible Heat

5-r and 5-s. The data in Fig. 20 indicate that  $d\delta/d\theta > 0$  regardless of latitude and wave number in the ranges indicated in the figure. The latitudinal variation of  $d\alpha\theta/d\theta$  is indicated in Fig. 21, a result that is obtained from Eq. 7-j using the experimental data in Figs. 16 and 17 as well as the previous results for  $B/Af$  and  $d\delta/d\theta$ . Since  $\alpha\theta = \int (d\alpha\theta/d\theta)d\theta$ , a constant tilt  $\alpha$  would require a constant value of  $d\alpha\theta/d\theta$ ; thus, Fig. 12 shows that the tilt depends on the latitude. Since  $d\alpha\theta/d\theta$  may be approximated by the linear relation:

$$\frac{d\alpha\theta}{d\theta} \approx -0.62\theta + 0.61$$

in the range  $25 \leq \theta \leq 65^\circ$ , then

$$\alpha = 0.61 - 0.31\theta + b/\theta$$

where  $b$  is a constant of integration and  $\alpha$  as well as  $\theta$  are given in radians. This relation then indicates that the tilt becomes more pronounced as the latitude decreases, a trend already identified earlier (Starr, 1948). Figure 22 shows the latitudinal variation of the amplitude of the stream function, Eq. 5-v; the parameter  $kA/a$  is obtained from Eq. 7-g and the experimental data in Fig. 17. Figure 22 indicates that the amplitude of the stream function reaches a maximum at the middle latitudes. Figure 23 shows the latitudinal variation of the parameter  $B/Af$ , which is derived from Eqs. 7-h and 7-i as in the solution of  $k\delta$ . The parameter  $(1/A)(dA/d\theta)$  is shown in Fig. 24; it is derived from Eq. 7-k and the experimental data in Fig. 17. This parameter is independent of wave number as indicated by Eq. 7-k. Figure 25 shows the parameter  $(1/B)(dB/d\theta)$  as derived from Eq. 7-l and the experimental data in Fig. 19. Using Eq. 7-o, the reciprocal of the parameter  $2S(\theta)/a$  is as shown on the ordinate of Fig. 26; this figure indicates that  $S(\theta) \rightarrow \infty$  at  $\theta \approx 52$  deg N, i.e., at the latitude where  $dH_m/d\theta \rightarrow 0$  and  $M_{m,1} \rightarrow 0$  as indicated by Figs. 15 and 16. Note that these conditions exhibited by the experimental data in Figs. 15, 16, and 26 do satisfy Eq. 5-x, which is one of the two fundamental equations

that allow the determination of the large-scale transports of angular momentum and sensible heat, the other fundamental equation being 5-q that is derived from the laws of motion.

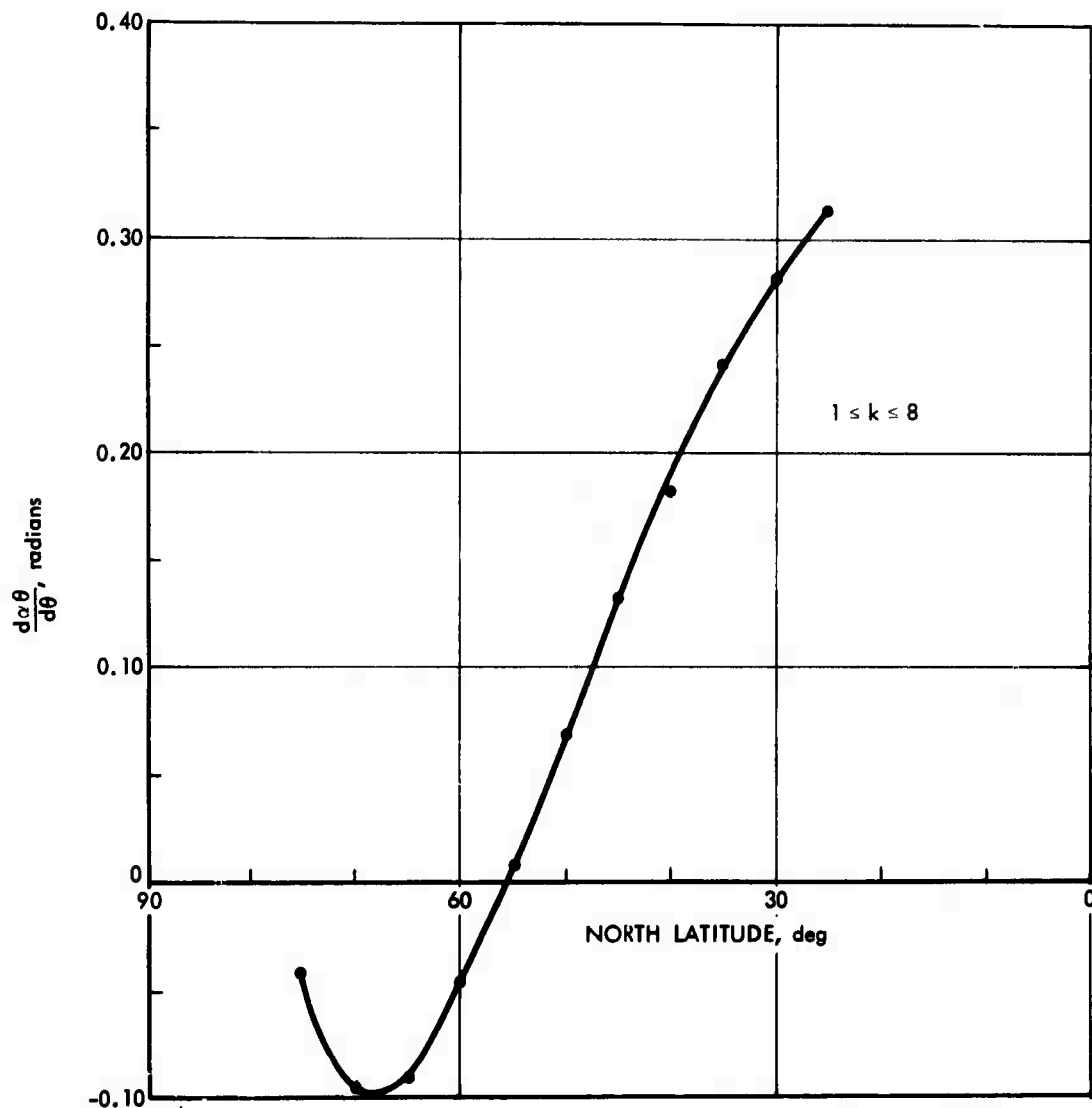


FIGURE 21. Value of  $d\alpha\theta/d\theta$  as Determined from the Oort-Rasmusson Annual Data (1971) for the Transports of Angular Momentum and Sensible Heat as Well as the Meridional Eddy Kinetic Energy

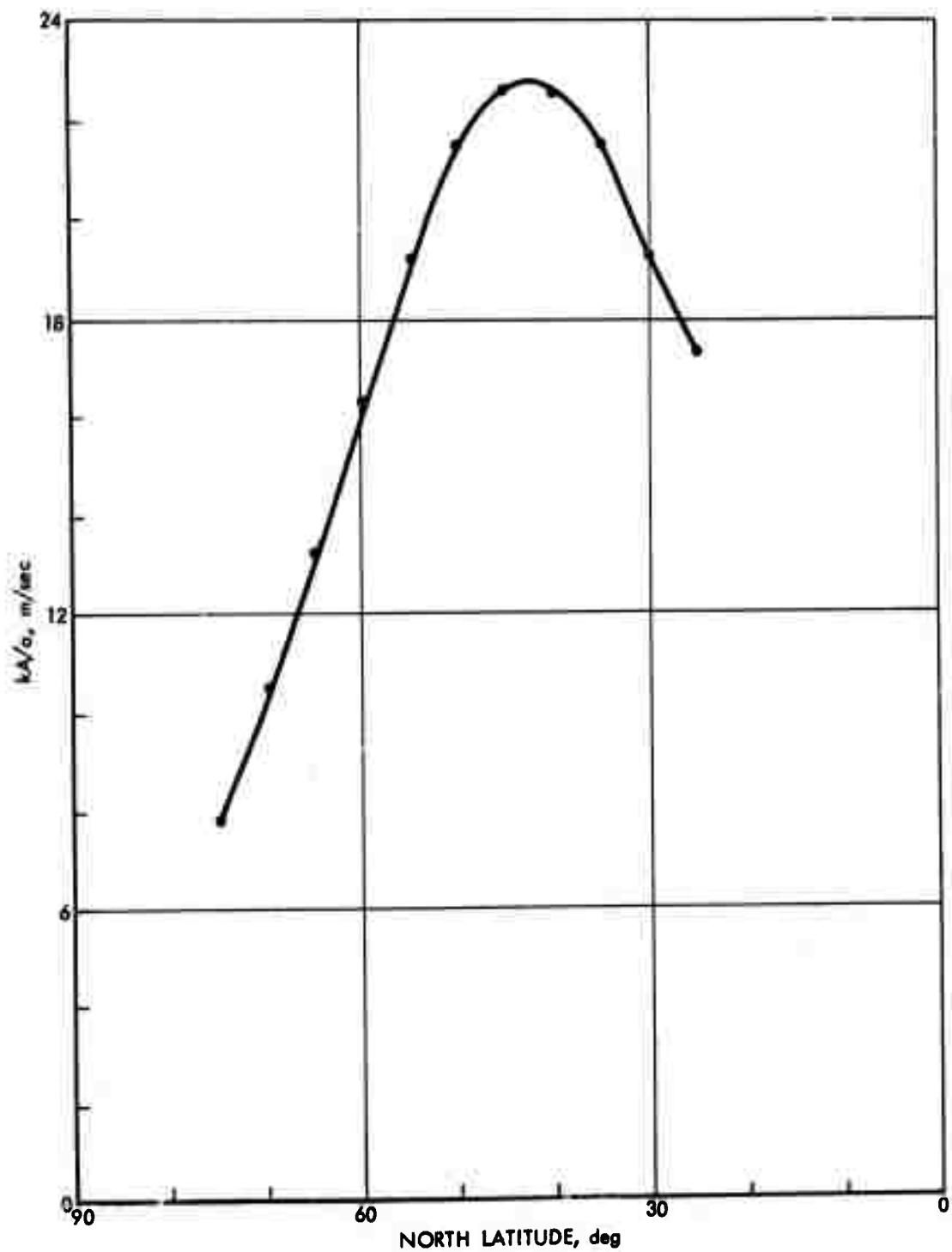


FIGURE 22. Value of  $kA/a$  as Determined from the Oort-Rasmusson Annual Data (1971) for the Meridional Eddy Kinetic Energy at 500 mb

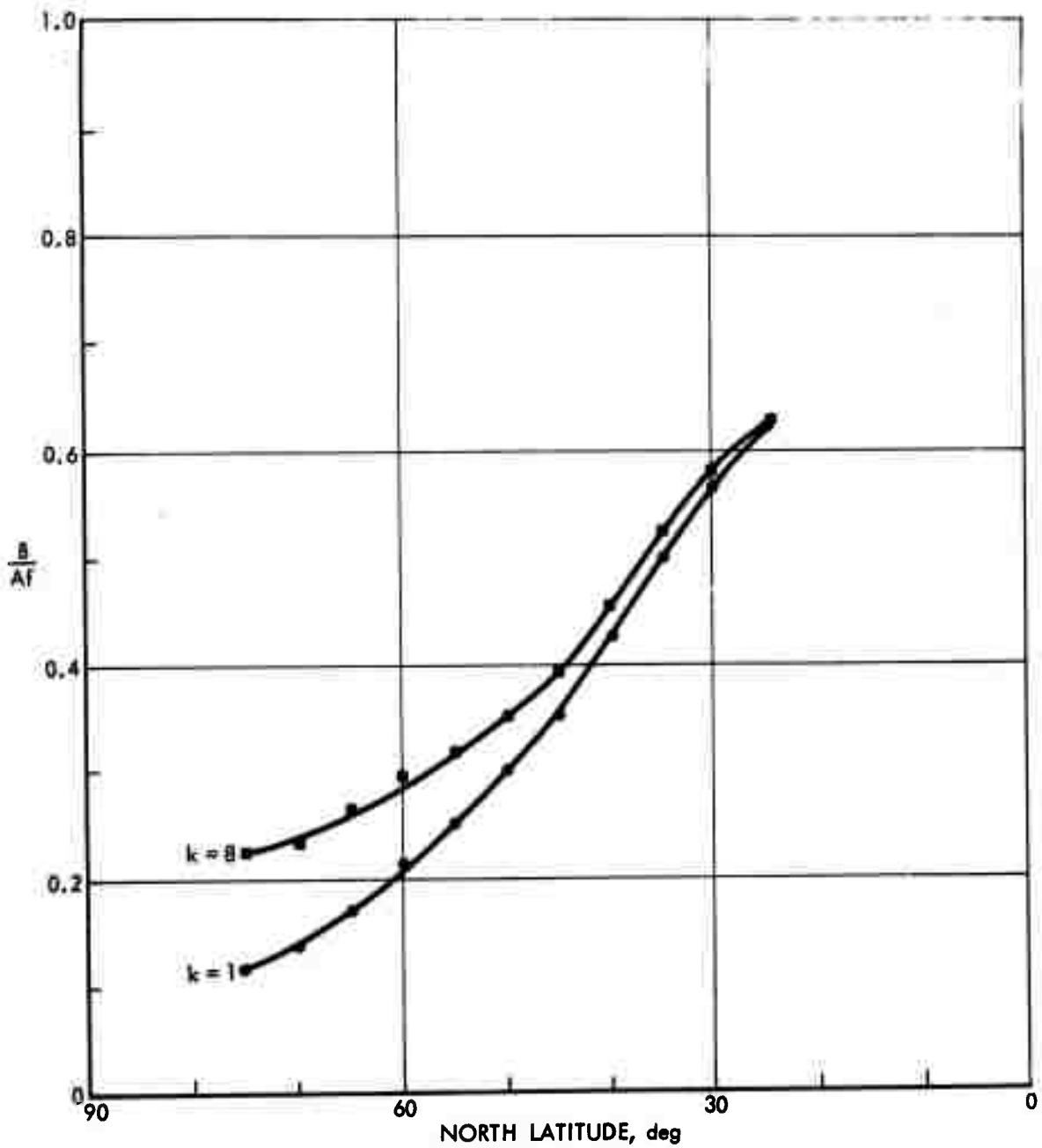


FIGURE 23. Value of  $B/Af$  as Determined from the Oort-Rasmuson Annual Data (1971) for the Meridional Eddy Kinetic Energy and the Transport of Sensible Heat

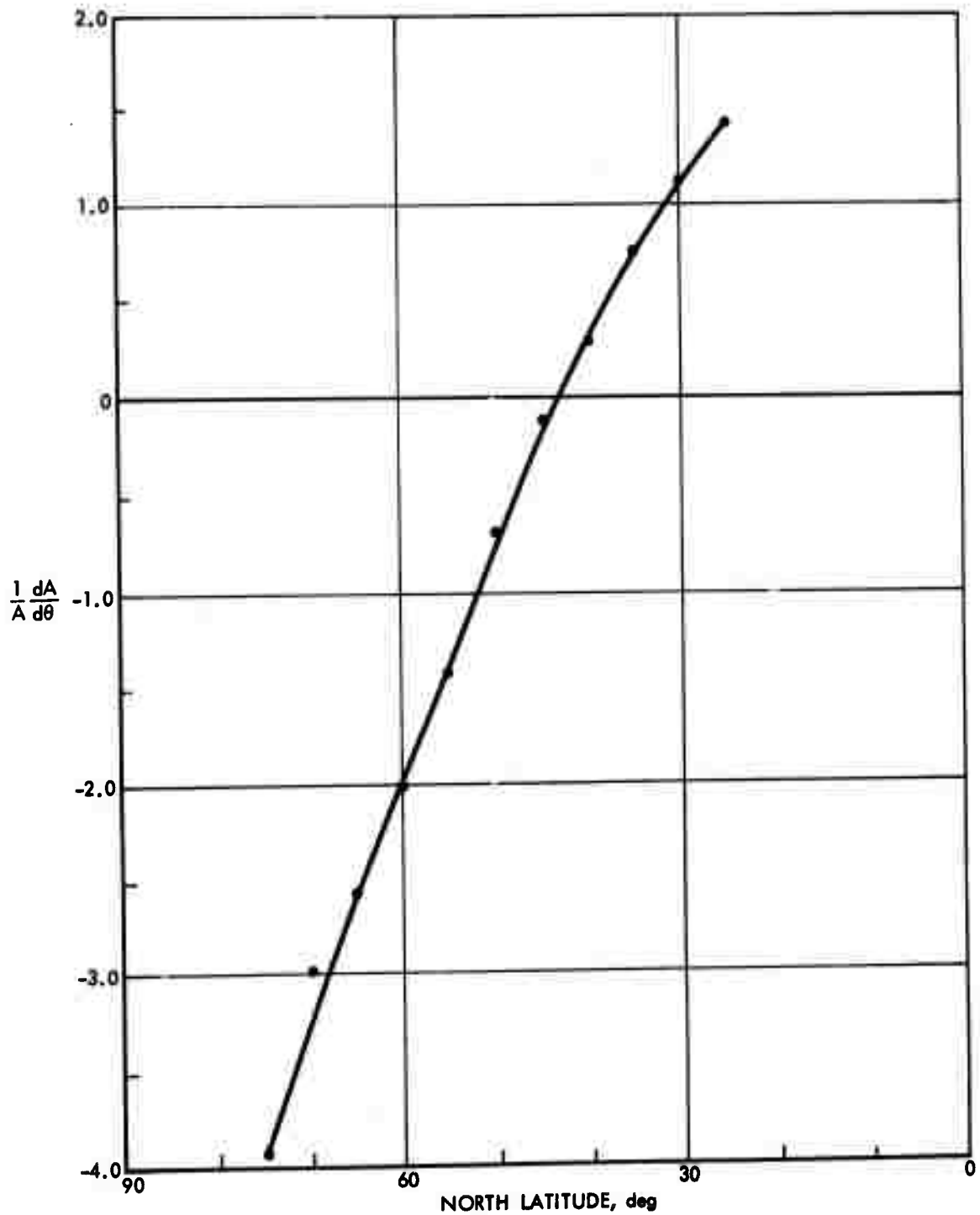


FIGURE 24. Value of  $(1/A) (dA/d\theta)$  as Determined from the Oort-Rasmusson Annual Data (1971) for the Meridional Eddy Kinetic Energy at 500 mb

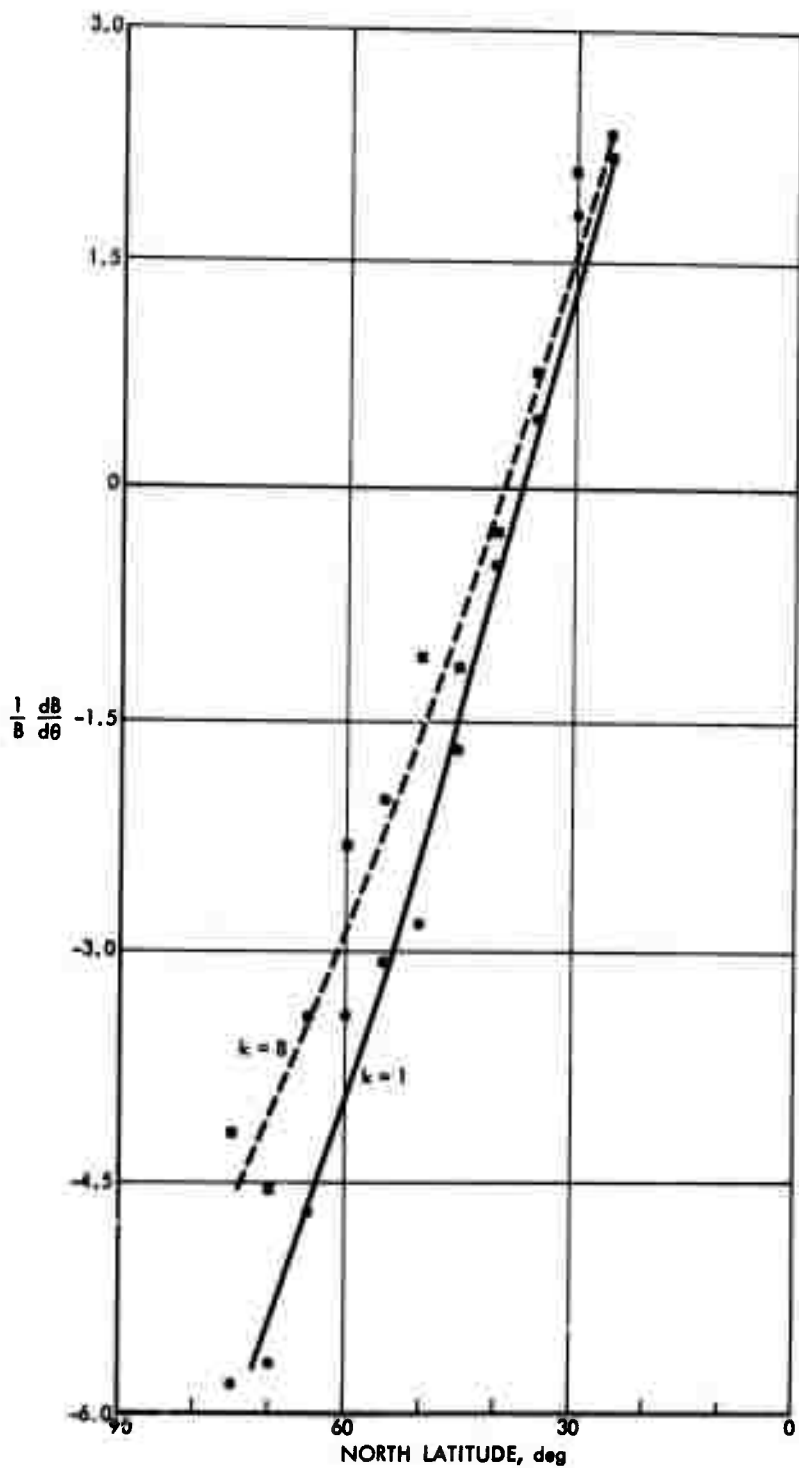


FIGURE 25. Value of  $(1/B) (dB/d\theta)$  as Determined from the Oort-Rasmusson Annual Data (1971) for the Meridional Eddy Kinetic Energy and the Transport of Sensible Heat

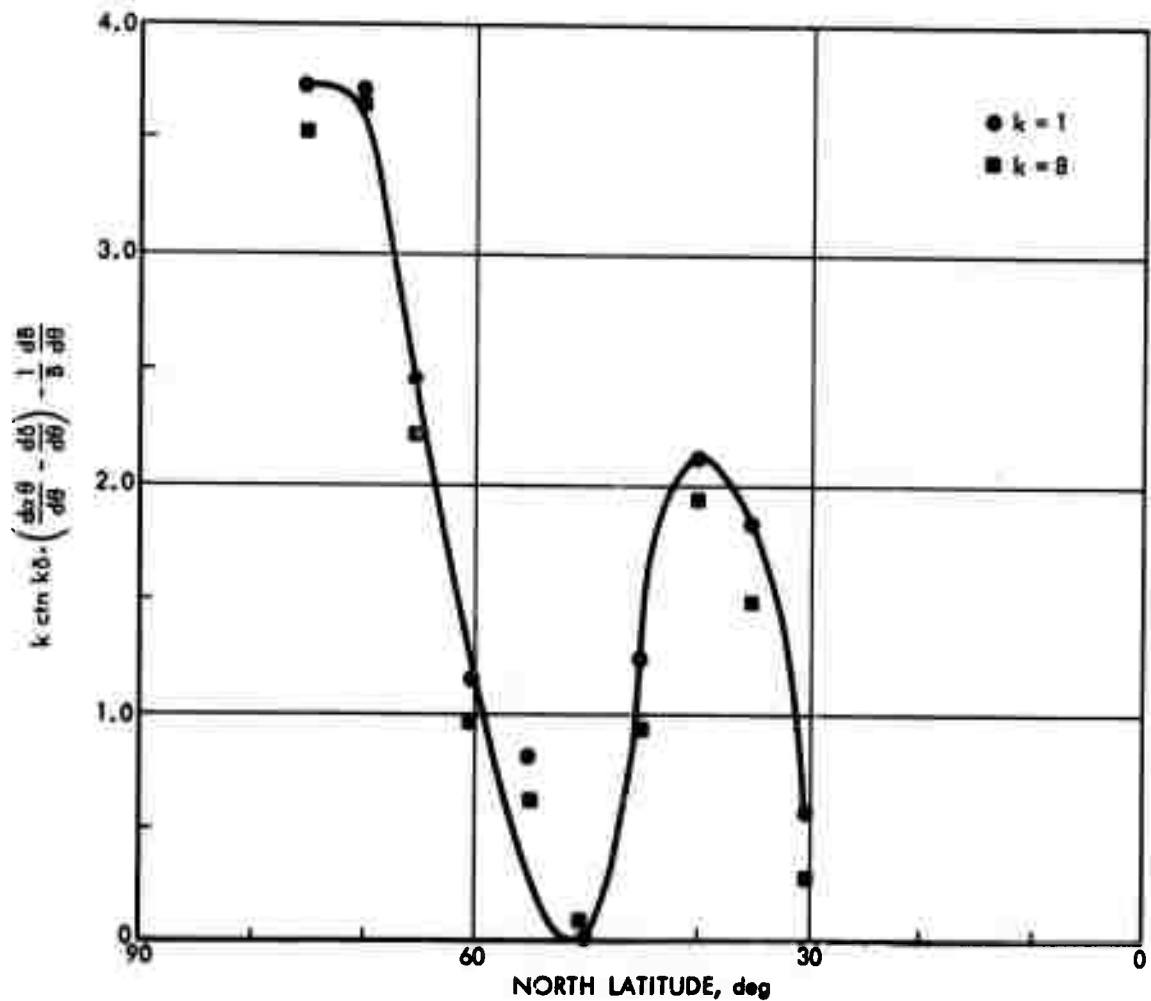


FIGURE 26. Reciprocal of  $2S/a$  Parameter as Determined from the Oort-Rasmusson Annual Data (1971) for the Eddy Zonal and Meridional Kinetic Energy as Well as the Transports of Sensible Heat and Angular Momentum

Figure 27 shows the ratio of the zonal eddy kinetic energy from the transient and eddy motions at the 250-mb level to the corresponding meridional eddy kinetic energy at the 500-mb level; these values were obtained from the most recent available experimental data (Oort-Rasmusson, 1971) and Eq. 7-m in the wave number range of interest for climate. This figure shows that a wave number of unity, corresponding to a wave length equal to a latitudinal circle with radius  $a \cos \theta$ ,

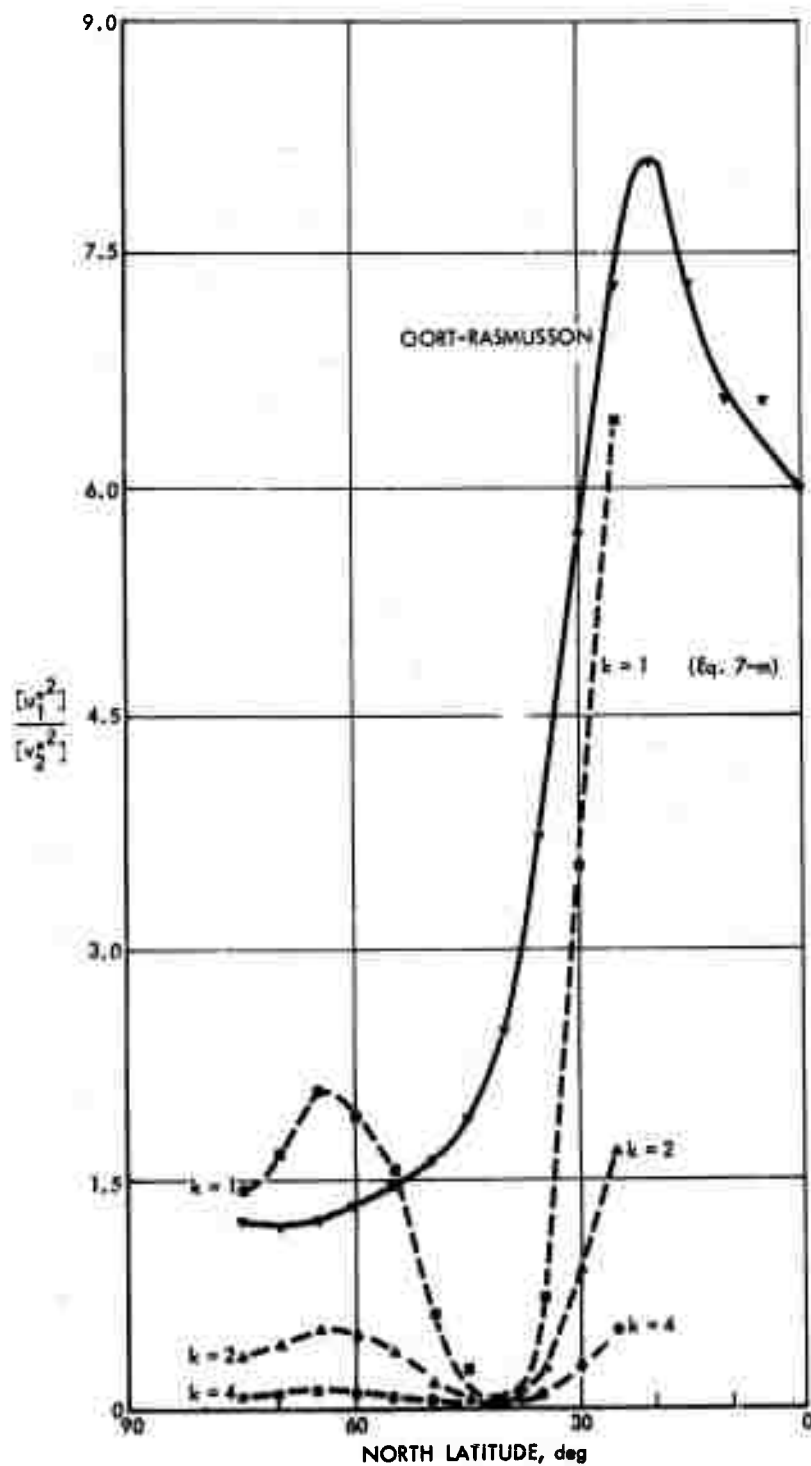


FIGURE 27. Ratio of Transient Plus Standing Zonal Eddy Kinetic Energy at 250 mb to the Corresponding Meridional Value at 500 mb. Solid Line Determined from Oort-Rasmusson Annual Data (1971). Dashed Lines Determined from Eq. 7-m.

yields the zonal eddy kinetic energy at the 250-mb level. The discrepancy at higher latitudes in the shape between the experimental and analytical curve for  $k = 1$  in Fig. 27 may be attributed to the shape exhibited by  $[u_1^{*2}]$  in Fig. 18 at those latitudes. Figure 20 indicates, then, that the phase lag parameter  $\delta \approx 0.1$  radian at a latitude corresponding to the maximum transport of sensible heat (Fig. 15).

IX. FORMULATION OF THE THEORY OF THE GENERAL CIRCULATION FOR  
CLIMATE BASED ON A VARIABLE TILT, PHASE LAG, AND  
AMPLITUDES OF THE BAROCLINIC DISTURBANCES

The experimental data for the transports of angular momentum and sensible heat, as well as for the meridional and zonal eddy kinetic energies, provide the following results:

1. A successful test of the formulation of the large-scale transports, as given by Eq. 5-x, at the latitude for maximum transport of sensible heat.
2. A wave number with a magnitude appropriate for climate that includes the effects of baroclinic disturbances and a non-homogeneous earth's surface.
3. The variation with latitude of the tilt and phase lag wave parameters as well as of the amplitudes of the stream function and temperature disturbances.

These results indicate that the assumptions of constant  $B$ ,  $\alpha$ , and  $\delta$  used for the evaluation of  $[\hat{u}_m^* \hat{v}_m^*] / m^4$  in the constant  $S$  model are not verified by the experimental data. Thus, all the limitations of the constant  $S$  theory described earlier can be removed by the calculation of a local  $S(\theta)$  as given by Eq. 7-0, a procedure that eliminates the need for a rather weak boundary condition at the pole to determine the constant  $S$ . Further, the available experimental data can be used to select boundary conditions at a latitude corresponding to near the north edge of the Hadley cell (where the ITCZ predominates, i.e., Figs. 6, 7); this procedure eliminates the need for the use of a non-existing geostrophic equilibrium near the equator, when considering

advertent modifications of the climate of the earth's surface at the middle and higher latitudes.\*

The modification of the constant S theory to allow the determination of the local  $S(\theta)$  parameter, as well as the meridional and zonal eddy kinetic energies at Levels 1 and 2, involves the use of expressions that relate the transports of sensible heat and angular momentum to the wave and amplitude parameters (i.e., Eqs. 5-y and 7-e), the approximation  $\bar{M}_m \approx \hat{M}_m \approx M_{m,1}$ , and the eddy kinetic energy at the 250-mb level. Thus, using a procedure similar to that for the derivation of Eq. 7-e, i.e., the identity  $\widehat{u_m^* v_m^*} = (1/2)\{\hat{u}_m^* \hat{v}_m^* + \bar{u}_m^* \bar{v}_m^*\}$ , and Eqs. 7-a through 7-d:

$$\hat{M}_m = \frac{H_m}{afm} \left\{ \left( 2 \frac{d\alpha\theta}{d\theta} - \frac{d\delta}{d\theta} \right) k \operatorname{ctn} k\delta + \frac{1}{A} \frac{dA}{d\theta} - \frac{1}{B} \frac{dB}{d\theta} \right\} \quad (7-p)$$

or

$$\left( 2 \frac{d\alpha\theta}{d\theta} - \frac{d\delta}{d\theta} \right) k \operatorname{ctn} k\delta + \frac{1}{A} \frac{dA}{d\theta} - \frac{1}{B} \frac{dB}{d\theta} = \frac{afm}{H_m} M_{m,1} \quad (7-q)$$

Note that the eddy kinetic energy equation could also be applied at Level 3; however, the approximation  $\bar{M}_m \approx \hat{M}_m$  used in Eq. 7-q yields no angular momentum at Level 3 as can formally be seen from the following relations:

$$[u_3^* v_3^*] = \frac{1}{4} [(\bar{u}^* - \hat{u}^*)(\bar{v}^* - \hat{v}^*)] = \frac{1}{4m^2} [(\bar{u}_m^* - \hat{u}_m^*)(\bar{v}_m^* - \hat{v}_m^*)]$$

---

\* Numerical calculations using the Mintz-Arakawa model (Gates, 1971) for two conditions representing the current Arctic environment and that of a postulated Arctic without the ice indicate no changes at these low latitudes in the temperature, the geopotential height, and the east-west winds in the lower (i.e., 1000-, 800-, and 400-mb levels) troposphere (Warshaw and Rapp, 1972).

Expanding the right-hand side of this expression and using the identities for  $\overline{u_m^* v_m^*}$  as well as  $\widehat{u_m^* v_m^*}$ :

$$[u_3^* v_3^*] = \frac{m^2}{2} (\overline{M}_m - \widehat{M}_m) \quad (7-r)$$

Similarly

$$[u_1^* v_1^*] = \frac{1}{4} [(\overline{u}^* + \widehat{u}^*)(\overline{v}^* + \widehat{v}^*)] = \frac{1}{4m^2} [(\overline{U}_m^* + \widehat{U}_m^*)(\overline{V}_m^* + \widehat{V}_m^*)]$$

or

$$[u_1^* v_1^*] = \frac{m^2}{2} (\overline{M}_m + \widehat{M}_m) = m^2 \widehat{M}_m = m^2 M_{m_1} \quad (7-s)$$

Thus, the approximation  $\overline{M}_m \approx \widehat{M}_m$  implies that the dynamics in the lower half of the atmosphere are relatively unimportant as compared with those of the upper half of the atmosphere.

The kinetic energy per unit mass for the horizontal motion in the troposphere is given by (Lorenz, 1967)

$$\frac{dK_e}{dt} = -\frac{1}{\rho} \vec{U} \cdot \vec{\nabla}_z p + \vec{U} \cdot \vec{F} \quad (8-a)$$

where  $K_e = (1/2) \vec{U} \cdot \vec{U} = (1/2)(u^2 + v^2)$ . Using the condition of vertical hydrostatic equilibrium and the geostrophic potential  $\phi = gz$ ,

$$\vec{\nabla}_z p = \rho g \vec{\nabla}_p z = \rho \vec{\nabla} \phi$$

Thus, Eq. 8-a becomes

$$\frac{dK_e}{dt} = -\vec{U} \cdot \vec{\nabla} \phi + \vec{U} \cdot \vec{F} \quad (8-b)$$

Equation 8-b must then be included in the set of primitive Eqs. 5-e through 5-h.

Using the continuity and hydrostatic equations (5-g and 5-h) in Eq. 8-b, making use of spherical coordinates, taking the zonal average, separating the eddy and circulation terms, and using  $\partial/\partial t \rightarrow 0$  for climate, Eq. 8-b can be written in the following form (Appendix B):

$$\begin{aligned} \frac{m}{a} \frac{\partial}{\partial \theta} \left\{ \frac{[K_E][v]}{m} + \frac{[K_E v^*]}{m} + \frac{[\phi^* v^*]}{m} \right\} + \frac{\partial}{\partial p} \left\{ [K_E][\omega] + [K_E \omega^*] + [\phi^* \omega^*] \right\} \\ + \frac{R}{p} [T^* \omega^*] - [u^* F_\lambda^* + v^* F_\theta^*] - \left\{ \frac{m^2}{a} \frac{\partial}{\partial \theta} \frac{[u^* v^*]}{m^2} + \frac{\partial [u^* \omega^*]}{\partial p} \right\} [u] \\ - \left\{ \frac{\tan \theta}{a} [u^{*2}] + \frac{m}{a} \frac{\partial}{\partial \theta} \frac{[v^{*2}]}{m} + \frac{\partial [v^* \omega^*]}{\partial p} \right\} [v] = 0 \quad (8-c) \end{aligned}$$

where

$$K_E = \frac{1}{2} \vec{u}^* \cdot \vec{u}^* + [\vec{u}] \cdot u^* = \frac{1}{2} u^{*2} + \frac{1}{2} v^{*2} + [u] u^* + [v] v^*$$

and

$$[K_E] = \frac{1}{2} [u^{*2}] + \frac{1}{2} [v^{*2}] \equiv K^*$$

When applying Eq. 8-c to the 250-mb level, some of the terms in this equation may be simplified through the use of the relations for the eddy winds (Eqs. 7-a through 7-d), the geostrophic equilibrium, the boundary conditions for  $\omega$  (Fig. 13), and the continuity equation (5-g). Thus, the second term in the first bracket yields

$$[K_{E_1} v_1^*] = \frac{1}{2} [u_1^{*2} v_1^*] + \frac{1}{2} [v_1^{*3}] + [u_1] [u_1^* v_1^*] + [v_1] [v_1^{*2}]$$

The triple correlations in the right-hand side of this expression vanish, as it can be seen from the following:

$$[u_1^{*2} v_1^*] = \frac{1}{8} [(\bar{u}^* + \hat{u}^*)^2 (\bar{v}^* + \hat{v}^*)] = \frac{1}{8m^3} [(\bar{u}_m^* + \hat{u}_m^*)^2 (\bar{v}_m^* + \hat{v}_m^*)]$$

Expanding the product  $(\bar{u}_m^* + \hat{u}_m^*)^2 (\bar{v}_m^* + \hat{v}_m^*)$ , using Eqs. 7-a through 7-d, and taking the zonal average of each of the six individual terms in this product, the results contain the zonal average of cubic terms given by the product of sines and cosines; e.g.,  $[\sin^c \eta \cos^d \eta]$ ,  $[\cos^c \eta \cos^d (\eta + k\delta)]$ ,  $[\cos^c \eta \sin^d (\eta + k\delta)]$ ,  $[\sin^c \eta \cos^d (\eta + k\delta)]$ ,  $[\sin \eta \cos \eta \sin (\eta + k\delta)]$ , etc., where  $c + d = 3$  and either  $c$  or  $d$  take values 0, 1, 2, or 3. Since the zonal average of each of these cubic products vanishes,  $[u_1^{*2} v_1^*] = 0$ . Similarly, since

$$[v_1^{*3}] = \frac{1}{8} [(\bar{v}^* + \hat{v}^*)^3] = \frac{1}{8m^3} [(\bar{v}_m^* + \hat{v}_m^*)^3]$$

the results contain again four cubic terms involving the expression  $[\cos^c \eta \cos^d (\eta + k\delta)]$ . Hence  $[v_1^{*3}] = 0$ . Thus, using Eq. 7-s:

$$[K_{E_1} v_1^*] = m^2 [u_1] M_{m_1} + [v_1] [v_1^{*2}] \quad (8-d)$$

where  $[v_1^{*2}]$  is given by Eq. 7-f. The third term in the first bracket of Eq. 8-c vanishes, as it can be seen from the use of the geostrophic equilibrium, i.e.

$$[\phi_1^* v_1^*] = \frac{m}{f} \left[ \phi_1^* \frac{\partial \phi_1^*}{\partial x} \right] = \frac{m}{2f} \left[ \frac{\partial \phi_1^{*2}}{\partial x} \right] = 0 \quad (8-e)$$

The first term in the second bracket of Eq. 8-c may be written as:

$$\frac{\partial}{\partial p} [K_E] [\omega] = \frac{\partial}{\partial p} K^*[\omega] = \frac{0 - K_2^*[\omega_2]}{0 - p_2} = \frac{2 K_2^*[\omega_2]}{p_4}$$

Since the continuity equation with the boundary conditions for  $\omega$  yields

$$D_1 = - \frac{(\partial \omega)}{(\partial p)_1} = - \frac{\omega_0 - \omega_2}{0 - p_2} = - \frac{\omega_2}{p_2}$$

one can write

$$\frac{2 [\omega_2]}{p_4} = \frac{[\omega_2]}{p_2} = -[D_1] = - \frac{m}{a} \frac{\partial}{\partial \theta} \frac{[v_1]}{m}$$

or

$$\frac{\partial}{\partial p} [K_E] [\omega] = - K_2^* \frac{m}{a} \frac{\partial}{\partial \theta} \frac{[v_1]}{m} \quad (8-f)$$

The condition  $[\hat{F}] = -[\hat{F}]$  that was used in Eqs. 5-n and 5-o implies  $[F_1] = 0$ , hence  $[F_1^*] = 0$ . Thus, using Eq. 7-s as well as Eqs. 8-d through 8-f, and the notation  $\partial [X\omega^*]/\partial p = 2 [X_2\omega_2^*]/p_4$  where  $X_2$  denotes  $K_{E,2}$ ,  $\phi_2^*$ ,  $u_2^*$  or  $v_2^*$ , Eq. 8-c applied at the upper half of the atmosphere yields:

$$\begin{aligned} & \frac{m}{a} \frac{\partial}{\partial \theta} \left\{ \frac{K_1^*[v_1]}{m} + m [u_1] M_{m_1} + \frac{[v_1][v_1^{*2}]}{m} \right\} - \frac{m}{a} K_2^* \frac{\partial}{\partial \theta} \frac{[v_1]}{m} + 2 \frac{[K_{E_2}\omega_2^*]}{p_4} \\ & + 2 \frac{[\phi_2^*\omega_2^*]}{p_4} + \frac{R}{p_1} [T_1^*\omega_1^*] - \left\{ \frac{m^2}{a} \frac{\partial}{\partial \theta} M_{m_1} + 2 \frac{[u_2^*\omega_2^*]}{p_4} \right\} [u_1] \\ & - \left\{ \frac{\tan \theta}{a} [u_1^{*2}] + \frac{m}{a} \frac{\partial}{\partial \theta} \frac{[v_1^{*2}]}{m} + 2 \frac{[v_2^*\omega_2^*]}{p_4} \right\} [v_1] = 0 \quad (8-g) \end{aligned}$$

Multiplying Eq. 8-g by  $a/m$ , collecting the two terms involving  $M_{m,1}$ , and using  $\omega_1 = (1/2) \omega_2$  as a result of a linear interpolation for  $\omega_1$ , from neighboring levels, Eq. 8-g yields:

$$\begin{aligned} & \frac{\partial}{\partial \theta} \left\{ \frac{[v_1]}{m} K_1^* + \frac{[v_1]}{m} [v_1^{*2}] \right\} + M_{m_1} \frac{\partial}{\partial \theta} [u_1] m \\ & \quad - K_2^* \frac{\partial}{\partial \theta} \frac{[v_1]}{m} - [v_1] \frac{\partial}{\partial \theta} \frac{[v_1^{*2}]}{m} - [v_1][u_1^{*2}] \sin \theta \\ & + \frac{2a}{mp_4} \left\{ [K_{E_2} \omega_2^*] + [\phi_2^* \omega_2^*] + R [T_1^* \omega_2^*] - [u_2^* \omega_2^*][u_1] - [v_2^* \omega_2^*][v_1] \right\} = 0 \end{aligned} \quad (8-h)$$

Equation 8-h is the final form of the eddy kinetic energy equation at the 250-mb level. The last bracket contains all the relevant vertical transports, which have a large coefficient through the appearance of the radius of the earth. A systematic description of each term in this equation is given below.

The meridional circulation at the 250-mb level is given by the expression  $[v_1] = (m^2/af) (dM_{m,1}/d\theta)$ . The zonal average of the eddy kinetic energy,  $K_1^*$ , can be defined in terms of the wave parameters and the amplitude of the baroclinic disturbances with the aid of Eqs. 7-f, 7-m, and 7-g. The zonal circulation,  $[u_1]$ , is obtained from Eq. 5-j; i.e., expanding the operator  $d/dt$  with the aid of Eq. 5-g, using spherical coordinates for  $\vec{v} \cdot \vec{v}$ , taking the zonal average, setting  $\partial[v]/\partial t = 0$  and using  $[\vec{v}] = 0$ :

$$\frac{m}{a} \frac{\partial}{\partial \theta} \left\{ \frac{[v_1]^2}{m} + \frac{[v_1^{*2}]}{m} \right\} = - \frac{\tan \theta}{a} \left\{ [u_1]^2 + [u_1^{*2}] \right\} - f[u_1] - \frac{2}{p_4} [v_2^* \omega_2^*] - \frac{1}{a} \frac{\partial [\phi_1]}{\partial \theta}$$

Multiplying through by  $a/\tan \theta$  and rearranging terms, this expression is reduced to an algebraic equation for the zonal circulation at Level 1, i.e.,

$$\begin{aligned}
& [u_1]^2 + a f \operatorname{ctn} \theta \cdot [u_1] + [u_1^{*2}] - [v_1]^2 - [v_1^{*2}] + 2 \operatorname{ctn} \theta [v_1] \frac{\partial [v_1]}{\partial \theta} \\
& + \operatorname{ctn} \theta \frac{\partial}{\partial \theta} [v_1^{*2}] + \frac{2a}{p_4} [v_2^* \omega_2^*] \operatorname{ctn} \theta + \operatorname{ctn} \theta \frac{\partial [\phi_1]}{\partial \theta} = 0 \quad (8-i)
\end{aligned}$$

where  $\partial[\phi_1]/\partial\theta$  is evaluated by using the hydrostatic equation together with a linear representation of an emagram giving the  $\ln p$  vs.  $T$  properties for air; i.e., using the relation  $\phi = \partial\phi/\partial p - p\partial\phi/\partial p$  and Eq. 5-h:

$$[\phi_1] = \frac{[\phi_0 p_0] - [\phi_2 p_2]}{0 - p_2} + R [T_1] = [\phi_2] + R [T_1]$$

Applying Eq. 5-h at Level 3 with  $\phi_4 = gz_4 = 0$ :

$$[\phi_2] = \frac{2}{3} R [T_3]$$

hence

$$[\phi_1] = \frac{2}{3} R [T_3] + R [T_1] \quad (8-j)$$

Since the constant  $\gamma^2$  is related to the static stability parameter at Level 2 as:

$$\gamma^2 = \frac{1}{2} p_2^2 \frac{\partial \phi}{\partial p} \frac{\partial}{\partial p} \ln \theta_{p_2} = -\frac{1}{2} p_2^2 \frac{RT}{p} \frac{\partial}{\partial p} \ln \theta_{p_2}$$

or

$$\gamma^2 = -\frac{1}{2} R p_2 \Gamma_2$$

where  $\Gamma_2$  is the static stability parameter at Level 2 given by

$$\Gamma_2 = \frac{\partial[T_2]}{\partial p} - \frac{R}{c_p} \frac{[T_2]}{p_2} = \frac{[T_3] - [T_1]}{p_3 - p_1} - \frac{2}{7} \frac{[T_2]}{p_2} = \frac{1}{p_2} \left( [T_3] - [T_1] - \frac{2}{7} [T_2] \right)$$

then

$$[T_3] - [T_1] = \frac{2}{7} [T_2] - \frac{2}{R} \gamma^2 \quad (8-k)$$

From a linear relationship in an emagram (Kurihara, 1970):

$$[T_2] = \left( 1 - \frac{\ln 2}{\ln 3} \right) [T_1] + \frac{\ln 2}{\ln 3} [T_3] \quad (8-l)$$

From Eqs. 8-k and 8-l:

$$[T_1] = \left( 1 - \frac{2}{7} \frac{\ln 2}{\ln 3} \right) [T_2] + 2 \frac{\ln 2}{\ln 3} \frac{\gamma^2}{R}$$

and

$$[T_3] = \frac{1}{7} \left( 9 - 2 \frac{\ln 2}{\ln 3} \right) [T_2] - 2 \left( 1 - \frac{\ln 2}{\ln 3} \right) \frac{\gamma^2}{R}$$

Substituting these expressions for  $[T_1]$  and  $[T_3]$  in Eq. 8-j, and evaluating  $\partial[\phi_1]/\partial\theta$ :

$$\frac{\partial[\phi_1]}{\partial\theta} = \left( \frac{13}{7} - \frac{10}{21} \frac{\ln 2}{\ln 3} \right) R \frac{\partial[T_2]}{\partial\theta}$$

or

$$\frac{\partial[\phi_1]}{\partial\theta} = 1.56 \frac{\partial[\hat{\phi}]}{\partial\theta} \quad (8-m)$$

Note that the term  $\partial[T_2]/\partial\theta$  in Eq. 8-m cannot be obtained from the application of energy Eq. 5-f at Level 2 to determine  $[T_2]$ , because  $[\hat{v}_m] = 0$ . Since geostrophic Eq. 5-r as applied to the long-term zonal circulation yields  $\partial[\phi_1]/\partial\theta = -af[u_{g1}]$ , the linear term in  $[u_1]$  in Eq. 8-i is approximately equal to the term containing  $\partial[\phi_1]/\partial\theta$  in the same equation. Thus, Eq. 8-i expresses the degree of departure from geostrophic equilibrium for the long-term zonal circulation.

The zonal average of the eddy kinetic energy at Level 2,  $K_2^*$ , can be evaluated with the aid of Eq. 7-g for  $[v_2^{*2}]$  and the expression for  $[u_2^{*2}]$ . The latter can be evaluated from  $u_2^{*2}$ , which is derived in a manner similar to  $v_2^{*2}$ , i.e., from geostrophic Eq. 5-r,  $u_2^* = (1/2m) \hat{u}_m^*$ . However, Figs. 17 and 18 indicate that  $[u_2^{*2}] \approx [v_2^{*2}]$  or  $K_2^* \approx [v_2^{*2}]$ .

The vertical transports involving  $\omega_2^*$  in the eddy kinetic energy Eq. 8-h are very small (Lorenz, 1967) and their transient values become unmeasurable (Oort, 1971).<sup>\*</sup> Nevertheless, the vertical transports can be evaluated by using the relations  $\omega_2 = -p_2 D_1 = -\frac{1}{2} p_2 \hat{D} = -\frac{1}{4} p_4 \hat{D}$ , (Appendix A), i.e.,

$$\omega_2^* = -\frac{1}{4} \frac{p_4}{a} \left( \frac{\partial \hat{u}_m^*}{\partial \lambda} + m \frac{\partial}{\partial \theta} \frac{\hat{v}_m^*}{m^2} \right)$$

or after using Eqs. 7-a and 7-c,

$$\omega_2^* = \frac{1}{4} \frac{p_4}{a} \frac{mkB}{af} \text{ctn } \theta \cdot \cos(\eta + k\delta) \quad (8-n)$$

Note that the large term  $a/p_4$  in the coefficient of the vertical transports in Eq. 8-h is cancelled out by its reciprocal in the coefficient of Eq. 8-n. Each of the vertical transports in Eq. 8-h is evaluated as follows:

<sup>\*</sup> Private communication.

$$[K_{E_2} \omega_2^*] = [u_2^* \omega_2^*] [u_2] \quad (8-o)$$

since the triple correlations vanish and  $[\nabla] = 0$ ; the zonal circulation at Level 2 in Eq. 8-o is given by the average of the values at Levels 1 and 3, i.e.,

$$[u_2] = \frac{1}{2} ([u_1] + [u_3]) = \frac{1}{2} [u_1] \left( 1 + \frac{[u_3]}{[u_1]} \right)$$

where  $[u_3]/[u_1] < 1$ . The transport  $[u_2^* \omega_2^*]$  is evaluated by using  $u_2^* = (1/2 m) \bar{u}_m^*$ . Hence,

$$[u_2^* \omega_2^*] = \frac{1}{2m} [\bar{u}_m^* \omega_2^*]$$

Equations 7-b, 8-n, and 5-y then yield:

$$[u_2^* \omega_2^*] = \frac{1}{4} \frac{mp_4}{a} \frac{kH_m \text{ctn } \theta}{af} \left( \frac{d\alpha\theta}{d\theta} \cdot \text{ctn } k\delta + \frac{1}{k} \frac{1}{A} \frac{dA}{d\theta} \right) \quad (8-p)$$

The transport  $[\phi_2^* \omega_2^*]$  is evaluated by using  $\phi_2^* = (1/2) \bar{\phi}^*$  and Eq. 8-n; the parameter  $\bar{\phi}^*$  is obtained from the geostrophic Equation 5-s, i.e.,  $\nabla_m^* = (m^2/af)(\partial \bar{\phi}^*/\partial \lambda)$ . Integration of this equation with the aid of Eq. 7-d yields  $\bar{\phi}^* = fA \sin \eta$ . Thus:

$$[\phi_2^* \omega_2^*] = - \frac{1}{4} \frac{mp_4}{a} H_m \text{ctn } \theta \quad (8-q)$$

The transport  $R [T_1^* \omega_2^*]$  or  $2R [T_1^* \omega_1^*]$  can be estimated by taking an average between the corresponding values at Levels 0 and 2. The transport  $[T_0^* \omega_0^*]$  vanishes because  $\omega_0^* = 0$ , while the transport  $[T_2^* \omega_2^*]$  is evaluated by using  $\bar{\phi}^* = RT_2^*$  and Eq. 8-n. The result is:

$$R [T_2^* \omega_2^*] = [\hat{\phi}^* \omega_2^*] = 0 \quad (8-r)$$

Since  $[T_0^* \omega_0^*] = [T_2^* \omega_2^*] = 0$ , its average  $[T_1^* \omega_1^*] = 0$ . The transport  $[v_2^* \omega_2^*]$  is evaluated by using  $v_2^* = (\frac{1}{2m}) \bar{v}_m^*$  and Eq. 8-n; the result is then as follows:

$$[v_2^* \omega_2^*] = \frac{1}{4} \frac{km}{af} \cdot \frac{mp^4}{a} \cdot H_m \text{ ctn } \theta \cdot \text{ctn } k\delta \quad (8-s)$$

The theoretical determination of the meridional and zonal kinetic energy terms at Levels 1 and 2 in Figs. 17 and 18, as well as the parameters in Figs. 20 through 27, can be obtained from the numerical integration of the foregoing system of equations. These numerical integrations can start with initial conditions at low latitudes that are determined from these figures. The initial conditions involve, for example, the terms that appear in Eq. 7-q, i.e.,  $M_{m,1}$ ,  $H_m$ ,  $d\alpha\theta/d\theta$ ,  $d\delta/d\theta$ ,  $\delta$ ,  $d \ln A/d\theta$ , and  $d \ln B/d\theta$ . The basic Equation 5-q yields then  $dM_{m,1}/d\theta$  for a given value of the eigenvalue parameter  $\gamma^2$ ; likewise, Eq. 5-x yields  $dH_m/d\theta$  from the initial values for  $H_m$ ,  $M_{m,1}$ , and  $S$ . The problem is then reduced to the determination of four derivatives, i.e.,  $d^2\alpha\theta/d\theta^2$ ,  $d^2\delta/d\theta^2$ ,  $d^2 \ln A/d\theta^2$ , and  $d^2 \ln B/d\theta^2$ , which are obtained from the simultaneous solution of four ordinary differential equations. These equations are given by Eq. 8-h and by three equations obtained through differentiating Eqs. 7-e and 7-q once and differentiating Eq. 5-y twice; the second derivative of  $H_m$  which then appears can be evaluated from the differentiation of Eq. 5-x or 5-z. Similarly, the second derivative of  $M_{m,1}$ , which appears in  $d[v_1]/d\theta$  in Eq. 8-h, can be obtained from Eq. 5-q. The numerical integrations can be performed until the eigenvalue parameter  $\gamma^2$  is found to satisfy the boundary condition  $H_m \rightarrow 0$  as  $\theta \rightarrow \pi/2$ .

The solution of the foregoing system of equations yields the dynamics induced by the heating rates of Eq. 1; note that they are decoupled from the transport of water vapor by two-dimensional turbulence. The converse is not true, however, for the large-scale transport

of water vapor is coupled to the dynamics through the continuity equation for water vapor. Equation 5-c applies to either a gas or a liquid; however, it is usually assumed that liquid water falls out immediately upon forming from condensation. Thus, the continuity equation for water vapor is given by a modification of Eq. 5-c to include the effects of condensation and diffusion from mainly the vertical gradient of moisture. Since differentiation of Eq. 5-c yields the expression  $d\rho/dt = -\rho \vec{\nabla} \cdot \vec{V}$  for air, the respective equation for water vapor is given by (e.g., Washington and Kasahara, 1970):

$$\frac{d\rho_w}{dt} = -\rho_w \vec{\nabla} \cdot \vec{V} + M_w + \rho E_w \quad (9-a)$$

where  $\rho_w$  denotes the density of water vapor,  $M_w$  the rate of condensation of water vapor per unit volume, and  $E_w$  the rate of change of water vapor content per unit mass due to mainly the vertical diffusion of water vapor. Equation 9-a can be written in terms of either the specific humidity or the mixing ratio, which are defined as the amounts of water vapor per unit mass of moist or dry air, respectively. Since the specific humidity differs only slightly from the mixing ratio, the use of either one is approximately interchangeable. If the specific humidity is denoted by  $q$ , i.e. (e.g., Willett and Sanders, 1959):

$$q = \frac{\rho_w}{\rho} = \frac{0.622 e}{p - 0.378e} \approx 0.622 \frac{e}{p} \quad (9-b)$$

where  $e$  denotes the partial pressure of water vapor, Eq. 9-a and the use of the relation  $q d\rho/dt = -\rho q \vec{\nabla} \cdot \vec{V}$  yields

$$\frac{dq}{dt} = \frac{M_w}{\rho} + E_w \quad (9-c)$$

which in the coordinate system of Eq. 5-g (e.g., Holloway and Manabe, 1971) yields:

$$\frac{m}{a} \frac{\partial}{\partial \theta} \frac{[vq]}{m} + \frac{\partial}{\partial p} [\omega q] = \left[ \frac{M_w}{\rho} \right] + [E_w] \quad (9-d)$$

Applying Eq. 9-d to the atmospheric column in Fig. 1, and denoting the vertical average for each term by  $\chi_2 = \int_0^1 \chi d(p/p_4)$  where  $\chi$  denotes  $[vq]$ ,  $[\omega q]$ ,  $[M_w/\rho]$ , and  $[E_w]$ :

$$\frac{m}{a} \frac{\partial}{\partial \theta} \frac{[v_2^* q_2^*]}{m} = \left[ \frac{M_w}{\rho} \right]_2 + [E_{w_2}] \quad (9-e)$$

Note that the first term in the right-hand side of Eq. 9-e is related to the heat released from condensation,  $C$ , in Eq. 1 as follows:

$$C = L \int_0^\infty M_w dz = \frac{p_4}{g} L \int_0^1 \frac{M_w}{\rho} d \left( \frac{p}{p_4} \right)$$

or

$$C = \frac{p_4}{g} L \left[ \frac{M_w}{\rho} \right]_2 \quad (9-f)$$

where  $L$  denotes the latent heat of condensation. Also, if  $Q_c$  denotes the heating rate per unit mass, i.e.,  $Q_c = L M_w/\rho$ , Eq. 9-f can be written:

$$C = \frac{p_4}{g} Q_{c_2} \quad (9-g)$$

Similarly, the rate of evaporation per unit mass over the oceans that is injected into the atmospheric column can be related to  $[E_{w,2}]$ . Note that the transport of specific humidity as given by Eq. 9-e can be expressed as the difference of the rates of evaporation from the earth and precipitation upon the earth (i.e., Fig. 6); this result is, of

course, in agreement with that derived by using Eq. 6 with  $X = q$  (Lorenz, 1967). The transport of water vapor itself in Eq. 9-e can be evaluated directly as a function of latitude, since the vapor pressure is a function of temperature (e.g., Petterssen, 1956); thus, from Eq. 9-b,  $q^*$  becomes proportional to  $\hat{\phi}^*$ . It is then seen that through the transport of water vapor, the dynamics of the troposphere control the amounts of evaporation from the earth and precipitation upon the earth.

The application of the foregoing equations to the problem of advertent modification of the climate of the earth's surface at middle and high latitudes involves the use of a procedure for iterating  $T_2(\theta)$  for a given advertent modification of the earth's surface albedo at those latitudes. The occurrence of evaporation and condensation in the atmosphere is caused primarily by the changing capacity of the air for water vapor, which depends entirely upon the air temperature (e.g., Willett and Sanders, 1959). Thus, the use of an arbitrary initial  $T_2(\theta)$ , together with Eqs. 1 and 2, generates the function  $q_f(\theta)$ , which in turn yields the dynamics as well as the humidity transports. The subsequent iteration of  $T_2(\theta)$  may then proceed until Eq. 9-e is satisfied. Thus, this iteration procedure starts with the use of an a priori modification of the parameterization of the troposphere heating, say, for example, at the middle and high latitudes as the result of the advertent modification of the Arctic Ocean's surface albedo (Fig. 14). Therefore, this a priori modification must account for the effects present in Eqs. 1 and 2, i.e., the latent heat  $C$ , the local albedo of the atmosphere ( $S_a$ ) and the earth's surface ( $S_s$ ), etc.

It is emphasized that the main assumption in the foregoing system of equations based on the current climate is the important role of the dynamics of the upper half relative to those of the lower half of the troposphere, i.e.,  $\bar{M} \approx \hat{M} \approx M_1$  or  $M_3/M_1 \ll 1.0$  (Table 3). Because the transport of angular momentum in the upper half of the troposphere controls the meridional cell structure of the general circulation, which prevails even during the two extremes of the interglacial and

glacial cycles of climate during the current Pleistocene Epoch, the assumption concerning the relative role of the dynamics in the upper half of the troposphere becomes applicable to the general circulation of the atmospheric air for any climate.

## X. RESULTS AND CONCLUDING REMARKS

Considerations of the feasibility of advertent climate modification at the higher latitudes of the United States involve the answers to four key subquestions, which are identified in Section II. This paper seeks to answer the first or initial subquestion through the formulation of a model for the general circulation for climate that emphasizes physical phenomenology. This model is based on a variable (i.e., as a function of latitude) tilt from the meridian for both the flow and temperature disturbances, a variable phase lag between the flow and temperature disturbances, and a variable amplitude of these baroclinic disturbances. Results from this formulation are as follows:

1. The use of this model utilizing experimental data for the long-term statistics of the general circulation (i.e., the annual zonal averages of the transports of angular momentum and sensible heat as well as the meridional and zonal eddy kinetic energies at the 250- and 500-mb levels) allows the semi-experimental determination of parameters that are difficult to measure directly, i.e., the wave and amplitude parameters of the baroclinic disturbances, the wave number appropriate for climate, and the vertical transports (i.e., Figs. 20 through 27, and Eqs. 8-o through 8-s). These results, for example, indicate quantitatively that the tilt of the baroclinic disturbances becomes predominant as the latitude decreases, which is in agreement with previous qualitative experimental observations (Starr, 1948). Also, the wave number appropriate for climate, and including the effects of baroclinic disturbances as well as of a nonhomogeneous earth's surface, is of the order of unity.

2. There is good agreement between the experimental value of the middle latitude, at which the large-scale transport of angular momentum vanishes as the transport of sensible heat reaches a maximum value (Figs. 15, 16), with the corresponding latitude value that is determined from the semi-experimental values of the wave and amplitude parameters of the baroclinic disturbances (Fig. 26, Eqs. 7-o and 5-x). This agreement constitutes then a successful local test of the basic formulation of the baroclinic disturbances for the determination of the large-scale transports of angular momentum and sensible heat by two-dimensional turbulence (i.e., Eqs. 5-v and 5-w).
3. The model based on variable wave and amplitude parameters of the baroclinic disturbances indicates that the large-scale transports of angular momentum and sensible heat by two-dimensional turbulence do depend on the zonal circulation (i.e., Eqs. 8-h and 8-i), a result that resolves the puzzle of the constant S theory which, by implicit assumption, yields the result that the transports are independent of the zonal circulation (Smagorinsky, 1964). The model based on variable wave and amplitude parameters of the baroclinic disturbances indicates further that the transports of angular momentum and sensible heat are also coupled to the vertical transports as given by Eqs. 8-h and 8-o through 8-s.
4. The model based on variable wave and amplitude parameters of the baroclinic disturbances requires only one eigenvalue parameter, which involves the static stability of a tropospheric column; this result implies that there is no need, as in the constant S model, for the use of a rather weak boundary condition at the north pole in order to establish the magnitude of the parameter S through most of the latitudinal range of the northern hemisphere.

The model based on variable wave and amplitude parameters of the baroclinic disturbances may also modify an important conclusion

that is derived from the constant  $S$  model, which indicates that the same multiple of the transports of angular momentum and sensible heat as well as of the poleward heat flux satisfies the fundamental equations of the model (i.e., Eqs. 5-q and 5-x with  $S$  a constant). This would then mean that the transports scale directly with the magnitude of the poleward heat flux, i.e., that only the shape of the poleward heat flux function (Fig. 14) determines the two or three meridional cell structures (e.g., Fig. 5) corresponding, respectively, to the two extremes of interglacial or glacial climates of middle and high latitudes during the current Pleistocene Epoch. Thus, the shape of the poleward heat flux function would determine the type of the climate, while the amplitude of the poleward heat flux would fix the intensity of the particular type of climate. However, the model based on variable wave and amplitude parameters indicates that  $S$  is a function of latitude, which depends on the meridional and zonal eddy kinetic energy as well as on the vertical transports; hence, the foregoing conclusion from the constant  $S$  model may become invalid.

The formulation of the model based on variable wave and amplitude parameters of the baroclinic disturbances remains to be tested for the current climate. This test requires the following two steps: (1) to obtain for latitudes greater than about 30 degrees (Fig. 20) the theoretical values of the transports of sensible heat and angular momentum (Figs. 15, 16) based on  $S(\theta)$  as well as the theoretical values of the meridional and zonal eddy kinetic energy at the 250- and 500-mb levels (Figs. 17, 18); and (2) to include (at the same latitudes) comparisons of theoretical values for the statistics of the water vapor (Eq. 9-e) with corresponding experimental values from the Oort-Rasmusson data. This latter consideration might require a thermodynamic parameterization of the moisture flux based, for example, on seasonal data for the current climate.

The model based on variable wave and amplitude parameters of the baroclinic disturbances could then be applied to conditions of an Arctic Ocean without sea ice, which corresponds to the interglacial

environment of the current Pleistocene Epoch. This procedure would use known boundary conditions at low latitudes and properly modified functions of the poleward heat flux at middle and high northern latitudes (Fig. 14); such calculations would thus provide a test of the iteration procedure for the solution of the problem of advertent modification of the earth's climate at middle and high latitudes.

The model based on variable wave and amplitude parameters of the baroclinic disturbances could next be used to answer the second and third subquestions identified earlier in the key questions in advertent climate modification (Section II), i.e., the predictability of changes of the climate of the earth's surface at middle and high latitudes of the northern hemisphere, and the sensitivity of the magnitude of the long-term statistics of the general circulation to advertent modifications of parameters such as the earth's surface albedo, etc. The transitive or intransitive nature of the advertent changes of climate at middle and high northern latitudes could be investigated numerically with this model by attempting to find an extra solution for the conditions of an Arctic Ocean without sea ice. The sensitivity of the long-term statistics of the general circulation could subsequently be investigated numerically with this model by using parametric perturbations of the poleward heat flux at the middle and high northern latitudes.

Preliminary investigations of the fourth subquestion concerning the technology for advertent climate modification at the higher northern latitudes are given in Section VI. In-depth investigations of this subquestion must await positive answers to the second and third subquestions.

## XI. REFERENCES

- Arakawa, A., 1966. "Computational Design for Long-Term Numerical Integration of the Equations of Atmospheric Motion," *Journal of Computational Physics*, Vol. 1, No. 1, July 1966, pp. 119-143.
- Bell, Barbara, 1953. "Solar Variation as an Explanation of Climate Change," *Climate Change - Evidence, Causes and Effects*. Harlow Shapley, Harvard University Press, Cambridge, 1953.
- Budyko, M.I., 1956. "The Heat Balance of the Earth's Surface." Translated by N.A. Stepanova, U.S. Weather Bureau, 1958.
- Budyko, M.I., 1966. "Polar Ice and Climate," *Proceedings of the Symposium on the Arctic Heat Budget and Atmospheric Circulation*, Memorandum RM-5233-NSF, December 1966, The Rand Corporation, Santa Monica, California.
- Budyko, M.I., 1969. "The Effect of Solar Radiation Variations on the Climate of the Earth, *Tellus*, 21, 611-619.
- Budyko, M.I., 1970. Comments on "A Global Climatic Model Based on the Energy Balance of the Earth-Atmosphere System," *Journal Applied Meteorology*, 8, 310.
- Charney, J.G. and Phillips, N.A., 1953. *Journal of Meteorology*, 10, p. 71.
- Charney, J.G., 1959. "On the Theory of the General Circulation of the Atmosphere," *The Atmosphere and the Sea in Motion*, Rockefeller Institute Press, New York, 1959.
- Faegre, A., 1972. "An Intransitive Model of the Earth-Atmosphere-Ocean System," *Journal of Applied Meteorology*, Vol. 11, No. 1, February 1972.
- Fairbridge, R.W., 1961. "Convergence of Evidence on Climatic Change and Ice Ages," *Annals New York Academy of Sciences*, Vol. 95, October 1961.

- Gates, W.L., et al, 1971, "A Documentation of the Mintz-Arakawa Two-Level Atmospheric General Circulation Model," R-877, ARPA, December 1971, The Rand Corporation, Santa Monica, California.
- Haurwitz, B., 1948. "The Motion of Atmospheric Disturbances on the Spherical Earth," Journal of Marine Research 3, pp. 254-267.
- Hidalgo, H., 1969. "Satellite Measurements of Atmospheric Parameters," Research Paper P-505, Institute for Defense Analyses, Science and Technology Division, December 1969.
- Hidalgo, H. and Vauglio-Laurin, R., 1970. "Description of Atmospheric Turbulences for Linear Propagation of Laser Beams," Research Paper P-600, Institute for Defense Analyses, Science and Technology Division, July 1970.
- Holloway, J.L. and Manabe, S., 1971. "Simulation of Climate by a Global Circulation Model," Monthly Weather Review, Vol. 99, No. 5, May 1971.
- Houghton, H.G. "On the Annual Heat Balance of the Northern Hemisphere," Journal of Meteorology, Vol. 11, No. 1, February 1954.
- Julian P.R., Washington W.M., Hembree L., Ridley C., 1970. "On the Spectral Distribution of Large-Scale Atmospheric Kinetic Energy," Journal of the Atmospheric Sciences, Vol. 27, May 1970.
- Kasahara, A. and Washington, W.M. "General Circulation Experiments with a Six-Layer NCAR Model, Including Orography, Cloudiness and Surface Temperature Calculations," Journal of Atmospheric Sciences, July 1971.
- Kornfield, J. and Hasler, A.F., 1969. "A Photographic Summary of the Earth's Cloud Cover for Year 1967," Journal Applied Meterology, Vol. 8, pp. 687-700.
- Kurihara, Y., 1970. "A Statistical-Dynamical Model of the General Circulation of the Atmosphere," Journal of the Atmospheric Sciences, September 1970.
- London, J., 1957. "A Study of the Atmospheric Heat Balance," AF 19(122)-165, (ASTIA No. 117227) New York University, Department of Meteorology and Oceanography, July 1957.

Lorenz, E.N., 1967. "The Nature and Theory of the General Circulation of the Atmosphere," World Meteorological Organization.

Lorenz, E.N., 1968. "The Predictability of a Flow which Possesses Many Scales of Motion," Tellus XXI (1969), 3, 289-307.

Lorenz, E.N., 1968. "Climatic Determinism," Causes of Climatic Change, Meteorological Monographs, Vol. 8, No. 30, February 1968.

Lorenz, E.N., 1970. "Climatic Change as a Mathematical Problem," Journal of Applied Meteorology, Vol. 9, No. 3, June 1970.

MacCracken, M.C., 1969. "Ice Age Theory Analysis by Computer Model Simulation," UCRL-71888 Parts I and II. Lawrence Radiation Laboratory, University of California, Livermore.

Maykut, G.A., 1969. "A Thermodynamic Model of Sea Ice," Thesis towards Doctor of Philosophy degree, University of Washington, Seattle, Washington. (Also, Journal of Geophysical Research, Oceans and Atmospheres, Vol. 76, No. 6, February 20, 1971).

Miller, A. and Thompson, J.C. "Elements of Meteorology," Charles E. Merrill Publishing Company, Columbus, Ohio, 1970.

Mintz, Y., 1964. "Very Long-Term Global Integration of the Primitive Equations of Atmospheric Motion," Proceedings of the WMO/IUGG. Symposium on the Research and Development Aspects of Long-Range Forecasting, Boulder, Colorado, 1964, WMO Technical Note, No. 66, 1965, pp. 141-167.

Mitchell, J.M., 1968. Editor, "Causes of Climatic Change," Meteorological Monographs, Vol. 8, No. 34, February 1968, American Meteorological Society, Boston, Massachusetts.

Monin, A.S., 1970. "The Atmospheric Boundary Layer," Annual Review of Fluid Mechanics, Vol. 2, 1970, Annual Reviews Inc., 4139 El Camino Way, Palo Alto, California 94306, U.S.A.

Oort, A.H. and Rasmusson, E.M., 1971. "Atmospheric Circulation Statistics," NOAA Professional Paper 5, U.S. Department of Commerce. Superintendent of Documents, U.S. Government Printing Office, Washington, D.C. 20402.

Phillips, N.A., 1956. "The General Circulation of the Atmosphere: A Numerical Experiment," Quarterly Journal of the Royal Meteorological Society, Vol. 82, No. 352, April 1956.

Pike, A.C., 1970. "The Inter-Tropical Convergence Zone Studied with an Interacting Atmosphere and Ocean Model," Proceedings of the Symposium on Tropical Meteorology, June 2-11, 1970, University of Hawaii, Honolulu, Hawaii.

Petterssen, S., 1956. "Weather Analysis and Forecasting," Volume II, McGraw-Hill Book Company, New York.

Rapp, R.R., 1970. "Climate Modification and National Security," P-4476, October 1970, The Rand Corporation, Santa Monica, California.

Rossby, C.G. "The Atmosphere and the Sea in Motion," Rockefeller Institute Press in Association with Oxford University Press, New York, 1959.

Sadler, J.C., 1969. "Average Cloudiness in the Tropics from Satellite Observations," Honolulu, East-West Center Press.

Saltzman, B. and Vernekar, A.D., 1971. "An Equilibrium Solution for the Axially-Symmetric Component of the Earth's Macro-climate," Journal of Geophysical Research, Oceans and Atmospheres, Vol. 76, No. 6, February 20, 1971.

Schell, I.I., 1961. "Recent Evidence about the Nature of Climate Changes and Its Implications," Annals New York Academy of Sciences, Vol. 95, October 1961.

Schell, I.I., 1971. On Mathematical and "Natural" Models for the Study of Climate Changes, Journal of Applied Meteorology, Vol. 10, No. 6, December 1971, pp. 1344-1346.

Sellers, W.D., 1969. "A Global Climatic Model Based on the Energy Balance of the Earth-Atmosphere System," Journal Applied Meteorology, 8, pp. 392-400.

Sellers, W.D., 1970. Reply. Journal of Applied Meteorology, 8, p. 311.

Shapiro, A.H., 1953. "The Dynamics and Thermodynamics of Compressible Fluid Flow," Vol. I, The Ronald Press Company, New York.

Smagorinsky, J., 1958. "On the Numerical Integration of the Primitive Equations of Motion for Baroclinic Flow in a Closed Region," Monthly Weather Review, Vol. 86, No. 12, December 1958.

Smagorinsky, J., 1963. "General Circulation Experiments with the Primitive Equations: I. The Basic Experiment," Monthly Weather Review, Vol. 91, No. 3, March 1963.

Smagorinsky, J., 1964. "Some Aspects of the General Circulation," Quarterly Journal of the Royal Meteorological Society, Vol. 90, No. 383, January 1964.

Starr, V.P., 1948. "An Essay on the General Circulation of the Earth's Atmosphere," Journal of Meteorology, Vol. 5, No. 2, April 1948. Also see "Observational Studies of the Atmospheric Circulation," Scientific Report No. 2, Planetary Circulations Project, Department of Meteorology, Massachusetts Institute of Technology, Cambridge, Massachusetts.

Thompson, P.D., 1957. "Uncertainty of initial state as a factor in the predictability of large scale atmospheric flow patterns," Tellus 9, 275-295.

Thompson, P.D., 1961. "Numerical Weather Analysis and Prediction," The Macmillan Company, New York.

Warshaw, M. and Rapp, R.R., "An Experiment on the Sensitivity of a Global Circulation Model: Studies in Climate Dynamics for Environmental Security," R-908, ARPA, February 1972, The Rand Corporation, Santa Monica, California.

Washington, W.M. and Kasahara, A., 1970. "A January Simulation Experiment with the Two-Layer Version of the NCAR Global Circulation Model," Monthly Weather Review, Vol. 98, No. 8, August 1970.

Willett, H.C., 1953. "Atmospheric and Oceanic Circulation as Factors in Glacial-Interglacial Changes of Climate," Climate Change - Evidence, Causes and Effects, Harlow Shapley, Harvard University Press, Cambridge, Massachusetts.

Willett, H.C. and Sanders, F., 1959. Descriptive Meteorology, Academic Press, Inc., New York, 1959.

## APPENDIX A

### DERIVATION OF ZONAL MOMENTUM AND ENERGY EQUATIONS AND S WAVE-PARAMETER

This appendix gives a more detailed but unified presentation of all the assumptions that are used in (1) the derivation of the two zonal Equations 5-k and 5-l as well as the energy Equation 5-m from the set of primitive Equations 5-e through 5-h, and (2) the use of the mechanisms of the tilt and phase lag of the baroclinic disturbances (Fig. 12, Section VII) which leads to Eq. 5-x.

#### 1. ZONAL MOMENTUM AND ENERGY EQUATIONS

The scalar Eq. 5-i can be written in the Mercator ( $x, y$ ) coordinates instead of the spherical ( $\lambda, \theta$ ) coordinates through the transformations  $dx = a d\lambda$  and  $dy = a d\theta/\cos \theta$ . The zonal and meridional winds in the Mercator plane then become  $u_m = dx/dt = a d\lambda/dt$  and  $v_m = dy/dt$  or  $v_m = a \cos^{-1} \theta d\theta/dt$ , while the relationship between the Mercator winds and actual winds becomes  $u = u_m \cos \theta$  and  $v = v_m \cos \theta$ . Substituting this expression for  $u$  in Eq. 5-i, the Mercator zonal wind is given by (Sagorinsky, 1958):

$$\frac{du_m}{dt} = \frac{2}{a} u_m v_m \sin \theta + f v_m - \frac{1}{\cos^2 \theta} \frac{\partial \phi}{\partial x} + \frac{1}{\cos \theta} F_x \quad (\text{A-1})$$

where the operator  $d/dt$  is given by  $\partial/\partial t + u_m \partial/\partial x + v_m \partial/\partial y + \omega \partial/\partial p$ . After expanding the operator  $d/dt$  in Eq. A-1, using the notation  $m = \cos^{-1} \theta$ , the transformation  $dy = a m d\theta$ , and noting the identity

$$v_m \frac{\partial u_m}{\partial y} - \frac{u_m v_m}{a} \sin \theta = m v_m \frac{\partial}{\partial y} \left( \frac{u_m}{m} \right)$$

the local derivative of the zonal wind becomes

$$\frac{\partial u_m}{\partial t} = -u_m \frac{\partial u_m}{\partial x} - mv_m \frac{\partial}{\partial y} \left( \frac{u_m}{m} \right) - \omega \frac{\partial u_m}{\partial p} + \left( \frac{u_m}{a} + 2\Omega \right) v_m \sin \theta - m^2 \frac{\partial \phi}{\partial x} + mF_x$$

(A-2)

The application of Eq. A-2 at Levels 1 and 3 (Fig. 13, Section VII) requires the evaluation of the term  $\omega \partial u_m / \partial p$  at these levels; with the notation  $\hat{\chi} = \chi_1 - \chi_3$ , the term at Level 1 becomes

$$\omega_1 \left( \frac{\partial u_m}{\partial p} \right)_1 \approx -\omega_1 \frac{u_{m_1} - u_{m_3}}{p_3 - p_1} = -\frac{\omega_1 \hat{u}_m}{\Delta p}$$

The value of  $\omega_1$  is obtained from the continuity Eq. 5-g after its transformation to the Mercator plane; denoting the horizontal divergence  $\vec{v} \cdot \vec{U}$  by D, using spherical coordinates in  $\vec{v} \cdot \vec{U}$  and the foregoing transformations for both the coordinates and the winds, one obtains:

$$D \equiv \vec{v} \cdot \vec{U} = \frac{m}{a} \left( \frac{\partial u}{\partial \lambda} + \frac{\partial}{\partial \theta} \frac{v}{m} \right) = \frac{\partial u_m}{\partial x} + m^2 \frac{\partial}{\partial y} \left( \frac{v_m}{m^2} \right) = -\frac{\partial \psi}{\partial p}$$

hence

$$D_1 = -\left( \frac{\partial \psi}{\partial p} \right)_1 = -\frac{\omega_0 - \omega_2}{0 - p_2} = -\frac{\omega_2}{\Delta p}$$

Similarly

$$D_3 = \frac{\omega_2}{\Delta p} = -D_1$$

with the notation  $\bar{\chi} = \chi_1 + \chi_3$ ,  $\bar{D} = 0$ , while  $\hat{D} = 2D_1$ . Interpolating linearly for  $\omega_1$  and  $\omega_3$  from neighboring levels,  $\omega_1 = \omega_3 = \omega_2/2$ . Thus

$$\omega_1 \left( \frac{\partial u_m}{\partial p} \right)_1 = - \frac{\omega_1 \hat{u}_m}{\Delta p} = \frac{1}{4} \hat{D} \hat{u}_m$$

Using the identity

$$\hat{u}_m = 2 u_{m_1} - \bar{u}_m$$

and

$$\frac{\hat{D}}{2} = D_1 = \frac{\partial}{\partial x} u_{m_1} + m^2 \frac{\partial}{\partial y} \left( \frac{v_{m_1}}{m^2} \right)$$

then

$$\omega_1 \left( \frac{\partial u_m}{\partial p} \right)_1 = u_{m_1} \frac{\partial}{\partial x} u_{m_1} + u_{m_1} m^2 \frac{\partial}{\partial y} \left( \frac{v_{m_1}}{m^2} \right) - \frac{\hat{D} \bar{u}_m}{4}$$

Substituting this result in Eq. A-2 at Level 1, and noting that  $u_{m_1} v_{m_1} \sin \theta/a = -m u_{m_1} v_{m_1} dm^{-1}/dy$ , Eq. A-2 at Level 1 can be put in the form

$$\frac{\partial}{\partial t} u_{m_1} = - \frac{\partial}{\partial x} u_{m_1}^2 - m^4 \frac{\partial}{\partial y} \left( \frac{u_{m_1} v_{m_1}}{m^4} \right) + \frac{\hat{D} \bar{u}_m}{4} + f v_{m_1} - m^2 \frac{\partial \phi_1}{\partial x} + m F_{x_1} \quad (A-3)$$

Similarly, Eq. A-2 when applied to Level 3 yields

$$\frac{\partial}{\partial t} u_{m_3} = - \frac{\partial}{\partial x} u_{m_3}^2 - m^4 \frac{\partial}{\partial y} \left( \frac{u_{m_3} v_{m_3}}{m^4} \right) - \frac{\hat{D}u_m}{4} + f v_{m_3} - m^2 \frac{\partial \phi_3}{\partial x} + m F_{x_3} \quad (A-4)$$

Equations A-3 and A-4 are similar, except for the change in sign of  $\hat{D}u_m/4$ , which comes about from the use of  $u_{m_3}$  instead of  $u_{m_1}$ , i.e., the identity  $-\hat{u}_m = 2u_{m_3} - \bar{u}_m$ . Adding Eqs. A-3 and A-4 one obtains

$$\frac{\partial \bar{u}_m}{\partial t} = - \frac{\partial \bar{u}_m^2}{\partial x} - m^4 \frac{\partial}{\partial y} \left( \frac{\bar{u}_m \bar{v}_m}{m^4} \right) + f \bar{v}_m - m^2 \frac{\partial \bar{\phi}}{\partial x} + m \bar{F}_x$$

while subtracting Eq. A-4 from Eq. A-3 yields

$$\frac{\partial \hat{u}_m}{\partial t} = - \frac{\partial \hat{u}_m^2}{\partial x} - m^4 \frac{\partial}{\partial y} \left( \frac{\hat{u}_m \hat{v}_m}{m^4} \right) + \frac{\hat{D}u_m}{2} + f \hat{v}_m - m^2 \frac{\partial \hat{\phi}}{\partial x} + m \hat{F}_x$$

Taking the zonal average of these equations, defined by

$$[\chi] \equiv \frac{1}{2\pi a} \int_0^{2\pi a} \chi \, dx$$

one gets

$$\frac{\partial [\bar{u}_m]}{\partial t} = -m^4 \frac{\partial}{\partial y} \frac{[\bar{u}_m \bar{v}_m]}{m^4} + m [\bar{F}_x] \quad (A-5)$$

$$\frac{\partial [\hat{u}_m]}{\partial t} = -m^4 \frac{\partial}{\partial y} \frac{[\hat{u}_m \hat{v}_m]}{m^4} + \frac{[\hat{D}u_m]}{2} + f [\hat{v}_m] + m [\hat{F}_x] \quad (A-6)$$

where in the derivation of Eq. A-5, the term  $[\bar{v}_m]$  drops out, because of  $\bar{v} = 0$  as well as the boundary condition  $v_m = 0$  at the equator and the poles at both levels and at any time,  $t$ . By using the identity

$$\overline{\chi_m v_m} = \frac{1}{2} (\overline{\chi_m} \overline{v_m} + \widehat{\chi_m} \widehat{v_m})$$

and the definitions  $\overline{\chi_m} = [\overline{\chi_m}] + \overline{\chi_m}^*$ ,  $\widehat{\chi_m} = [\widehat{\chi_m}] + \widehat{\chi_m}^*$  one gets the following result

$$[\overline{u_m v_m}] = \frac{1}{2} [\widehat{u_m}] [\widehat{v_m}] + [\overline{u_m^* v_m^*}]$$

Hence, Eq. A-5 becomes (Smagorinsky, 1964)

$$\frac{\partial [\overline{u_m}]}{\partial t} = -m^4 \frac{\partial}{\partial y} \frac{[\widehat{u_m}] [\widehat{v_m}]}{2m^4} - m^4 \frac{\partial \overline{M_m}}{\partial y} + m [\widehat{F}_x] \quad (\text{A-7})$$

(Eq. 5-k, Section VII)

where  $M_m$  denotes a quantity proportional to the nonlinear eddy flux of angular momentum, i.e.,

$$M_m = [\overline{u_m^* v_m^*}] / m^4$$

Similarly, by using the identity

$$\widehat{\chi_m v_m} = \frac{1}{2} (\widehat{\chi_m} \widehat{v_m} + \overline{\chi_m} \overline{v_m})$$

one gets

$$[\widehat{u_m v_m}] = \frac{1}{2} [\overline{u_m}] [\widehat{v_m}] + [\widehat{u_m^* v_m^*}]$$

and Eq. A-6 becomes

$$\frac{\partial [\widehat{u_m}]}{\partial t} = -\frac{m^4}{2} \frac{\partial}{\partial y} \frac{[\overline{u_m}] [\widehat{v_m}]}{m^4} - m^4 \frac{\partial}{\partial y} \frac{[\widehat{u_m^* v_m^*}]}{m^4} + \frac{[\widehat{D}\overline{u_m}]}{2} + f[\widehat{v_m}] + m[\widehat{F}_x]$$

From the condition  $\bar{D} = 0$ , and the definitions  $D = [D] + D^*$ ,  
 $u_m = [u_m] + u_m^*$ , the third term in the right-hand side of this equation becomes

$$\frac{1}{2} [\widehat{D}u_m] = [D][u_m] + [D^*u_m^*]$$

Expanding the first term in the right-hand side of  $\partial[\hat{u}_m]/\partial t$  and using the definition  $D = \partial u_m/\partial x + m^2 \partial(v_m/m^2)/\partial y$  together with  $[\bar{v}_m] = 0$  in  $[D][u_m]$ , the expression for  $\partial[\hat{u}_m]/\partial t$  reduces to the following form:

$$\frac{\partial[\hat{u}_m]}{\partial t} = -\frac{m^2}{2} [\hat{v}_m] \frac{\partial}{\partial y} \frac{[u_m]}{m^2} - m^4 \frac{\partial}{\partial y} \frac{[u_m^*v_m^*]}{m^4} + [D^*u_m^*] + f[\hat{v}_m] + m[\hat{F}_x]$$

or rearranging terms

$$\frac{\partial[\hat{u}_m]}{\partial t} = f[\hat{v}_m] - \frac{m^2}{2} [\hat{v}_m] \frac{\partial}{\partial y} \frac{[u_m]}{m^2} + m^2 \left\{ -m^2 \frac{\partial \hat{M}_m}{\partial y} + \frac{[D^*u_m^*]}{m^2} \right\} + m[\hat{F}_x]$$

Using the condition  $[\bar{v}_m] = 0$ , and the definition of the vertical component of the relative vorticity  $\zeta = \partial v_m/\partial x - m^2 \partial(u_m/m^2)/\partial y$  which yields  $[\zeta] = -m^2 \partial([u_m]/m^2)/\partial y$ , the expression for  $\partial[\hat{u}_m]/\partial t$  may be written as follows (Smagorinsky, 1964)

$$\frac{\partial[\hat{u}_m]}{\partial t} = [v_m][f + \zeta] + m^2 \left\{ -m^2 \frac{\partial \hat{M}_m}{\partial y} + \frac{[D^*u_m^*]}{m^2} \right\} + m[\hat{F}_x] \quad (A-8)$$

(Eq. 5-4, Section VII)

Equations A-7 (5-k) and A-8 (5-l) have been derived from the zonal component of Eq. 5-e (Section VII) and the continuity Eq. 5-g (Section VII) as applied to Levels 1 and 3. The energy Equation 5-f (Section VII) together with the hydrostatic relation 5-h (Section VII) are applied at Level 2 (i.e., Fig. 1, Section III). Since Eq. 5-f can be rewritten as

$$\frac{d \ln T}{dt} = \frac{R}{c_p} \frac{w}{p} + \frac{Q}{c_p T}$$

and the definitions of  $w$  and the potential temperature,  $\theta_p$ , where  $\theta_p = (p_4/p)^{R/c_p} \cdot T$ , yield

$$\frac{d \ln T}{dt} = \frac{R}{c_p} \frac{w}{p} + \frac{d \ln \theta_p}{dt}$$

the energy Equation 5-f at Level 2 becomes

$$\frac{d}{dt} \ln \theta_{p_2} = \frac{Q_2}{c_p T_2}$$

Since Eq. 5-h (Section VII) yields  $\rho_2 = -\hat{p}/\hat{\phi} = p_2/\hat{\phi}$  or  $T_2 = \hat{\phi}/R$ , the above expression becomes with the use of the definition of  $\theta_p$ :

$$\frac{d\hat{\phi}}{dt} = \frac{R}{c_p} Q_2$$

Note that this expression with  $\hat{\phi} = RT_2$  is compatible with Eq. 5-f at Level 2 only because the term involving the "vertical" velocity  $w_2$  (i.e.,  $w = dp/dt = -\rho g w$ ) is small compared with  $Q_2/c_p$ . Using the operator  $d/dt$  in the Mercator plane and  $2\vec{U}_2 = \vec{U}_1 + \vec{U}_3 = \vec{U}$ , the energy equation at Level 2 becomes

$$\frac{\partial \hat{\phi}}{\partial t} = -\left(\frac{\vec{U}_m}{2} \frac{\partial \hat{\phi}}{\partial x} + \frac{\vec{V}_m}{2} \frac{\partial \hat{\phi}}{\partial y}\right) - w_2 \left(\frac{\partial \hat{\phi}}{\partial p}\right)_2 + \frac{R}{c_p} Q_2$$

Using the condition  $\vec{\nabla} = \partial \vec{U}_m / \partial x + m^2 \partial (\vec{V}_m / m_2) \partial y = 0$ , the foregoing equation can be put in the following form:

$$\frac{\partial \hat{\phi}}{\partial t} = -\frac{\partial}{\partial x} \left(\frac{\hat{\phi} \vec{U}_m}{2}\right) - m^2 \frac{\partial}{\partial y} \left(\frac{\hat{\phi} \vec{V}_m}{2m^2}\right) - w_2 \frac{\partial \hat{\phi}}{\partial p} + \frac{R}{c_p} Q_2$$

The third term in the right-hand side may be evaluated with the aid of the continuity equation and the definition of  $\theta_p$ ; this latter condition yields  $\partial(\ln \theta_{p,2})/\partial p = (1/\hat{\theta}) \partial \hat{\theta}/\partial p$ . Thus,  $\omega_2 \partial \hat{\theta}/\partial p$  may be expressed as  $\gamma^2 \hat{D}$  where  $\gamma^2 = (1/2)p_2^2 (\partial \hat{\theta}/\partial p) (\partial \ln \theta_{p,2}/\partial p)$ . The energy equation at Level 2 becomes

$$\frac{\partial \hat{\theta}}{\partial t} = -\frac{\partial}{\partial x} \left( \frac{\partial \bar{Q}_m}{2} \right) - m^2 \frac{\partial}{\partial y} \left( \frac{\partial \bar{v}_m}{2m^2} \right) - \gamma^2 \hat{D} + \frac{R}{c_p} Q_2$$

Taking the zonal average, using  $[\bar{v}_m] = 0$ , and the definition of  $\hat{D}$  together with the fact that  $\gamma^2$  is constant, the foregoing equation becomes (Smagorinsky, 1964):

$$\frac{\partial [\hat{\theta}]}{\partial t} = -m^2 \frac{\partial}{\partial y} H_m - \gamma^2 m^2 \frac{\partial}{\partial y} \frac{[\hat{v}_m]}{m^2} + \frac{R}{c_p} [Q_2] \quad (\text{A-9})$$

(Eq. 5-m, Section VII)

where  $H_m$  denotes a quantity proportional to the nonlinear eddy flux of sensible heat, i.e.,

$$H_m = \frac{[\bar{v}_m^* \hat{\theta}^*]}{2m^2}$$

## 2. THE S WAVE-PARAMETER

A feature of the circulation in middle and higher latitudes that is almost as prominent as hydrostatic equilibrium is geostrophic equilibrium, i.e., the approximate balance between the Coriolis force and the horizontal pressure gradient force in Eq. 5-e (Section VII). The geostrophic equilibrium then yields  $-f\vec{k} \times \vec{U} = \vec{\nabla}\phi$ , or equivalently,  $\vec{U} = (1/f)\vec{k} \times \vec{\nabla}\phi$ . Using spherical coordinates for  $\vec{\nabla}\phi$ , the relationship between the Mercator winds and actual winds, and separating the circulation and eddy motions, one obtains:

$$\hat{u}_m^* = -\frac{m^2}{f} \frac{\partial \hat{\phi}^*}{\partial y} = -\frac{m}{af} \frac{\partial \hat{\phi}^*}{\partial \theta} \quad (\text{A-10})$$

(Eq. 5-r, Section VII)

$$\hat{v}_m^* = \frac{m^2}{f} \frac{\partial \hat{\phi}^*}{\partial x} = \frac{m^2}{af} \frac{\partial \hat{\phi}^*}{\partial \lambda} \quad (\text{A-11})$$

(Eq. 5-s, Section VII)

The differentiation of the expression for  $H_m$ , use of the condition  $\bar{D}^* = 0$  in the product  $[\hat{\phi}^* D_1^*]$ , and use of Eqs. A-10 (5-r) and A-11 (5-s) yields

$$\frac{1}{f} \frac{\partial H_m}{\partial y} = \frac{[\hat{u}_m^* \hat{v}_m^*]}{2m^4} - \frac{[\hat{u}_m^* \hat{v}_m^*]}{2m^4}$$

Expanding  $\hat{M}_m = [\hat{u}_m^* \hat{v}_m^*]/m^4$ , the foregoing expression becomes

$$\hat{M}_m - \frac{1}{f} \frac{\partial H_m}{\partial y} = \frac{[\hat{u}_m^* \hat{v}_m^*]}{m^4} \quad (\text{A-12})$$

The condition  $\bar{D}^* = 0$  yields the stream function  $\psi^*$  in the following form:

$$\hat{u}_m^* = -m^2 \frac{\partial \psi^*}{\partial y} = -\frac{m}{a} \frac{\partial \psi^*}{\partial \theta} \quad (\text{A-13})$$

(Eq. 5-t, Section VII)

$$\hat{v}_m^* = m^2 \frac{\partial \psi^*}{\partial x} = \frac{m^2}{a} \frac{\partial \psi^*}{\partial \lambda} \quad (\text{A-14})$$

(Eq. 5-u, Section VII)

Thus, the two spectral modes ( $\hat{U}_m^*$  and  $\hat{V}_m^*$ ) of the eddy winds are given by Eqs. A-10, A-11, A-13, A-14 and the analytical description of the baroclinic disturbances. i.e.,

$$\psi^* = A \sin \eta \quad (\text{A-15})$$

(Eq. 5-v, Section VII)

$$\hat{\phi}^* = B \sin (\eta + k\delta) \quad (\text{A-16})$$

(Eq. 5-w, Section VII)

where  $\eta = k(\lambda - \alpha\theta)$ . Substituting these results in the expression for  $H_m^*$ , one gets:

$$H_m^* = \frac{kAB}{2a} [\sin (\eta + k\delta) \cos \eta] = \frac{kAB}{4a} \sin k\delta \quad (\text{A-17})$$

(Eq. 5-y, Section VII)

Assuming that B,  $\alpha$ , and  $\delta$  in Eq. A-16 (5-w) are nearly constant,

$$\frac{[\hat{U}_m^* \hat{V}_m^*]}{m^4} = \frac{k^2 \alpha AB}{a^2 f m} [\cos (\eta + k\delta) \cos \eta] = \frac{k^2 \alpha AB \cos k\delta}{2a^2 f m} \quad (\text{A-18})$$

Note that the conditions of constant B and  $\delta$  used in the derivation of Eq. A-18 imply from Eq. A-17 that  $H_m^*$  is proportional to A. Combining Eqs. A-17 and A-18:

$$\frac{[\hat{U}_m^* \hat{V}_m^*]}{m^4} = \frac{H_m^*}{f m S} \quad (\text{A-19})$$

where

$$S = \frac{a \tan k\delta}{2\alpha k} \quad (\text{A-20})$$

Combining Eqs. A-12 and A-19:

$$\hat{M}_m = \frac{1}{F} \left( \frac{dH_m}{dy} + \frac{H_m}{mS} \right) \quad (\text{A-21})$$

(Eq. 5-x, Section VII)

## APPENDIX B

### DERIVATION OF EDDY KINETIC ENERGY EQUATION

This appendix gives a more detailed derivation of the eddy kinetic energy Equation 8-c (Section IX) from Eq. 8-b (Section IX), i.e.,

$$\frac{dK_e}{dt} = -\vec{U} \cdot \vec{\nabla} \phi + \vec{U} \cdot \vec{F} \quad (\text{B-1})$$

(Eq. 8-b, Section IX)

which must be added to the set of primitive Equations 5-e through 5-h (Section VII). Multiplying the continuity Equation 5-g through by  $-\phi$  and adding the result to B-1 (8-b):

$$\frac{dK_e}{dt} = -\vec{\nabla} \cdot \phi \vec{U} - \frac{\partial \phi \omega}{\partial p} + \omega \frac{\partial \phi}{\partial p} + \vec{U} \cdot \vec{F}$$

Using Equation 5-h, to eliminate  $\partial \phi / \partial p$  yields

$$\frac{dK_e}{dt} = -\vec{\nabla} \cdot \phi \vec{U} - \frac{\partial \phi \omega}{\partial p} - \frac{RT\omega}{p} + \vec{U} \cdot \vec{F} \quad (\text{B-2})$$

Since  $\vec{U} = [\vec{U}] + \vec{U}^*$ , the kinetic energy  $K_e$  may be expressed as follows:

$$K_e = K_Z + K_E \quad (\text{B-3})$$

where  $K_Z$  and  $K_E$  denote, respectively, the zonal and eddy kinetic energies, which are defined as follows:

$$K_Z = \frac{1}{2} [\vec{U}] \cdot [\vec{U}] = \frac{1}{2} [u]^2 + \frac{1}{2} [v]^2$$

and

$$K_E = \frac{1}{2} \vec{U}^* \cdot \vec{U}^* + [\vec{U}] \cdot \vec{U}^* = \frac{1}{2} u^{*2} + \frac{1}{2} v^{*2} + [u] u^* + [v] v^*$$

Substituting Eq. B-3 in B-2, the individual time rate of change of the eddy kinetic energy is given by

$$\frac{dK_Z}{dt} + \frac{dK_E}{dt} = -\vec{\nabla} \cdot \phi \vec{U} - \frac{\partial \phi \omega}{\partial p} - \frac{RT\omega}{p} + \vec{U} \cdot \vec{F} \quad (B-4)$$

where  $dK_Z/dt = [\vec{U}] \cdot d[\vec{U}]/dt$ . Multiplying the continuity Equation 5-g through by  $\chi$ , adding the result to the expression for  $d\chi/dt$ , letting  $\chi = K_E$ , using spherical coordinates for  $\vec{\nabla} \cdot \chi \vec{U}$ , and taking the zonal average:

$$\frac{d}{dt} [K_E] = \frac{\partial}{\partial t} [K_E] + \frac{m}{a} \frac{\partial}{\partial \theta} \frac{[K_E v]}{m} + \frac{\partial}{\partial p} [K_E \omega]$$

which, with the zonal average of the right-hand side of Eq. B-4, yields:

$$\begin{aligned} \frac{dK_Z}{dt} + \frac{\partial}{\partial t} [K_E] + \frac{m}{a} \frac{\partial}{\partial \theta} \frac{[(K_E + \phi) v]}{m} + \frac{\partial}{\partial p} [(K_E + \phi) \omega] \\ = -\frac{R}{p} [T\omega] + [\vec{U} \cdot \vec{F}] \end{aligned} \quad (B-5)$$

Separating the eddy and circulation terms in Eq. B-5, i.e., using  $\chi = [\chi] + \chi^*$  where  $\chi$  denotes successively the geopotential, the meridional wind, the individual time rate of change of the pressure, and the temperature:

$$\frac{\partial}{\partial t} [K_E] + \frac{m}{a} \frac{\partial}{\partial \theta} \left\{ \frac{[K_E][v]}{m} + \frac{[K_E v^*]}{m} + \frac{[\phi^* v^*]}{m} \right\} + \frac{\partial}{\partial p} \left\{ [K_E][\omega] + [K_E \omega^*] + [\phi^* \omega^*] \right\} + T_{e_2} = 0 \quad (B-6)$$

where the term  $T_{e_2}$  denotes

$$T_{e_2} = (dK_Z/dt)^* + \frac{R}{p} [T^* \omega^*] - [u^* F_\lambda^* + v^* F_\theta^*]$$

and  $(dK_Z/dt)^*$  the eddy terms in  $dK_Z/dt$  or  $[\vec{U}] \cdot d[\vec{U}]/dt$ , i.e., in  $[u] d[u]/dt + [v] d[v]/dt$ . The expression for  $(dK_Z/dt)^*$  can then be obtained by taking the zonal average of Eqs. 5-i and 5-j (Section VII), expanding the individual time derivatives in a manner similar to that of  $d[K_E]/dt$ , and performing the operation  $[u] d[u]/dt + [v] d[v]/dt$ . Each of these two latter terms will yield two eddy components corresponding to the last two terms in the right-hand side of  $d[X]/dt$ , where  $X$  denotes successively  $[u]$  and  $[v]$ . Each quadratic term in the right-hand side of Eqs. 5-i and 5-j yields an additional eddy component, so that the six eddy components in  $(dK_Z/dt)^*$  are as follows:

$$\left( \frac{dK_Z}{dt} \right)^* = \frac{[u]}{a} \tan \theta [u^* v^*] - \frac{[v]}{a} \tan \theta [u^{*2}] - T_{e_3}$$

where the term  $T_{e_3}$  denotes the four terms in the individual time derivatives, i.e.,

$$T_{e_3} = [u] \left\{ \frac{m}{a} \frac{\partial}{\partial \theta} \frac{[u^* v^*]}{m} + \frac{\partial}{\partial p} [u^* \omega^*] \right\} + [v] \left\{ \frac{m}{a} \frac{\partial}{\partial \theta} \frac{[v^{*2}]}{m} + \frac{\partial}{\partial p} [v^* \omega^*] \right\}$$

Noting that the two terms involving the angular momentum  $[u^*v^*]$  can be reduced to a single one, i.e.,

$$\frac{[u]}{a} \left\{ \tan \theta [u^*v^*] - m \frac{\partial [u^*v^*]}{\partial \theta} \right\} = - \frac{[u]}{a} m^2 \frac{\partial [u^*v^*]}{m^2}$$

and using  $\partial [K_E]/\partial t = 0$ , Eq. B-6 reduces to the form of Eq. 8-c (Section IX), (Kurihara, 1970).